Genetic basis of rhizoid development in the liverwort *Marchantia polymorpha*



Suvi Honkanen

Magdalen College

Department of Plant Sciences

University of Oxford

A thesis submitted for the degree of Doctor of Philosophy (D. Phil.)

Michaelmas 2015

Genetic basis of rhizoid development in the liverwort *Marchantia polymorpha*

Suvi Honkanen
Magdalen College
Department of Plant Sciences
University of Oxford

A thesis submitted for the degree of Doctor of Philosophy (D. Phil.)
Michaelmas 2015

Abstract

The evolution of specialised rooting structures was one of the key morphological innovations that allowed the first multicellular plants to colonise land more than 470 million years ago. The first land plants likely resembled modern bryophytes with a rooting structure that consists of filamentous rooting cells called rhizoids, which are morphologically similar to the root hairs of vascular plants. This thesis describes identification of genes required for rhizoid development in a model bryophyte, the liverwort *Marchantia polymorpha.* The aim was to identify the conserved and novel aspects of the gene regulatory networks for filamentous rooting cell development in land plants. *Agrobacterium*-mediated T-DNA transformation of haploid *M. polymorpha* spores was used to generate 150,000 *M. polymorpha* T-DNA insertion lines, which were screened for defects in rhizoid development. 204 rhizoid defective mutants were isolated which allowed identification of 25 genes required for *M. polymorpha* rhizoid development. The role of the class I *RSL* (*ROOT HAIR DEFECTIVE SIX-LIKE*) genes as positive regulators of root hair and rhizoid differentiation was found to be conserved between liverworts and vascular plants. This suggests that the class I *RSL* gene mechanism is ancient and originated before the two lineages diverged more than 440 million years ago. Furthermore, the *M. polymorpha* class I *RSL* gene Mp*RSL1* is required for development of gemmae and mucilage papillae, which similarly to rhizoids form from single epidermal cells that elongate to form an outgrowth. Moreover, Mp*RSL1* is under negative feedback regulation of the *FEW RHIZOIDS1* (*FRH1*) microRNA. Many genes required for rhizoid elongation were similar with those required for root hair elongation, suggesting that these genes are likely to have been part of the genetic network downstream of class I *RSL* genes in the common ancestor of liverworts and vascular plants.

Acknowledgements

- Liam Dolan –Thank you for giving me the opportunity to work on this project. I am grateful for the numerous inspirational discussions and all the guidance I have received throughout my DPhil.
- Jane Langdale, Javier Agusti and Holger Breuninger –Thank you for all the advice and encouragement, it has been invaluable.
- Anna, Bruno, Clemence, Clement, Chulmin, Giulia, Helene, Reka, Sandy, Sourav, Susanna, Thomas and Victor –Thank you for your friendship, patience and all the entertaining conversations that made the lab such a wonderful place to work at.
- Owen –Thank you for all those more or less scientific discussions at the University Club.
- Brendan –Thank you for being my rock. I love you.
- Many of the above for reading drafts of this thesis.
- My friends and family for all the support I have received.
- My grandparents, whose stories and collection of nonfiction books influenced me more than I realised at the time.

- Justin Goodrich and Hugh Dickinson for their constructive feedback on this thesis.
- Mario Arteaga-Vazquez for sharing the *M. polymorpha* small RNA sequencing data and for running the miRNA target prediction.
- Steve Kelly for bioinformatics.
- John Baker for photography.
- Gem Toes for being such an excellent graduate administrator.
- Helen, Pauline and Lida for their help in the lab.
- Source BioScience for sequencing.
- European Research Council (ERC) and Biotechnology and Biological Sciences Research Council (BBSRC) for funding.
- Gatsby Plants Network for support.

Table of Content

Abstract **2**

Acknowledgements **3**

Table of Content **4**

Supplementary files available on CD **7**

List of Abbreviations **9**

Chapter 1: Introduction **10**

1.1. The colonisation of land 13
1.2. The first land plants evolved from Streptophyte algae 14
1.3. The first land plants are likely to have resembled extant bryophytes 16
1.4. The origin and evolution of vascular plants 19
1.5. Many genetic mechanisms that control morphological complexity in flowering plants are likely to have ancient origins 20
1.6. Elaboration of developmental mechanisms during the evolution of vascular plants 22
1.7. Evolution of rooting structures 25
1.8. Conserved basic helix-loop-helix transcription factors regulate initiation and elongation of root hairs and rhizoids 26
1.9. Auxin promotes root hair and rhizoid development 28
1.10. Root hairs and rhizoids elongate by tip growth 30
1.11. Patterning of root hairs and rhizoids 31
1.12. The liverwort *M. polymorpha* as a model organisms for studying the evolution of filamentous rooting cells 33

Chapter 2: Materials and Methods **38**

2.1. Plant material and bacterial strains 39
2.2. Plant growth conditions 39
2.3. Plant transformation 40
2.4. Isolation of mutants defective in rhizoid development 41
2.5. Analysis of co-segregation and T-DNA copy number 43
2.6. Constructs 44
T-DNA mutagenesis 44
Over-expression constructs 44
Promoter-reporter constructs 45
2.7. DNA extraction 46
2.8. Thermal asymmetric interlaced PCR (TAIL-PCR) 46
2.9. RNA extraction, cDNA synthesis and quantitative RT-PCR 47
RNA extraction 47
cDNA synthesis and qRT-PCR 48
qRT-PCR data analysis 48
2.10. Rapid amplification of cDNA ends (RACE) PCR 49
2.11. Small RNA enriched RNA extraction and Stem-loop PCR 49
2.12. Microscopy and image analysis 50
Light microscopy 50
Confocal microscopy 50
Image processing 51
2.13. Sequence retrieval, alignment and phylogeny construction 51

Chapter 3: Genetic screen for *M. polymorpha* mutants defective in rhizoid development 53
3.1. Summary 54
3.2. Introduction 55
3.3. Results and discussion 59
3.3.1. Screening of 150,000 *M. polymorpha* T-DNA insertion lines resulted in identification of 204 rhizoid defective mutants 59
Inheritance of the rhizoid defective phenotype 61
Co-segregation analysis 61
Mutants with abnormal T-DNA insertion sequences 64
T-DNA copy number 64
3.3.2. Twenty-five genes involved in *M. polymorpha* rhizoid development identified 66
3.3.3. Twenty-four of the 25 *M. polymorpha* rhizoid development genes have predicted homologs in Arabidopsis 71
3.3.4. Many Arabidopsis multicopy genes are present as a single gene in *M. polymorpha* .. 88
3.3.5. Many of the *M. polymorpha* rhizoid development genes are likely to have a conserved role in filamentous rooting cell development 91
3.3.6. Similar genes are required for cell wall synthesis and cell wall integrity during the elongation of rhizoids and root hairs 92
CSLD genes are required for the development of tip growing cells in *M. polymorpha,* Arabidopsis and rice 92
A predicted xyloglucan-specific galacturonosyltransferase is required for filamentous rooting cell development in both *M. polymorpha* and Arabidopsis 93
Catharanthus roseus RLK1-like family proteins are required for cell wall integrity in *M. polymorpha* and Arabidopsis 95
3.3.7. Rhizoid elongation requires genes associated with actin cytoskeleton dynamics and vesicle transport machinery 98
3.3.8. The *M. polymorpha* rhizoid defective mutants identify 14 genes with a novel role in filamentous rooting cell development 99
3.3.9. The first mutants with defects in six previously uncharacterised plant genes define genes required for rhizoid development 100
3.3.10 Technical considerations 100
Gain-of-function mutants 100
Coverage of the screen 102
3.4. Conclusion 104

Chapter 4: The *M. polymoprha* class I *RSL* gene *MpRSL1* is a positive regulator of rhizoid precursor cell differentiation 106
4.1. Summary 107
4.2. Introduction 108
4.3. Results 111
4.3.1. The class I *RSL* gene *MpRSL1* is required for rhizoid development in *M. polymorpha* 111
MpRSL1 is required for rhizoid precursor cell differentiation 112
4.3.2. *MpRSL1* is a positive regulator of rhizoid precursor cell differentiation 112
The 35S-promoter on the T-DNA is likely to be responsible for the elevated *MpRSL1* expression in the gain-of-function mutants 118
4.3.3. *MpRSL1* function is not restricted to rhizoid development 118
MpRSL1 is required for gemmae development 119
MpRSL1 is required for the development of epidermal papillae 120
MpRSL1 is likely to be required for the induction of reproductive development or the formation of sexual reproductive structures 120
4.4. Discussion 122

Chapter 5: *FEW RHIZOIDS1* is a novel negative regulator of *MpRSL1* and rhizoid precursor cell differentiation 126
5.1. Summary 127
5.2. Introduction 128
5.3. Results 130
5.3.1. Identification of a novel regulator of rhizoid precursor cell differentiation 130
The few rhizoid phenotype of *Mpfrh1-2* and *Mpfrh1-3* is inherited and co-segregates with the hygromycin resistance marker on the T-DNA 133
The *Mpfrh1* mutant lines are defective in reproductive development 134
5.3.2. *MpFRH1* negatively regulates the development of rhizoid precursor cells and rhizoids 135
5.3.3. *MpFRH1* negatively regulates the development of epidermal papillae and gemmae 137
5.3.4. *MpFRH1* negatively regulates *MpRSL1* transcript levels 138
5.3.5. *MpRSL1* positively regulates *MpFRH1* transcript level 140
5.3.6. *MpFRH1* functions as RNA 141
5.3.7. *MpFRH1* is a pri-miRNA gene that gives rise to a 21 bp MpFRH1 miRNA 146
The mature MpFRH1 miRNA is present in wild type and *MpFRH1*^{GOF} *M. polymorpha* 148
5.3.8. MpFRH1 miRNA targets *MpRSL1* 150
5.3.9. The FRH1 miRNA target site on class I *RSL* gene transcripts is conserved across liverworts 151
5.3.10. The *MpFRH1* promoter is expressed in rhizoid precursor cells, rhizoids and epidermal papillae 153
MpFRH1 promoter may be expressed during gemma development 157
MpFRH1 expression pattern coincides with the expected *MpRSL1* expression pattern and the pattern of *MpRSL1* activity 157
5.4. Discussion 158

Chapter 6: General discussion 167

Appendices 173
Materials and methods Appendix 174
Chapter 3 Appendix 177
Chapter 5 Appendix 182

References 184

Supplementary files available on CD

Supplementary file 1 –TAIL-PCR band sequences containing the T-DNA insertion flanking genomic sequences of the rhizoid defective mutants

Supplementary file 2 –multiple sequence alignment of Arabidopsis and *M. polymorpha* ALBA-like proteins used for phylogeny construction (Phylip format)

Supplementary file 3 –multiple sequence alignment of Arabidopsis and *M. polymorpha* CSLD proteins used for phylogeny construction (Phylip format)

Supplementary file 4 –multiple sequence alignment of Arabidopsis and *M. polymorpha* FBA proteins used for phylogeny construction (Phylip format)

Supplementary file 5 –multiple sequence alignment of Arabidopsis and *M. polymorpha* class A and class B GATA proteins used for phylogeny construction (Phylip format)

Supplementary file 6 –multiple sequence alignment of Arabidopsis and *M. polymorpha* IRE-like proteins used for phylogeny construction (Phylip format)

Supplementary file 7 –multiple sequence alignment of Arabidopsis and *M. polymorpha* PI4Kα proteins used for phylogeny construction (Phylip format)

Supplementary file 8 –multiple sequence alignment of Arabidopsis and *M. polymorpha* PTI-like proteins used for phylogeny construction (Phylip format)

Supplementary file 9 –multiple sequence alignment of Arabidopsis and *M. polymorpha* RHM-like proteins used for phylogeny construction (Phylip format)

Supplementary file 10 –multiple sequence alignment of Arabidopsis and *M. polymorpha* SRI3-like proteins used for phylogeny construction (Phylip format)

Supplementary file 11 –multiple sequence alignment of Arabidopsis and *M. polymorpha* CrRLK1L proteins used for phylogeny construction (Phylip format)

Supplementary file 12 –multiple sequence alignment of Arabidopsis and *M. polymorpha* TMT proteins used for phylogeny construction (Phylip format)

Supplementary file 13 –multiple sequence alignment of Arabidopsis and *M. polymorpha* WDL family proteins used for phylogeny construction (Phylip format)

Supplementary file 14 –multiple sequence alignment of Arabidopsis and *M. polymorpha* XF-like proteins used for phylogeny construction (Phylip format)

Supplementary file 15 –multiple sequence alignment of Arabidopsis and *M. polymorpha* class XI and class VIII myosin proteins used for phylogeny construction (Phylip format)

Supplementary file 16 –multiple sequence alignment of Arabidopsis and *M. polymorpha* XUT-like proteins used for phylogeny construction (Phylip format)

List of Abbreviations

APT	*ADENINE PHOSPHORIBOSYL TRANSFERASE*
bHLH	basic helix-loop-helix
BLAST	Basic Local Alignment Search Tool
bp	basepair
CTAB	Cetyltrimethylammonium bromide
CUL	*CULLIN*
DNA	Deoxyribonucleic acid
FRH	*FEW RHIZOIDS*
IRE	*INCOMPLETE ROOT HAIR ELONGATION*
kb	kilobasepair
LRL	*Lotus japonicus ROOTHAIRLESS1-LIKE*
miRNA	microRNA
Mya	million years ago
NLS	nuclear localisation signal
ORF	open reading frame
PCR	polymerase chain reaction
qRT-PCR	quantitative real-time PCR
RACE-PCR	rapid amplification of cDNA ends PCR
RNA	ribonucleic acid
RSL	*ROOT HAIR DEFECTIVE SIX-LIKE*
Sd	standard deviation
SRI	*SHORT RHIZOIDS*
TAIL-PCR	thermal asymmetric interlaced PCR
WT	wild type
YFP	yellow fluorescent protein

Chapter 1

Introduction

The first land plants evolved from streptophyte freshwater algae and colonised land sometime more than 470 million years ago (Mya). Over time, evolution of morphological and developmental complexity in the diploid sporophyte generation of land plants resulted in a range of adaptations that allowed plants to flourish in the terrestrial environment. The establishment of land plants permanently changed the climate and created the basis for all terrestrial ecosystems, and therefore was crucial for the subsequent emergence and spread of animals on land.

The evolution of a specialised rooting structure that anchors the plant on its substrate and facilitates efficient uptake of nutrients and water was one of the key morphological adaptations that allowed the first plants to colonise land. The first land plants are likely to have closely resembled modern bryophytes, with haploid dominant life-cycles and rooting structures consisting of filamentous rooting cells called rhizoids, which are morphologically similar to root hairs of vascular plants (Edwards *et al*., 1995; Taylor, 1995; Wellman *et al*., 2003; Kerp *et al*., 2005; Taylor *et al*., 2005).

When and where did the gene regulatory network for the first land plant rooting systems originate? What was the identity of the genes that regulated the development of the rooting system of the earliest land plants? We can begin to answer these questions by identifying components of the genetic network that regulates the development of rhizoids, filamentous rooting cells that make up the rooting system in the early diverging groups of land plants, bryophytes. Defining the genetic mechanisms controlling rhizoid development in bryophytes allows us to

elucidate which aspects of this gene regulatory network are similar with the gene regulatory network that controls root hair development in vascular plants. Those genetic mechanisms that are conserved between bryophytes and vascular plants are likely to be ancient and to have been present in the early land plants before the two lineages diverged more than 443 Mya (Steemans *et al*., 2009).

This thesis describes the identification of genes that regulate rhizoid development in a bryophyte model species, the liverwort *M. polymorpha*, carried out to identify the conserved and novel aspects of the gene regulatory network for filamentous rooting cell development in land plants. This chapter provides an overview on the evolution of developmental mechanisms in land plants, and outlines the key characteristics of *M. polymorpha* development. Chapter 2 provides details of the methods used in this study. Chapter 3 describes a forward genetic screen of *M. polymorpha* T-DNA insertion lines carried out to isolate a collection of mutants defective in rhizoid development. Rhizoid development can be divided into two distinct stages; i) differentiation of epidermal cells into rhizoid precursor cells and ii) elongation of rhizoids by tip growth. The role of a subset of the genes associated with rhizoid elongation is further discussed in chapter 3, while chapters 4 and 5 focus on the genetic mechanisms that regulate rhizoid precursor cell differentiation.

1.1. The colonisation of land

The colonisation of land by multicellular plants more than 470 Mya was one of the key events in the history of life on our planet (Kenrick and Crane, 1997). The transition of plants from an aquatic environment to a terrestrial setting resulted in exposure to many novel stresses such as UV radiation, gravity, desiccation and large variations in temperature. To cope with these stresses a range of adaptations evolved in the land plant lineage by the beginning of Carboniferous era 360 Mya (Taylor *et al*., 2009). The development of waxy cuticles protected plants against UV-radiation and desiccation, and the evolution of stomata facilitated gas exchange through this thick cuticle (Edwards *et al.*, 1998; Beerling *et al*., 2001). The evolution of broad leaves increased the capture of sunlight resulting in enhanced photosynthetic output (Beerling *et al*., 2001). Development of vascular tissue increased the efficiency of long distance water transport through the plant and subsequent thickening of the vascular tissue provided structural support that allowed the evolution of tall trees (Taylor *et al*., 2009). The evolution of rooting structures enabled plants to take up nutrients and water from the soil. Furthermore, the development of extensive rooting systems in land plants accelerated weathering processes through increased mechanical disruption of rocks as well as acidification of soils by root exudates (Raven and Edwards, 2001). This increase in weathering had a major impact on long-term geochemical carbon cycling due to enhanced release of calcium and magnesium silicate minerals in surface soils, and their subsequent sequestering of CO_2 to long-term carbon storage (Berner, 1998). Increased sequestering of CO_2 reduced the concentration of CO_2 in the atmosphere, which led to global climate cooling (Berner 1991, 1994). Overall,

the evolution of morphological complexity in the land plant lineage allowed plants to colonise diverse habitats, creating the base for most terrestrial ecosystems and resulting in permanent climate change, both of which facilitated the subsequent colonisation of land by metazoan organisms (Becker and Marin, 2009).

1.2. The first land plants evolved from Streptophyte algae

All land plants (embryophytes) form a monophyletic group, whose common ancestor evolved within the group of freshwater streptophyte algae (Fig. 1.1). Within streptophyte algae, either Charales (Karol *et al*., 2001; Qiu *et al*., 2006), Coleochaetales (Finet *et al*., 2010) or most convincingly Zygnematales (Turmel *et al*., 2006; Wodniok *et al*., 2011; Timme *et al*., 2012; Wickett *et al*., 2014) has been resolved as the algal sister group to all land plants based on molecular phylogenetic studies. Many cellular features considered characteristic of land plants, such as plasmodesmata, a phragmoplast, hexameric cellulose synthases and growth from a defined apical cell, evolved within the streptophyte algae providing further support to their phylogenetic relationship with land plants (reviewed in Graham *et al*., 2000). However, Streptophyte algae lack other key features that evolved in the land plant lineage, such as a life-cycle alternating between multicellular haploid and diploid generations, retention of the zygote on the maternal tissue and growth from a defined apical cell with three cutting faces resulting in the formation of complex 3D architecture (Graham *et al*., 2000; Niklas and Kutschera, 2009).

The extant members of the streptophyte algal lineages most closely related to land plants are morphologically relatively simple. Charales bear the highest level of complexity with multicellular nodes that give rise to branching filaments and multicellular rhizoids (reviewed in McCourt *et al*., 2004). Coleochaetales are small and either filamentous or disc-shaped, while Zygnematales contain both single-celled and multicellular filamentous forms that reproduce by the unusual method of conjugation (McCourt *et al*., 2004). Some species within Zygnematales, such as those belonging to the genus Spirogyra, also develop rhizoids that are unicellular and thought to function in anchorage (Inoue *et al*., 2002). The simple morphology within the extant Zygnematales has been suggested to result from secondary simplification, whereas the reproductive method of Zygnematales is thought to be a derived character (Turmel *et al*., 2007; Wodniok *et al*., 2011). Unfortunately the fossil record of the streptophyte algae is poor and therefore does not provide clues to the morphology of the immediate algal ancestors of land plants.

In contrast to streptophyte algae, in which the zygote is the only diploid cell, the life-cycles of all land plants are characterised by alternation between haploid and diploid phases, both of which are multicellular (Niklas and Kutschera, 2009). During the evolution of vascular plants the diploid sporophyte generation increased in complexity, coupled with reduction of the haploid gametophyte phase (Graham *et al.*, 2000). As a result, the gametophytes of flowering plants only comprise a few cells embedded in the parent sporophyte tissue. By contrast, in the basal land plants bryophytes (liverworts, mosses and hornworts) the gametophyte phase is dominant and nourishes the growth of the simple sporophyte. According to the

now widely accepted antithetic theory (Bower 1908), the multicellular diploid sporophyte generation originates from the intercalation of mitotic divisions into the zygote developmental program before meiosis, resulting in a diploid embryo that is retained and nutritionally dependent on the parental gametophyte tissues. The evolution of morphological complexity in this diploid sporophyte generation then resulted in the dominant, nutritionally independent sporophyte observed in vascular plants today.

1.3. The first land plants are likely to have resembled extant bryophytes

The first land plants are likely to have resembled extant bryophytes. Some phylogenetic studies suggest liverworts are the basal group of land plants (Dombrovska and Qiu, 2004; Qiu *et al*., 2006), while more recent studies have resolved alternative topologies, in which hornworts or a monophyletic bryophyte clade form the earliest diverging group (Cox *et al*., 2014; Wickett *et al*., 2014) (Fig. 1.1). Consistent with the antithetic theory, the sporophytes of bryophytes are small, morphologically relatively simple and nutritionally dependent on the parent gametophyte tissue, potentially representing an evolutionary intermediate between the single-cell diploid phase of the algal ancestor of land plants and the complex sporophytes of vascular plants.

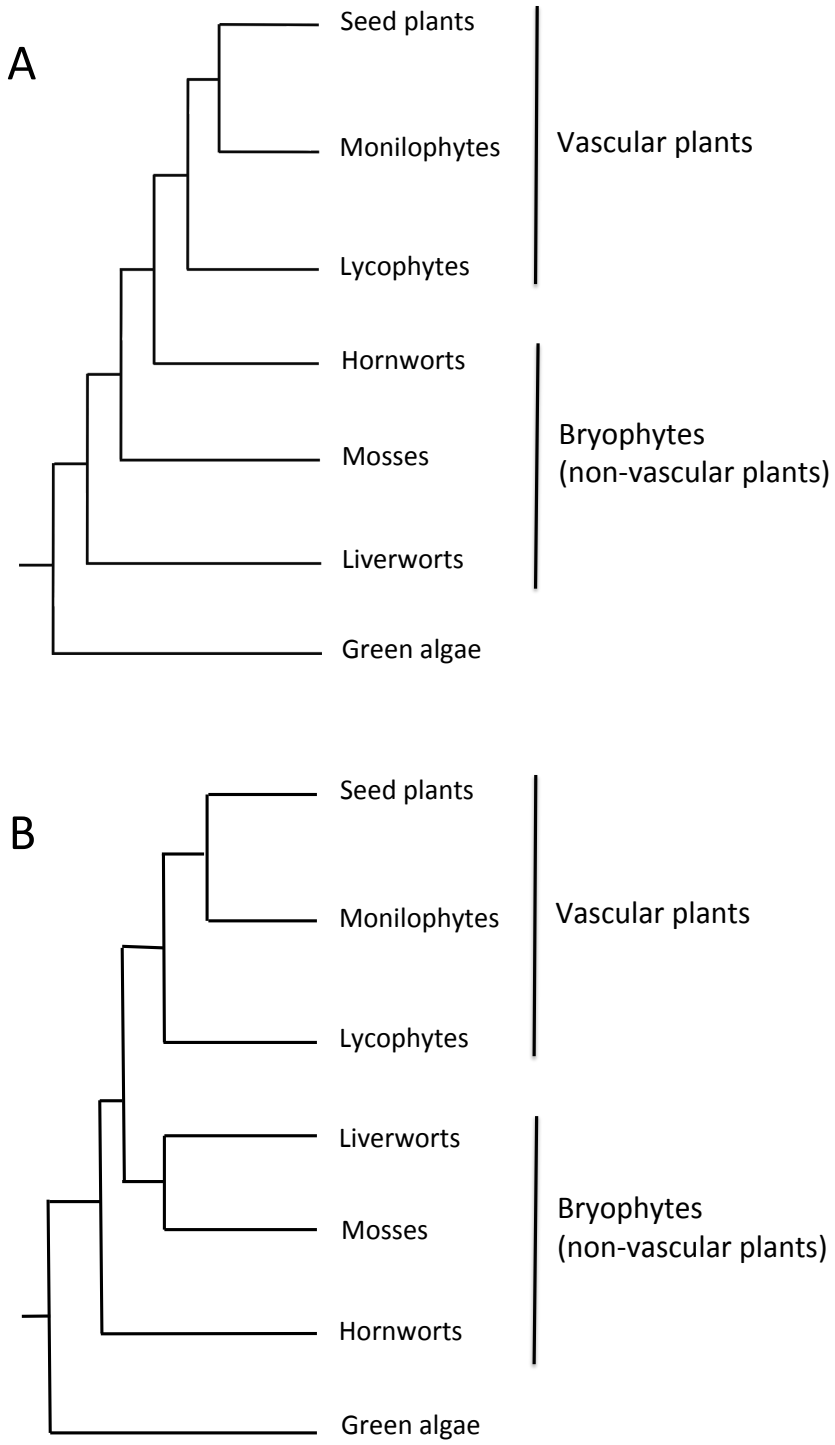

Figure 1.1 Streptophyte phylogenies recovered in molecular phylogenetic studies. A) Streptophyte phylogeny after Qiu *et al.*, 2006 based on nucleotide sequences of 67 chloroplast genes from 36 species and 6 non-chloroplastic genes from 193 species. B) Streptophyte phylogeny after Wickett *et al*., 2014 based on first and second codon position nucleotides for 674 nuclear genes from 102 species.

The fossil record suggests the earliest land plants were similar to liverworts. The first evidence for the colonisation of land by plants is the appearance of spores in the fossil record from the mid-Ordovician period (around 470 Mya) onwards (Wellman and Gray, 2000). The ultrastructure of the walls surrounding these spores is remarkably similar to that of modern liverwort spores (Taylor, 1995; Wellman *et al*., 2003). Moreover, features of fossilised tissue fragments found associated with similar spores also suggests liverwort affinities (Edwards *et al*., 1995). However, the oldest liverwort megafossils originate from around 390 Mya (Hernick *et al*., 2008), which may be due to poor preservation of liverwort gametophyte tissues (Wellman and Gray, 2000). Some of the earliest well preserved land plant megafossils, such as those found in the early-Devonian Rhynie Chert (410 Mya) in Scotland, show alternation between physiologically independent haploid and diploid generations, both of which are multicellular and show similar levels of morphological complexity (Taylor *et al*., 2009). The Rhynie Chert plants were already vascularised, possessed stomata and had rhizoids on both gametophyte and sporophyte generations (Edwards *et al*., 1998; Kerp *et al*., 2005; Taylor *et al*., 2009). Liverworts retain many features of the gametophytes of these earliest well-preserved land plant megafossils in comparison to other extant plant groups, supporting their position at the base of the land plant phylogenetic tree (Kerp *et al*., 2005; Taylor *et al*., 2005).

1.4. The origin and evolution of vascular plants

Most of the basic morphological features characteristic of land plants evolved in the sporophyte generation of vascular plants during the Silurian-Devonian era (443-360 Mya). The appearance of trilete spores in the fossil record at approximately 443 Mya is thought to mark the emergence of the first vascular plants, and therefore the diversification of the bryophyte and vascular plant lineages (Steemans *et al*., 2009). The first vascular plant megafossils have been dated back to around 425 Mya (Edwards and Feehan, 1980; Gensel, 2008); however, the oldest well-preserved fossilised vascular tissues originate from around 415 Mya (Edwards *et al.,* 1992). The diversification of lycophyte and euphyllophyte (monilophytes and seed plants) lineages occurred soon after the emergence of the first vascular plants (Kenrick and Crane, 1997). Many of the characteristics of vascular plants; axial roots, leaves and secondary growth, evolved independently in the lycophyte and euphyllophyte lineages during the Devonian period (Raven and Edwards, 2001; Gensel, 2008). The euphyllophyte lineage further diverged giving rise to the monilophytes (ferns and horsetails) and seed plants, after which the first seed-bearing species evolved within the seed plant lineage (Linkies *et al.,* 2010). By the end of the Devonian era 360 Mya the evolution of morphological complexity in the sporophyte generation had led to the emergence of tall trees with deep penetrating rooting systems that created the basis for the Earth's first forest ecosystems (Stein *et al*., 2012). Flowers only evolved in the seed plant lineage by 125 Mya, after which flowering plants (angiosperms) rapidly diversified and form the vastly most species diverse group of land plants today (Friis *et al*., 2001).

1.5. Many genetic mechanisms that control morphological complexity in flowering plants are likely to have ancient origins

The morphology of the extant streptophyte algae suggests the algal ancestor of land plants is likely to have had multicellular haploid generation and unicellular diploid generation. Furthermore, in the basal groups of land plants, bryophytes, the haploid gametophyte generation is morphologically more complex with rhizoids, photosynthetic tissue and branching indeterminate meristems, while the diploid sporophyte is small, has an unbranched determinate meristem and is nutritionally dependent on the haploid gametophyte. This suggests that some of the basic morphological features of land plants are likely to have first evolved in the haploid gametophyte generation. As the haploid and diploid stages of the land plant life-cycle share the same genetic material, it seems reasonable to hypothesise that some genetic components giving rise to the existing complexity in the gametophyte phase were recruited to drive the increasing morphological complexity in the sporophyte generation during evolution of vascular plants.

The haploid and diploid stages of the plant life-cycle use the same genetic material, but execute distinct developmental programs. The transition between the haploid and diploid developmental programs is regulated by class II *KNOTTED1-LIKE HOMEOBOX* (*KNOX*) genes. In the moss *P. patens*, loss of class II *KNOX* gene function results in activation of the haploid developmental program in the diploid generation without undergoing meiosis (Sakakibara *et al*., 2013). Therefore, the class II *KNOX* genes repress the haploid developmental program during the diploid phase in the wild type. Furthermore, the maintenance of the correct developmental

program is likely to involve epigenetic regulation. The polycomb repressive complex 2 (PRC2) represses gene expression by carrying out histone H3 lysine 27 trimethylation that promotes chromatin silencing. In the moss *P. patens,* loss of PRC2 components results in production of sporophyte-like structures in the gametophyte stage (Mosquna *et al*., 2009; Okano *et al*., 2009). These findings suggest that the sporophyte developmental program is repressed by a PRC2 dependent epigenetic mechanism during the gametophyte stage.

When and where did the genetic mechanisms that control morphological complexity in vascular plant sporophytes originate? We can elucidate this by investigating the function of homologous genes in the bryophyte lineage, which diverged from the lineage leading to vascular plants plants soon after the first plants colonised land (Steemans *et al*., 2009). If homologous genes carry out a similar function in bryophytes and vascular plants, such as the model flowering plant Arabidopsis, then the genetic mechanism is likely to have been present in the early land plants that were common ancestors of the two lineages.

Many genetic mechanisms are likely to have ancient origins in land plants. Similar genetic regulatory mechanisms control the development of root hairs in the diploid sporophytes of Arabidopsis and rhizoids in the haploid gametophyte of the moss *Physcomitrella patens* (discussed further below) (Menand *et al*., 2007; Tam *et al*., 2015). Furthermore, similar transcription factors regulate the development of the highly specialised Arabidopsis vascular tissue and morphologically simple *P. patens* water conducting cells (Xu *et al.,* 2014). A mechanism that regulates day-length dependent transition from vegetative to reproductive development is

conserved between the haploid gametophyte of the liverwort *M. polymorpha* and diploid sporophyte of Arabidopsis (Kubota *et al*., 2013). In addition, the major light receptors (Rensing *et al*., 2008; Komatsu *et al.,* 2014) and many aspects of ABA (Marella *et al*., 2006; Tougane *et al*., 2010) and auxin (Prigge *et al.*, 2010; Flores-Sandoval *et al*., 2015; Eklund *et al*., 2015; Kato *et al.*, 2015) perception and signaling appear to be conserved between bryophyte gametophytes and the Arabidopsis sporophyte. These findings suggest many developmental mechanisms have originated before the divergence of bryophytes and flowering plants.

1.6. Elaboration of developmental mechanisms during the evolution of vascular plants

While several ancient land plant genetic mechanisms probably first emerged in the haploid gametophyte generation, many of these mechanism have massively elaborated during the evolution of the flowering plant sporophyte body plan. The auxin signaling pathway provides an excellent example. In Arabidopsis, localised auxin synthesis and polar auxin transport give rise to dynamic auxin minimas and maximas that that are crucial for establishing patterns of tissue differentiation during a wide range of processes including lateral root initiation, floral organ development and leaf morphogenesis (Benkova *et al*., 2003). Binding of auxin to the auxin receptor TIR1 triggers degradation of Aux/IAA repressor proteins through the proteosomal pathway (Dharmasiri *et al*., 2005; Kepinski and Leyser, 2005). Degradation of Aux/IAAs releases auxin response factors (ARFs) that function as transcriptional regulators of auxin responsive genes. The Arabidopsis genome

encodes for 6 TIR1/AFBs, 29 Aux/IAAs and 23 ARFs (Vanneste and Friml, 2009). Distinct combinations of TIR1/AFBs, Aux/IAAs and ARFs are thought to respond to different threshold levels of auxin (Villalobos *et al.,* 2012). Furthermore, cell type specific differences in the expression levels of different *Aux/IAA* and *ARF* genes may contribute to the ability of auxin to elicit such a wide range of responses in different developmental contexts (Vanneste and Friml, 2009). In contrast, the liverwort *M. polymorpha* has a single *TIR1*-like gene, a single *Aux/IAA* gene and three *ARF* genes (Flores-Sandoval *et al*., 2015). These findings suggest that while the basic mechanism of auxin signaling is likely to have originated early in the evolution of the land plants, the signaling network has diversified and gained new roles during the evolution of vascular plants.

Post-transcriptional regulation of gene expression by 21-27 bp micro RNAs (miRNAs) is another mechanism that has ancient origins in land plants. The main genetic components of the miRNA biosynthesis pathway, as well as 12 families of miRNAs and their targets are likely to be conserved between bryophytes and angiosperms and therefore are likely to have been present in the common ancestor of the two lineages (Floyd and Bowman, 2004; Jones-Rhoades and Bartel, 2004; Axtell and Bartel, 2005; Axtell *et al*., 2007; Fattash *et al.,* 2007; Willman and Poethig, 2007; Addo-Quaye *et al*., 2009). However, many developmental processes these conserved miRNAs regulate in flowering plants, such as patterning of floral organs and patterning of vascular tissue differentiation in roots, only evolved much later within the vascular plant lineage. These findings indicate that while many of the regulatory interactions between the conserved miRNAs and their targets are

ancient, these genetic components were recruited to carry out novel developmental functions in the lineage leading to flowering plants. Therefore, while on a sequence level the origin of many genes that regulate land plant development can be traced back to the early land plants or their streptophyte algal ancestors transcriptome data (Floyd *et al*., 2006; Rensing *et al*., 2008; Timme and Delwiche, 2010; Sayou *et al.,* 2014; Dolan lab, unpublished data), further functional characterisation of the genes in different plant lineages is required to elucidate when these genes acquired their developmental roles.

Some genetic mechanisms only evolved in the sporophyte generation. For example, Class I *KNOTTED1-LIKE HOMEOBOX* (*KNOX*) genes are required for the maintenance of the Arabidopsis sporophyte indeterminate shoot apical meristem (Long *et al*., 1996; Hay and Tsiantis, 2010). In contrast, Class I *KNOX* genes are not involved in the maintenance of the indeterminate meristems in the haploid leafy gametophore of the moss *P. patens* (Sakakibara *et al*., 2008). Instead, *The P. patens* class I *KNOX* genes regulate spore coat development and the cell division pattern in the sporophyte (Singer and Ashton, 2007; Sakakibara *et al.*, 2008). Therefore, while the class I *KNOX* genes have sporophyte specific functions in both *P. patens* and Arabidopsis, these genes are likely to have acquired their role in meristem maintenance during the elaboration of the sporophyte body plan.

1.7. Evolution of rooting structures

In an aquatic environment plants can take up nutrients directly from the surrounding medium, whereas on land nutrients need to be acquired from the soil. One of the many adaptations that facilitated the transition of plants from water to dry land was the evolution of specialised rooting structures to carry out water and nutrient uptake as well as to anchor the plant on the substrate (Kenrick and Crane, 1997). The rooting structures of the gametophytes of the basal land plants bryophytes consist of tip-growing filamentous cells called rhizoids (Duckett *et al*., 2014). In contrast, the main rooting function of vascular plant sporophytes is carried out by roots, specialised axial organs that only evolved in the sporophyte generation (Raven and Edwards, 2001). In most species of vascular plants tip-growing filaments called root hairs grow as extensions of epidermal cells of the roots. In groups in which both generations are free-living (lycophytes and monilophytes) rhizoids form in the gametophyte, whereas root hairs form on the roots of the sporophyte. Hence a feature common to nearly all land plants is the presence of filamentous tip-growing rooting cells that form most of the interface between the plant and soil, and thus carry out important functions in water and nutrient uptake as well as anchoring the plant to the substrate.

More than 130 genes have been described as being involved in root hair development in the flowering plant Arabidopsis, mostly based on root hair defective mutants identified in mutant screens (Kwasniewski *et al*., 2012). In contrast, only a handful of genes are known to be involved in rhizoid development

in bryophytes almost entirely based on reverse genetic studies in the moss *P. patens.*

1.8. Conserved basic helix-loop-helix transcription factors regulate initiation and elongation of root hairs and rhizoids

The development of root hairs and rhizoids is partially regulated by the same genetic mechanisms. The *ROOT HAIR DEFECTIVE SIX-LIKE* (*RSL*) gene subfamily of basic helix-loop-helix (bHLH) transcription factors have been found to regulate rhizoid development in the haploid stage of the moss *P. patens* and root hair development in the diploid stage of the angiosperm Arabidopsis as well as in other vascular plants (*Oryza sativa, Brachypodium distachyon, Triticum aestivum*) (Menand *et al.*, 2007; Dolan lab unpublished data). The *RSL* transcription factors can be divided into two classes; class I *RSL* genes and class II *RLS* genes (Menand *et al*., 2007; *Yi et al*., 2010). In *A. thaliana*, class I *RSL* genes *RHD6* and *RSL1* are expressed in cells that give rise to root hairs (Masucci and Schiefelbein, 1994; Menand *et al.*, 2007). Class I *RSL* genes directly regulate the expression of the class II *RSL* gene RSL4, which is expressed later in the root hair development and regulates root hair elongation (Fig. 1.2; Yi *et al*., 2010). *P. patens* has two class I and four class II *RSL* genes. The *P. patens* homologues of the Arabidopsis class I *RSL* genes *RHD6* and *RSL1* (*PpRSL1* and *PpRSL2*) are required for the development of the multicellular *P. patens* rhizoids (Menand *et al*., 2007; Jang *et al*., 2011). Furthermore, constitutive over-expression of the two *P. patens* class I *RSL* genes converts most of the developing gametophore tissue into rhizoids, indicating that in moss class I *RSL* gene

expression is sufficient to trigger rhizoid initiation from cells that normally do not give rise to rhizoids (Jang *et al*., 2011). Expression of *PpRSL1* behind a strong constitutive 35S-promoter in the roothairless Arabidopsis *rhd6* mutant background rescues the root hair phenotype of this mutant indicating that the function of the class I RSL proteins is conserved between moss and flowering plants (Menand *et al*., 2007).

Lotus japonicus ROOTHAIRLESS1-LIKE (*LRL*) genes encode for a second subfamily of bHLH transcription factors involved in the regulation of root hair and rhizoid development (Karas *et al.*, 2009; Tam *et al*., 2015). The function of *LRL* genes was first identified in *Lotus japonicus*, in which mutations in a single *LRL* gene *LjRHL1* result in a hairless root phenotype indicating a non-redundant role in root hair initiation (Karas *et al*., 2005). Homologues of the *LRL* genes have also been characterised in rice (*OsRHL1*) and Arabidopsis (*AtLRL1, AtLRL2, AtLRL3*) (Ding *et al*., 2009; Karas *et al*., 2009). The three Arabidopsis *LRL* genes function redundantly to regulate root hair elongation, whereas root hair initiation is not affected (Karas *et al*., 2009; Bruex *et al*., 2012). Each of the three Arabidopsis *LRL* genes can rescue the phenotype of the *LjRHL1* mutant when over-expressed in lotus roots indicating functional conservation between the LRL proteins between these two species (Karas *et al*., 2009). Mutants for the rice *LRL* gene *OsRHL1* possess defects in root hair elongation as well as root epidermal cell patterning (Ding *et al.,* 2009). These findings suggest that the gene regulatory network around the *LRL* genes differs in these three angiosperm species. The moss *P. patens* has two *LRL* genes. Loss-of-function mutant for both of the *P. patens LRL* genes is rhizoidless (Tam *et al*., 2015),

indicating that like the *RSL* genes, *LRL* genes also have a conserved function as positive regulators of filamentous rooting cell development in a wide range of land plants.

Evolution of morphological complexity often occurs by evolution of cis-regulatory regions of genes that regulate development (Stern and Orgogozo, 2008, 2009). Cis-regulatory mutations can alter temporal and spatial expression patterns of developmental genes without compromising the functionality of the protein. In contrast, mutations within coding sequences are more likely to result in pleiotropic effects. Cis-regulatory evolution of *RSL* and *LRL* gene promoters may have resulted in recruitment of the gametophyte filamentous rooting cell module to function in a novel developmental context: on the sporophyte root epidermis.

1.9. Auxin promotes root hair and rhizoid development

The plant hormone auxin promotes the elongation of root hairs and rhizoids in a wide range of land plants including liverworts (Larue and Narayanaswami, 1956; Kaul *et al*., 1962; Maravolo and Voth, 1966; Ishizaki *et al*., 2012), mosses (Sakakibara *et al*., 2003; Fujita *et al*., 2008; Jang *et al*., 2011), ferns (Hickok and Kiriluk, 1984) and flowering plants (Pitts *et al*., 1998). In the moss *P. patens* exogenous auxin treatment enhances rhizoid growth, and is sufficient to induce ectopic rhizoid formation by promoting ectopic expression of the class I *RSL* genes *PpRSL1* and *PpRSL2* (Sakakibara *et al*., 2003; Jang *et al*., 2011). The *P. patens Pprsl1 Pprsl2* double mutant does not show enhanced rhizoid growth in response to auxin, indicating that the class I *RSL* genes are necessary for auxin-induced rhizoid growth

(Jang *et al*., 2011). In contrast, Arabidopsis auxin-induced root hair growth does not require the activity of class I *RSL* gene activity. Instead auxin enhances root hair elongation by up-regulating the transcription of a related class II *RSL* gene *RSL4* (Fig. 1.2; Masucci and Schiefelbein, 1994; Jang *et al*., 2011; Yi *et al*., 2010). This suggests auxin may promote growth of root hairs and rhizoids through modulating the levels of *RSL* gene expression in a wide range of land plants, however auxin is likely to feed into different parts of the network in different groups.

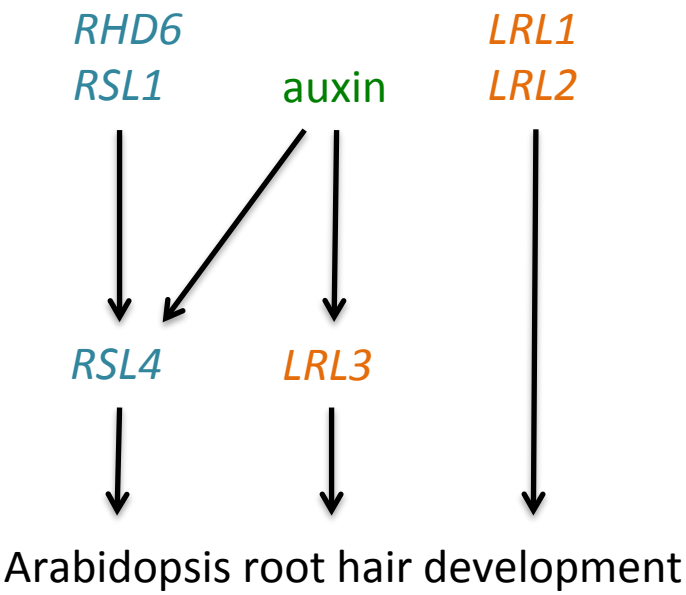

Figure 1.2 Simplified model of the genetic regulatory network for root hair development in Arabidopsis. The plant hormone auxin and basic helix-loop-helix transcription factors encoded by *RSL* genes and *LRL* genes function as positive regulators of Arabidopsis root hair development (Menand *et al*., 2007; Karas *et al*., 2009; Yi *et al*., 2010; Tam *et al*., 2015). Auxin and the class I *RSL* genes *RHD6* and *RSL1* positively regulate the expression of class II *RSL* gene *RSL4* and *LRL3,* which promote root hair development (Yi *et al*., 2010; Tam *et al*., 2015). *LRL1* and *LRL2* act as positive regulators of root hair development independently of the *RSL* genes and auxin (Tam *et al*., 2015)

1.10. Root hairs and rhizoids elongate by tip growth

Both root hairs and rhizoids elongate by tip growth, a mechanism of cell expansion in which growth is restricted to a small area at the apex of the cell (reviewed in Rounds and Bezanilla, 2013). Given that the role of the class I *RSL* genes and *LRL* genes as positive regulators of root hair and rhizoid development is conserved between Arabidopsis and *P. patens*, the function of many genes involved in root hair and rhizoid elongation may also be conserved.

Only a small number of genes associated with the organisation of the actin cytoskeleton have so far been described to be required for cell elongation in both root hairs and rhizoids. Continuous dynamic synthesis and disassembly of actin filaments that make up the actin cytoskeleton is required for appropriate vesicle transport during tip growth (Rounds and Bezanilla, 2013). Loss-of-function mutation in *ACTIN INTERACTING PROTEIN1* (*AIP1*) that promotes actin disassembly resulted in increased stability of actin filaments and reduced elongation of root hairs in Arabidopsis and rhizoids in *P. patens* (Augustine *et al*., 2011). Furthermore, disruption of ARP3A, a component of the actin cytoskeleton modifying Arp2/3 complex, resulted in defective rhizoid development (Finka *et al*., 2008). Phosphatidyl inositol phosphate kinases (PIPKs) are another class of genes required for actin cytoskeleton organisation during tip growth: mutations in PIPK encoding genes result in defective elongation of Arabidopsis root hairs and *P. patens* rhizoids (Kusano *et al*., 2008; Saavedra *et al*., 2011). PIPKs phosphorylate phosphoinositides (PIs): lipid signaling molecules found in cell membranes of eukaryotic cells. Distinct PIPKs phosphorylate the cytosolic myo-inositol head group of PIs at different

positions and therefore regulate the balance between the different forms of PIs. These different forms of PIs are thought have distinct signaling properties. Together these findings suggest that the actin cytoskeleton is important for appropriate cell elongation in both root hairs and rhizoids.

1.11. Patterning of root hairs and rhizoids

Nearly all vascular plants have root hairs, however the patterning of the root hair formation on the root epidermis shows large variation between species (Dittmer, 1940; reviewed in Dolan and Costa, 2001). Three types of root hair patterning have been identified in vascular plants (reviewed in Datta *et al*., 2011). Plants that have type I patterning can form a root hair from any cell of the root epidermis. In type II patterning each longitudinal root epidermal cell file consists of alternating short hair cells and longer non-hair cells. In plants that have type III patterning, such as Arabidopsis, the root epidermis consists of alternating longitudinal hair cell and non-hair cell files.

The molecular mechanisms that regulate root hair patterning in Arabidopsis function upstream of the class I *RSL* genes (Menand *et al*., 2007) and have been studied in great detail (e.g. Lee and Schiefelbein, 2002; Bernhardt *et al*., 2005; Koshino-Kimura *et al*., 2005; Song *et al*., 2011 and references therein). The Arabidopsis root hair patterning mechanism involves a protein complex composed of the basic helix-loop-helix transcription factor GL3, WD40 repeat protein TTG1 and R2R3 Myb protein WER. In non-root hair cells, GL3 activates the expression of

the homeodomain leucine-zipper protein GL2 (Koshino-Kimura *et al*., 2005). GL2 in turn represses the expression of the class I *RSL* gene *RHD6*, therefore repressing root hair formation in non-hair cells (Menand *et al*., 2007). GL3 also activates the expression of small single repeat Myb proteins CPC, TRY and ETC in non-hair cells (Koshino-Kimura *et al*., 2005). CPC, TRY and ETC move to the adjacent hair forming cells, where they inhibit the formation of the GL3-EGL3/TTG1/WER complex (Schellmann *et al*., 2002; Kurata *et al*., 2005). This represses *GL2* expression in hair forming cells, allowing the expression of the class I *RSL* gene RHD6 and therefore leading to root hair initiation (Menand *et al*., 2007). CPC and TRY also activate the expression of GL3 in hair cells, from which GL3 moves to the neighboring non-hair forming cells where it promotes non-hair cell fate (Bernardt *et al*., 2005). Therefore, the Arabidopsis root hair patterning mechanism is based on lateral inhibition in which both the hair cells and non-hair cells signal to the adjacent cells to acquire a different fate.

While the root hair patterning mechanism in Arabidopsis is well characterised, nothing is known about the genetic regulatory networks for root hair patterning in other vascular plants or bryophytes. Based on the phylogenetic distributions of different root hair patterns in seed angiosperms it is likely that the type III root hair patterning observed in Arabidopsis evolved multiple times within angiosperms; whereas type I patterning in which any cell of the root epidermis can differentiate into a root hair cell is considered as the ancestral condition (Clowes, 2000; Dolan and Costa, 2001). Therefore, details of the genetic mechanisms that

control root hair patterning in most vascular plants and rhizoid patterning in bryophytes remain to be discovered.

1.12. The liverwort *M. polymorpha* as a model organisms for studying the evolution of filamentous rooting cells

The liverwort *M. polymorpha* is emerging as a new bryophyte model species for studying the evolution of plant development. Unlike the bryophyte model species moss *P. patens*, *M. polymorpha* can be easily transformed by *Agrobacterium tumefaciens* during the haploid phase of its life-cycle, which allows powerful forward genetic screens to be carried out (Ishizaki *et al.*, 2008). *M. polymorpha* has a relatively short generation time, can easily be crossed, and can be propagated asexually from fragments, which makes analysing and maintaining the mutant lines convenient. In addition, homologous recombination has been successful in *M. polymorpha* (Ishizaki *et al*., 2013). These features of *M. polymorpha* make it a tractable bryophyte model genetic system.

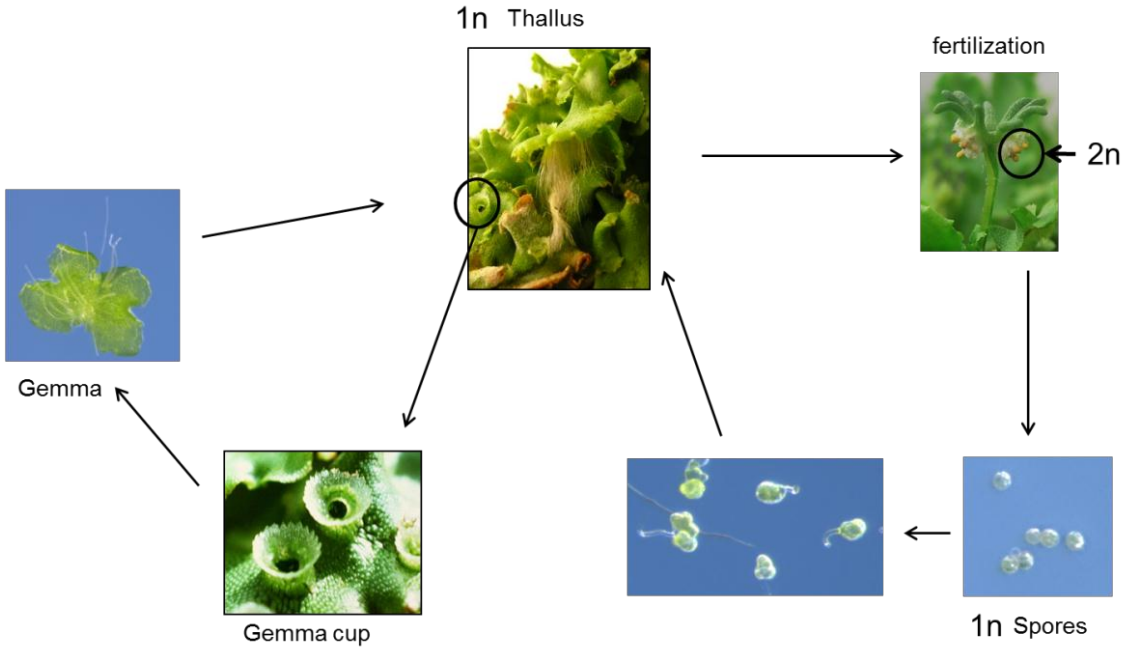

Figure 1.3 The life-cycle of the liverwort *M. polymorpha.* The mature haploid *M. polymorpha* gametophyte thallus develops either male or female reproductive structures, which produce the male and female gametes, respectively. After fertilisation the diploid sporophytes develop attached to the female reproductive structures. Each sporophyte consists of a short stalk and a sac-like sporangium that encloses the haploid spores, which after being released give rise to the next gametophyte generation. *M. polymorpha* gametophytes also undergo asexual reproduction by producing reproductive propagules called gemmae in gemma cups that form on the upper dorsal side the mature thallus.

The *M. polymorpha* life-cycle is illustrated in figure 1.3. In liverworts, rhizoids form during the dominant haploid gametophyte phase of the life-cycle, whereas the simple diploid sporophyte consists of a seta with a terminal sac-like sporangium enclosing the haploid spores. After being released from the sporangium the spores germinate and form a dorsiventral thallus. The first rhizoid emerges from a germinating spore before or soon after the first cell division (O'Hanlon, 1926).

Further rhizoids form at the base of the sporeling during later development and penetrate the growth substrate. *M. polymorpha* also reproduces asexually by fragmentation or production of asexual propagules called gemmae in cup-like structures on the dorsal side of the gametophyte thallus. Disc-shaped gemmae produce rhizoids on both sides soon after being dispersed from gemma cups prior to establishment of the dorsal-ventral axis, whereas in mature *M. polymorpha* rhizoid formation becomes restricted to the ventral side of the thallus (Taren, 1958; Ishizaki *et al*., 2012).

Mature *M. polymorpha* forms two types of rhizoids; smooth-walled rhizoids and tuberculate rhizoids that have peg-like inward protrusions of the cell walls, whereas juvenile stages (gemmae and young spores) only produce smooth rhizoids (McConaha, 1941; Duckett *et al*., 2014). Nearly all liverwort species have smooth rhizoids. In contrast, tuberculate rhizoids are only present in a subset of lineages and have been suggested to have evolved from smooth rhizoids (Duckett *et al*., 2014). Both smooth and tuberculate rhizoids are unicellular and grow as extensions of epidermal cells of the ventral thallus. The smooth rhizoids of a mature plant function in anchorage. They extend from rhizoid precursor cells in the ventral epidermis and are arranged in short longitudinal rows on both sides of the thallus midrib adjacent to scales that extend over the midrib. The rhizoid precursor cells are separated by non-rhizoid precursor cells, which undergo further divisions without enlargement resulting in regular spacing of larger rhizoid precursor cells surrounded by small non-rhizoid precursor cells (Voth and Hamner, 1940). The smooth rhizoids begin to elongate from the rhizoid precursor cells at a distance of

approximately 20 cells from the thallus apical cell (Voth and Hamner, 1940). Tuberculate rhizoids show more scattered initiation pattern, but similarly to smooth rhizoids they are initiated from epidermal cells of the ventral thallus. The tuberculate rhizoids grow along the ventral surface of the thallus forming lateral bundles towards the midrib (McConaha, 1941; Duckett *et al*., 2014). Smooth rhizoids can grow up to 30 mm long, whereas tuberculate rhizoids only grow to about 8 mm (Duckett *et al.,* 2014).

The lack of efficient internal water conductive system as well as presence of air chambers on the dorsal thallus makes liverworts particularly prone to desiccation (McConaha, 1941). Liverwort rhizoids have been shown to have the capability to transport water through capillary action, and therefore rhizoids have been suggested to play an important role in water uptake (McConaha, 1939, 1941; Duckett *et al.,* 2014). In contrast, the role of rhizoids in nutrient uptake in liverworts has not been demonstrated. However, the rhizoids do increase the surface area in contact with the substrate, which may facilitate nutrient uptake, and they are involved in forming associations with mycorrhizal fungi (Pocock and Duckett, 1985; Duckett *et al.*, 1991; Russel and Bulman, 2004; Duckett *et al*., 2014). These fungal associations may have played a crucial role in the colonisation of land by plants (Humphreys *et al.,* 2010).

The aim of the study described in this thesis was to identify genes that regulate the development of rhizoids in the early diverging group of land plants liverworts, using the liverwort *M. polymorpha* as a model organism. Elucidating the genetic mechanisms that control rhizoid formation in liverworts, such as *M.*

polymorpha, will allow us to estimate to which extent the development of rhizoids and root hairs is controlled by similar genes. This knowledge can then be used to identify which aspects of the gene regulatory network for the development of filamentous rooting cells, rhizoids and root hairs, are likely to have been present in the last common ancestor of land plants before the bryophyte and vascular plant lineages diverged more than 443 Mya (Steemans *et al*., 2009).

Chapter 2

Materials and Methods

Primer sequences and PCR cycling conditions are provided in the materials and methods appendix.

2.1. Plant material and bacterial strains

Male and female *M. polymorpha* accessions Tagaragaike-1 (Tak-1, male) and Tagaragaike-2 (Tak-2, female), kindly provided by K. Ishizaki (Kobe University, Japan), were used as wild type. *Agrobacterium tumefaciens* line GV3101 containing the helper plasmid pMP90 (Hellens *et al.,* 2000) was used in all plant transformations. *E. coli* strain XL-1 Blue was used in cloning.

2.2. Plant growth conditions

M. polymorpha was grown on sterile plates containing modified Johnson's medium (Johnson *et al*., 1957; 6 Mm KNO_3, 1 Mm $MgSO_4$, 4 Mm $Ca(NO_3)_2.4H_2O$, 25 µM KCl, 10 µM H_3BO_4, 1 µM $MnSO_4.4H_2O$, 1 µM $ZnSO_4.7H_2O$, 250 nM $CuSO_4.5H_2O$, 250 nM $(NH_4)_6Mo_7O_{24}.4H_2O$, 25 µM $FeSO_4.7H_2O$, 25 µM Na_2EDTA, 0.6 mM $NH_4H_2PO_4^{3-}$, 0.4 mM $(NH_4)_2SO_4$, 55.5 mM inositol, 0.533 g/l (w/v) MES) supplemented with 1 % (w/v) sucrose and 1.4 % (w/v) agar (Sigma cat#A9799), pH adjusted to 5.6. The amount of agar in the medium was reduced to 1 % (w/v) when plants were grown for RNA extraction to avoid damaging the rhizoids when detaching plants from the agar. The plates were placed horizontally in a Sanyo growth cabinet at 23 °C under constant white light illumination at intensity of 56 $\mu E.m^{-2}.s^{-1}$. For crossing plants were grown in a growth room at 23 °C under 16 hours light:8 hours dark photoperiod on 1:3 mixture of vermiculite and John Innes No. 2

compost. Sexual reproduction was induced by far-red light irradiation as described in Chiyoda *et al.,* 2008.

2.3. Plant transformation

Haploid *M. polymorpha* spores obtained from a cross between the wild type lines Tak-1 and Tak-2 were transformed as described in Ishizaki *et al*., 2008 by co-cultivation with Agrobacterium GV3101 containing a T-DNA transformation vector. Wild type spores contained in intact sporangia were collected, sterilised in 0.1 % (w/v) sodium dichloroisocyanurate (Sigma cat#218928) solution for 2 minutes and rinsed three times with sterile distilled water. The sporangia were crushed to release the spores before adding the spore solution to 25 ml of liquid M51C medium (Ono *et al*., 1979; 19.8 µM KNO_3, 5 µM NH_4NO_3, 1.5 µM $MgSO_4$, 2 µM $CaCl_2$, 2 µM KH_2PO_4, 110 nM EDTA-Fe(III), 1 µM Na_2MoO_4, 100 nM $CuSO_4$, 100 nM $CoCl_2$, 7 µM $ZnSO_4$, 40 µM $MnSO_4$, 49 µM H_3BO_3, 555 µM myo-inositol, 8 µM nicotinic acid, 5 µM pyridoxine hydrochloride, 30 µM thiamine hydrochloride, 2 mM L-glutamine, 0.1% w/v casein hydrolysate, 2 % w/v sucrose, pH 5.8) in a sterile Erlenmeyer flask. The liquid spore cultures were germinated in a growth cabinet at 23 °C under constant light intensity of 56 $\mu E.m^{-2}.s^{-1}$ for 6-7 days before transformation of sporelings by co-cultivation with agrobacterium for 1-2 days. After the transformation the sporelings were collected on a sterile 40 µm nylon mesh cell strainer (Fisher Scientific cat#22363547) and rinsed with 100 ml sterile distilled water. The sporelings were plated on antibiotic selection plates containing Johnson's medium with 10 mg/l hygromycin or 100 mg/l gentamycin to select for

plants with a T-DNA insertion, and 100 mg/l cefotaxime to kill the remaining Agrobacterium. After 10-14 days the antibiotic resistant transformant sporelings were clearly distinguishable and could be transferred from the selection plates to 12x12 cm square plates to be grown in uniform spacing. The transformant plants were grown on the square plates another 14 days before further analysis.

2.4. Isolation of mutants defective in rhizoid development

M. polymorpha plants transformed with the Agrobacterium containing the T-DNA transformation vector were screened for defective rhizoid phenotypes at the age of 1 month, and again about 2 weeks later. The workflow through the mutant screen is presented in figure 2.1. After the initial hygromycin selection the hygromycin resistant transformant plants were transferred on 12x12 cm square plates placing 8 plants in 7 rows, i.e. each plate containing 56 plants. The first round of screening was carried out after 14 days of growth on the square plates. During the first round of screening all plants considered to have a defective rhizoid phenotype were transferred to a fresh square plate, placing 12 plants on each plate. The second round of screening, in which the rhizoid defect was re-assessed, was carried out two weeks later to reduce the number of plants carried forward to further analysis and crossing with wild type.

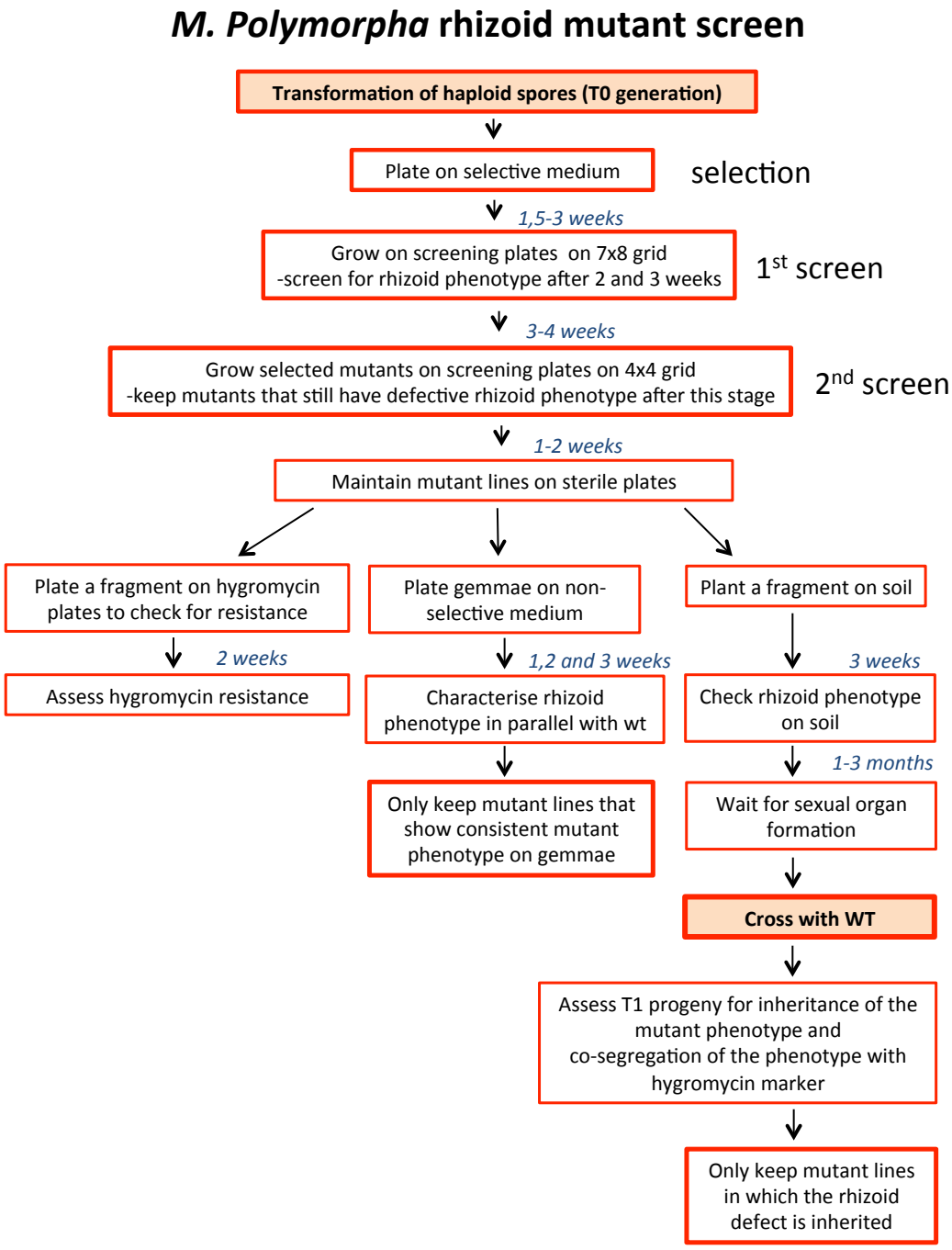

Figure 2.1 Workflow in the mutant screen to obtain a collection of *M. polymorpha* mutants with defective rhizoid phenotypes. Two rounds of screening were carried out, after which mutants with altered rhizoid phenotypes were assessed for hygromycin-resistance and rhizoid phenotype in gemmae. A fragment of each rhizoid mutant with a consistently altered phenotype was planted on soil for subsequent crossing with wild type. The T1 generation obtained was checked for inheritance of the mutant rhizoid phenotype as well as co-segregation of the mutant phenotype with the hygromycin-resistance marker.

2.5. Analysis of co-segregation and T-DNA copy number

The potential rhizoid defective mutants identified were crossed with a wild type plant of the opposite sex (Tak-1 or Tak-2). The resulting F1 spores were collected, sterilized and germinated on a petri dish for 14 days, after which approximately 224 F1 spores for each mutant line were moved on square plates placing 56 plants on each plate. After 2 weeks of growth on the square plates the F1 was assessed for inheritance of the rhizoid defective phenotype. If the defective rhizoid phenotype was inherited, the number of plants showing wild type and mutant phenotype was scored. A fragment of each F1 plant was then transferred on a plate containing 10 mg/l hygromycin and grown for 10 days before scoring the number and phenotype of hygromycin resistant plants to estimate the T-DNA insert number, and the mutant phenotype co-segregation with the hygromycin resistance marker. If the ratio of hygromycin resistant to hygromycin sensitive plants did not significantly differ from 1:1 ratio, the mutant line was concluded to have a single T-DNA insertion. If all hygromycin resistant plants showed the mutant phenotype and no hygromycin sensitive mutants were found, i.e. the defective mutant phenotype co-segregates with the hygromycin resistance marker, the rhizoid defect of the mutant was considered to have resulted from an insertion of an intact T-DNA into the gene responsible for the mutant phenotype. Rhizoid defective T-DNA mutant lines, in which the hygromycin resistance marker on the T-DNA co-segregated with the rhizoid defect after more than 100 F1 plants showing mutant phenotype had been assessed, were selected for identification of the T-DNA insertion site using TAIL-PCR (thermal asymmetric interlaced PCR). In addition, the T-DNA insertion site

was identified for mutants that were not successfully crossed by carrying out TAIL-PCR on the original mutant plant without crossing and co-segregation analysis.

2.6. Constructs

T-DNA mutagenesis

Agrobacterium transformed with the binary vector pCambia 1300 (http://www.cambia.org/daisy/bioforge_legacy/3726.html) was used to generate the *M. polymorpha* T-DNA insertion lines for the rhizoid mutant screen. The pCambia 1300 vector T-DNA sequence contains a gene for the plant antibiotic selection marker hygromycin driven by the Cauliflower mosaic virus 35S-promoter.

Over-expression constructs

MpFRH1 transcript sequence and *MpIRE* coding sequence were amplified from wild type cDNA using Phusion High-Fidelity DNA Polymerase (New England Biolabs cat#M0530L) in combination with gene specific primers. The resulting PCR product was recombined into the pCR8/GW/TOPO Gateway entry vector (Invitrogen cat#K2500-20). Gateway entry vectors containing the *MpFRH1* transcript variants were synthesised by Life Technologies GeneArt sequence synthesis service. To create over-expression vectors for plant transformation, LR reaction was carried out between a pCambia1300 based Gateway destination vector in which the expression of the gene at the Gateway site is driven by the OsActin promoter, and the Gateway entry vectors mentioned above.

Promoter-reporter constructs

The *MpFRH1* transcription start site was estimated based on Softberry TSSP promoter prediction (Solovyev & Shahmuradov, 2003). *MpFRH1* 3.5 kb promoter fragment including a predicted TATA box and 3.5 kb upstream sequence was amplified from wild type DNA using Phusion High-Fidelity DNA Polymerase (New England Biolabs cat#M0530L) in combination with gene specific primers. The resulting PCR fragment was cloned between *EcoRI* and *KpnI* restriction enzyme sites on HBp056; a pCambia1300 based plasmid containing 3x yellow fluorescent protein (YFP) fused to nuclear localisation signal sequence (NLS). The *proFRH1-3xYFP-NLS* fragment was then amplified using primers on the plasmid backbone, and cloned into pGEM-T Vector (Promega cat#A3600). The *ProFRH1-3xYFP-NLS* fragment was digested out of the pGEM-T Vector using *EcoRI* and cloned into the *EcoRI* site of pCambia1300.

To create a *MpIRE* promoter construct a 3.5 kb fragment upstream of the predicted coding sequence was amplified from wild type DNA using Phusion High-Fidelity DNA Polymerase (New England Biolabs cat#M0530L) in combination with gene specific primers containing 16 bp extensions complementary to the HBp187 plasmid. The *MpIRE* promoter fragment was recombined into *PmeI* site of HBp187 using In-Fusion HD Cloning Kit (Clontech cat#638910) following the manufacturer's protocol. On the resulting plasmid, a Gateway cassette was ligated behind the *MpIRE* promoter using Gateway Vector Conversion System (Life Technologies cat#11828-029). To make *proIRE::YFP-3xYFP-NLS* construct LR reaction was carried out between the HBp187 containing *proIRE-GW* and a HBp056 containing *3xYFP-*

NLS. To create a *proIRE::IRE* construct LR reaction was carried out between the HBp187 containing *proIRE-GW* and the *pCR8::IRE* construct described above.

2.7. DNA extraction

A 1x1 cm^2 thallus fragment was flash frozen in liquid nitrogen and ground using mortar and pestle. The resulting tissue powder was resuspended in 500 µl DNA extraction buffer (100 mM Tris-HCL pH 8, 1.4 M NaCl, 20 mM EDTA pH8, 2 % (w/v) CTAB) and incubated at room temperature for 15 minutes. DNA was then extracted twice using 250 µl phenol-chloroform-isoamyl alcohol (25:24:1) after which the DNA containing aqueous phase was collected. DNA was precipitated by adding 1 volume (500 µl) isopropanol followed by 10 minute centrifugation at 17,000 g. The resulting pellet was rinsed with 70 % EtOH, air dried and resuspended in 100 µl distilled H_2O.

2.8. Thermal asymmetric interlaced PCR (TAIL-PCR)

TAIL-PCR was carried out using MangoTaq DNA polymerase (Bioline cat#21078) with a set of nested primers for the left and right borders of the T-DNA (LB1 to LB3 and RB1 to RB3) in combination with six different random degenerate primers (AD1-6). For TAIL-PCR cycling conditions and primer sequences see the appendix 1. The resulting PCR products were gel purified using the QIAquick Gel Extraction Kit (Qiagen cat#28706) and sequenced from at Source BioSciences, Oxford. The T-DNA flanking genomic sequences were identified by aligning the TAIL-PCR product sequences against the *M. polymorpha* genome sequence (Dolan Lab,

unpublished) using the Basic Local Alignment Search tool (BLAST). The T-DNA insertion sites were verified by PCR with a genome specific primer designed 100-400 bp away from the predicted T-DNA insertion border in combination with one of the T-DNA border primers.

2.9. RNA extraction, cDNA synthesis and quantitative RT-PCR

RNA extraction

Total RNA was extracted from wild type and mutant *M. polymorpha* gemmae grown on agar plates for 15 days. Three biological replicate samples were prepared for each genotype. The tissue was flash frozen in liquid nitrogen and ground using mortar and pestle. The frozen homogenised tissue was carefully mixed with 700 µl TRIzol Reagent (Life Technologies cat#15596-018), incubated at 56 °C for 10 minutes and then spin down in a microcentrifuge at 17,000 g for 2 minutes. The supernatant was collected, and the subsequent steps of RNA extraction were carried out using the Direct-zol RNA miniprep kit (Zymo Research cat#2052) following the manufacturer's protocol. The amount of RNA was quantified using NanoDrop spectrophotometer (Thermo Fisher Scientific, USA). Based on the quantification all samples were diluted to the same concentration prior to DNAse treatment. The DNAse treatment was performed using the Turbo DNA-free kit (Life Technologies cat#AM2239). RNA integrity was verified by running an aliquot of each DNAse treated RNA sample on a 2 % (w/v) agarose gel stained with ethidium bromide.

cDNA synthesis and qRT-PCR

One µg of total RNA was used for cDNA synthesis. cDNA synthesis was carried out in a 20 µl reaction using Protoscript II reverse transcriptase (New England Biolabs cat#M0368) and oligo(dT) in the presence of Murin RNase inhibitor (New England Biolabs cat#M0314) according to the manufacturers protocol. For quantitative RT-PCR each cDNA sample was diluted 1:7. qRT-PCT was performed in the Applied Biosystems 7300 Real-Time PCR System (Life Technologies) with SensiMix SYBR Hi-ROX Kit (Bioline cat#QT605-05). Each biological replicate sample was run in three technical replicates.

qRT-PCR data analysis

qPCR data was first analysed using LinRegPCR v2012.0 (Ruijter *et al.*, 2009). LinRegPCR identifies the exponential part of the amplification curve and defines amplification efficiency individually for each technical replicate, after which it calculates the mean amplication efficiency for each primer pair. Based on this information, LinRegPCR then estimates the initial amount of template (N_0) in each technical replicate. Average N_0 values of the technical replicates were calculated for each biological replicate sample. The average N_0 for each biological replicate was then divided by the average reference gene N_0 of the sample. *MpAPT* and *MpCUL* were selected as reference genes based on *M. polymorpha* qPCR reference gene analysis (Saint-Marcoux *et al.*, 2015).

2.10. Rapid amplification of cDNA ends (RACE) PCR

To obtain the full-length *MpFRH1* transcript RACE-PCR was carried out using 5'/3' RACE Kit (Roche cat#03353621001) following the manufacturer's instructions. The RACE-PCR was performed using 1 µg of wild type RNA as template. The RNA used as a template for RACE-PCR was extracted and DNAse treated as for qRT-PCR.

2.11. Small RNA enriched RNA extraction and Stem-loop PCR

Wild type and mutant *M. polymorpha* gemmae were grown on agar plates for 15 days before harvesting the tissue. Small RNA enriched RNA preparations for stem-loop PCR were prepared using mirVana miRNA isolation kit (Life Technologies cat#AM1560) following the manufacturer's protocol. RNA concentration was estimated using NanoDrop spectrophotometer (Thermo Fisher Scientific, USA). All samples were diluted to 80 ng/µl, and DNAse treated using Turbo DNA-free kit (Life Technologies cat#AM2239). To verify the MpFRH1 miRNA, Stem-loop PCR was carried out as described in Varkonyi-Gasic *et al.*, 2007. First a MpFRH1 miRNA specific reverse transcription step was performed using Protoscript II reverse transcriptase (New England Biolabs cat#M0368) in the presence of Murin RNAse inhibitor (New England Biolabs cat#M0314) in a 20 µl reaction containing 320 ng small RNA enriched RNA and 1 µl of 1 µM MpFRH1 specific stem-loop primer. Subsequent PCR amplification of 2 µl reverse transcribed MpFRH1 miRNA was performed using PCRBIO Ultra Polymerase (PCR Biosystems cat#PB10.32-01) with MpFRH1 miRNA specific forward primer and a universal reverse primer. Resulting

amplification products were visualised on a 2 % agarose gel containing ethidium bromide.

2.12. Microscopy and image analysis

Light microscopy

Plants were imaged using a Leica DFC310 FX camera connected to a Leica M165 FC stereomicroscope. The rhizoid defects of the *M. polymorpha* mutant lines isolated in the screen were assessed by imaging gemmae from each mutant grown on plates containing Johnson's medium with 0.7 % Phytagel (Sigma cat#P8169) at 0, 2 and 10 days after plating. The mutants were classified into phenotypic groups based on their rhizoid phenotype in 10 day old gemmae.

Confocal microscopy

Confocal laser scanning microscopy was carried out with the Zeiss LSM510 Meta microscope using the Zeiss Plan-Neofluar 25x/0.8 water immersion lens with Argon/2 laser excitation at 488 nm in order to observe fluorescence emitted by YFP and chlorophyll at 505-550 nm and 645-710 nm, respectively. Fluorescence images were constructed by making maximum intensity projections from a Z-stack containing the epidermal cell layer of gemmae.

Image processing

All image processing was carried out using Fiji (Schindelin *et al*., 2012) and/or Adobe Photoshop CS4.

2.13. Sequence retrieval, alignment and phylogeny construction

All *M. polymorpha* transcript sequences were retrieved from a *M. polymorpha* transcriptome prepared by S. Kelly, H. Proust, G. Morieri, S. Hetherington and C. Champion. The transcriptome was previously assembled combining sequencing reads obtained from RNA extracted from 0 and 1 day old gemmae, dorsal thallus, rhizoids and thallus meristematic region. The genomic DNA sequences were obtained from *M. polymorpha* genome sequence generated by S. Kelly, H. Proust, G. Morieri, S. Hetherington and C. Champion.

The amino acid sequence for the proteins encoded by the putative rhizoid developmental genes identified in the mutant screen was estimated by first identifying the conserved domains on each transcript by using BLASTX in NCBI. The longest open reading frame that contained conserved domains was assumed to contain the coding sequence for the gene. The protein sequence from this ORF was then used as a query in NCBI BLASTP. Based on similarity of the predicted protein with orthologous proteins from other plants it was estimated whether the ORF on the transcript was likely to be complete.

Predicted orthologs for each rhizoid development gene were identified using OrthoFinder (Emms and Kelly, 2015) query for *V. carteri*, *C. reinhardtii*, *M.*

polymorpha, *P. patens*, *S. Kraussiana* and *A. thaliana* predicted proteins. Sequence alignment between each of the *M. polymorpha* rhizoid development genes and their predicted Arabidopsis orthologs identified by OrthoFinder was carried out using L-INS-i method in MAFFT version 7 (Katoh and Stanley, 2013). The sequence alignments were trimmed in BioEdit7.2.5 (Ibis Biosciences, USA) to remove the non-conserved poorly aligned regions, after which Maximum likelihood trees were constructed using PhyML 3.0 (Guindon *et al*., 2010). The resulting trees were visualised using MEGA6 (Tamura *et al*., 2013).

Chapter 3

Genetic screen for *M. polymorpha* mutants defective in rhizoid development

3.1. Summary

In the early diverging groups of land plants (bryophytes) the entire rooting system of the plant consists of rhizoids: tip growing filamentous rooting cells that are morphologically similar to root hairs of vascular plants. However, it is not known to which extent the development of rhizoids and root hairs is controlled by similar genes. Here, I describe a forward genetic screen performed to identify genes involved in rhizoid development in the bryophyte model species liverwort *Marchantia polymorpha*. *Agrobacterium*-mediated T-DNA transformation of haploid *M. polymorpha* spores was carried out to generate 150,000 *M. polymorpha* T-DNA insertion lines. Visual screening of these lines resulted in identification of 204 rhizoid defective mutants. Further analysis of the mutant lines has so far identified 25 genes required for rhizoid development. Most of these genes are predicted to function in processes also required for root hair elongation, such as cell wall synthesis and endocytic vesicle transport. For 11 of the 25 genes, mutations in similar Arabidopsis genes have been described to result in root hair defects. Therefore, many similar genes control the development of root hairs and rhizoids, suggesting that these genes are likely to have been part of a genetic network that functioned in the development of tip-growing cells in the common ancestor of liverworts and vascular plants.

3.2. Introduction

Rhizoids are filamentous tip-growing cells that constitute the entire rooting system of haploid free-living gametophytes of bryophytes. Root hairs are filametous tip-growing cells that form as extensions of epidermal cells on the axial roots in the diploid sporophyte generation of vascular plants (Raven and Edwards, 2001). Rhizoids and root hairs are morphologically similar, and carry out similar roles in nutrient and water uptake and anchorage. The basic helix-loop-helix transcription factors encoded by the class I *RSL* genes and *LRL* genes were first identified as positive regulators of root hair development in Arabidopsis (Masucci and Schiefelbein, 1994; Karas *et al*., 2009). Reverse genetic studies indicated that these genes also positively regulate the development of rhizoids in the moss *P. patens* (Menand *et al*., 2007; Tam *et al*., 2015). Therefore, the role of class I *RSL* genes and *LRL* genes as positive regulators of filamentous rooting cell development is conserved between bryophytes and flowering plants. This raises the question to what extent are the gene regulatory networks for root hair and rhizoid development conserved? Furthermore, identifying the conserved aspects of the gene regulatory network for filamentous rooting cell development allows us to identify which aspects of this network were likely to have been present in the last common ancestor of land plants before the bryophyte and vascular plant lineages diverged more than 443 Mya (Steemans *et al*., 2009).

Root hairs are a model system to study polarised cell expansion by tip growth in plants. The vast majority of the more than 130 genes that have been implicated in root hair development were first identified based on root hair

defective Arabidopsis mutants isolated in mutant screens (Kwasniewski *et al*., 2012). Further characterisation of these genes has resulted in great advances in understanding of many cellular processes required for root hair elongation (Reviewed in Datta *et al*., 2011). Root hairs have a cellular organisation characteristic of tip growing cells. The nucleus migrates into the elongating root hair during the early stages of root hair elongation (Galway *et al*., 1997). Most of the elongating root hair becomes occupied by a large central vacuole, while the apical region of the hair cell is highly enriched in vesicles (Galway *et al*., 1997). These vesicles continuously transport newly synthesised cell wall and plasma membrane components to the apex of the elongating cell through the exocytic vesicle transport pathway, while excess materials are recycled back through the endocytic vesicle transport pathway (Brandizzi and Wasteneys, 2013). The actin cytoskeleton is required for vesicle transport during root hair elongation. Consequently, disruption of the actin cytoskeleton dynamics results in cessation of tip growth (Rounds and Bezanilla, 2013). In contrast, treatment with drugs that interfere with microtubule stability results in curly root hairs without affecting the rate of elongation (Bibikova *et al*., 1999). Therefore, the microtubule component of the cytoskeleton is thought to be involved in defining the direction of cell elongation in root hairs but is not likely to be required for elongation in itself. Cell expansion at the tip of root hairs results from a balance between cell wall loosening and thickening, which is regulated by both cytosolic and apoplastic signalling molecules. In the cytosol, reactive oxygen species (ROS) produced by NADPH oxidase AtRHD2/AtRbohC activate Ca^{2+} influx at the apex, which in turn enhances exocytic vesicle transport and therefore promotes cell wall thickening (Foreman *et al.*, 2003).

In contrast, proton efflux at the apex of the tip of growing root hair results in local acidification of the extracellular space, which is thought to promote cell wall loosening (Monshausen *et al*., 2007). Alternating oscillations of ROS, Ca^{2+} and pH observed at the apex of elongating root hairs are thought to result in periodical cell wall thickening and loosening and therefore periodical oscillation in the rate of cell elongation (Monshausen *et al*., 2007). Arabidopsis root hairs and liverwort rhizoids are morphologically similar. Therefore, rhizoid elongation may also require genes associated with the processes described above.

Forward genetic studies, in which mutagenesis is carried out to isolate a collection of mutants defective in a particular process, offer a powerful method for identifying the genes involved in that process. Unlike reverse genetic studies, forward genetic screens are not biased by previous knowledge of factors involved. However, identifying the genes defective in the mutants isolated requires available genome sequence for the organism studied. So far, the only established bryophyte model species with a high quality, publicly available genome sequence is the moss *Physcomitrella patens* (Rensing *et al.,* 2008). Mutant screens in *P. patens* are complicated due to the difficulty of making genetic crosses, and due to a recent genome duplication that results in high levels of functional redundancy and makes it difficult to isolate loss-of-function mutants (Rensing *et al*., 2007). The liverwort *M. polymorpha* is emerging as a new bryophyte model species due to the availability of protocols for *Agrobacterium*-mediated T-DNA transformation of the dominant haploid stage of its life-cycle, the feasibility of its propagation and crossing, and the relatively small size of its genome (Ishizaki *et al*., 2008; Dolan lab, unpublished

data). Furthermore, the *M. polymorpha* genome has low levels of genetic redundancy; genes that are represented by large gene families in Arabidopsis are commonly present as single-copy genes in *M. polymorpha* (Dolan lab, unpublished data). Genome and transcriptome sequence data for *M. polymorpha* have been generated at our department (S. Kelly, H. Proust, G. Morieri, S. Hetherington, C. Champion, unpublished) and were available for use in this project.

This chapter describes a forward genetic screen carried out to identify components of the genetic network that regulates rhizoid development in the liverwort *M. polymorpha*. 150,000 *M. polymorpha* T-DNA insertion lines were generated using *Agrobacterium*-mediated T-DNA transformation and screened to isolate a collection of mutants defective in rhizoid development. Genes responsible for the defective rhizoid phenotypes in these mutant lines were identified using TAIL-PCR (thermal asymmetric interlaced PCR). Identification of the genes involved in rhizoid development in *M. polymorpha* revealed genes with characterised roles in root hair development in vascular plants, as well as novel regulators of filamentous rooting cell development.

3.3. Results and discussion

3.3.1. Screening of 150,000 *M. polymorpha* T-DNA insertion lines resulted in identification of 204 rhizoid defective mutants

M. polymorpha T-DNA insertion lines generated using *Agrobacterium*-mediated T-DNA transformation of haploid *M. polymorpha* sporelings were screened to isolate a collection of mutants defective in rhizoid development. A summary of the screen is presented in table 3.1. In total, 204 potential rhizoid defective mutants were isolated after generating and screening 150,000 *M. polymorpha* T-DNA insertion lines.

Table 3.1 Summary of the rhizoid mutant screen.

Summary of the mutant screen	
T-DNA insertion lines screened	150,000
potential rhizoid mutants isolated	204
backcrossed mutants	140
inherited mutation	120
T-DNA tagged backcrossed mutants	47
Total tagged mutants identified*	59

*mutant phenotype and hygromycin resistance gene co-segregate after backcrossing with wild type or multiple mutant alleles identified.

Overall, approximately 0.14 % of the T-DNA insertion lines screened had defects in rhizoid development. The frequency of different rhizoid defects observed is presented in figure 3.1. The most common type of rhizoid defect identified was short rhizoids (64.7 % of the mutants), while mutants with very short rhizoids formed the second most abundant group (17.2 %). Curly rhizoids were observed in

6.4 % of the mutants. Rhizoid development can be divided into two distinct stages; i) differentiation of epidermal cells into rhizoid precursor cells and ii) elongation of the rhizoid by tip growth. Mutants in all phenotype categories listed above have altered size or shape of rhizoids, and therefore are likely to be defective in the elongation stage. Mutants defective in rhizoid precursor cell differentiation, i.e. those mutants in which the number of rhizoids was altered, were relatively rare; 5.9 % of the mutants isolated had fewer rhizoids, while 5.3 % had more rhizoids compared to wild type. In total 11.2 % of the 204 mutants isolated were likely to be affected in genes involved in rhizoid precursor cell fate determination.

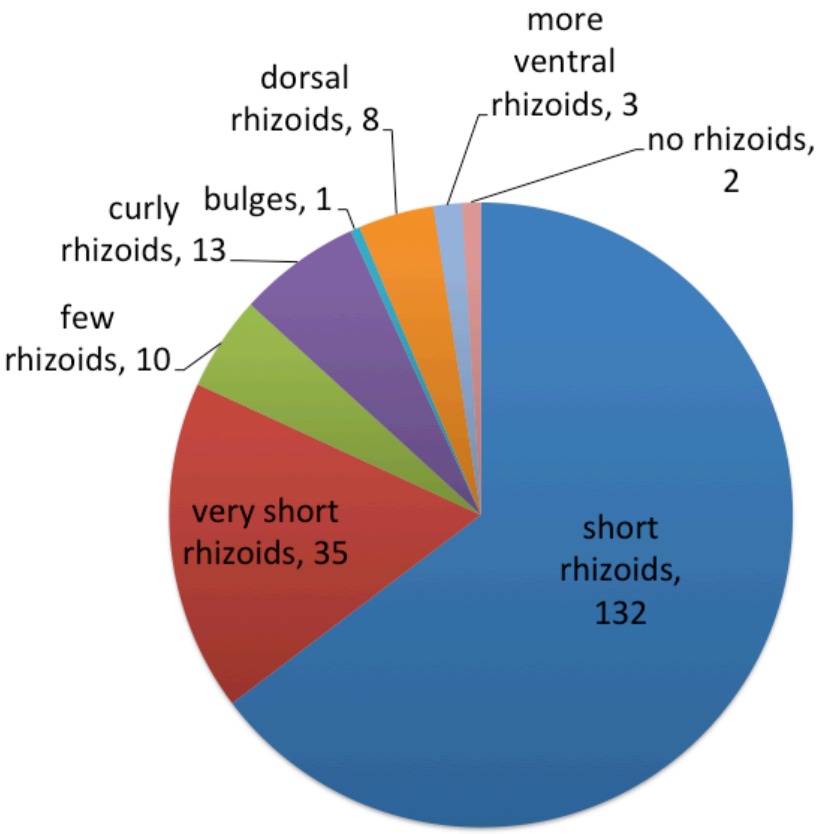

Figure 3.1 The frequency of different rhizoid defects in the screen for rhizoid defective *M. polymorpha* mutants. The number of mutant lines isolated for each phenotype category is shown. The total number of rhizoid defective mutants isolated was 204.

Inheritance of the rhizoid defective phenotype

The T-DNA lines isolated in the initial screen were backcrossed with wild type *M. polymorpha* in order to assess the inheritance of the mutant phenotype. Altogether 140 (68.6 %) of total potential rhizoid defective mutants were successfully backcrossed with wild type. Of the crossed mutant lines 120 (85.7 %) showed inheritance of the rhizoid defect in the F1 generation, verifying the rhizoid defect of the original mutant resulted from a change in the DNA sequence of the plant and could be passed on to the next generation.

Co-segregation analysis

The process of generating plant T-DNA insertion lines using *Agrobacterium*-mediated T-DNA transformation commonly induces mutations other than those caused by an insertion of an intact T-DNA sequence into the plant genome. In the lines in which the mutant rhizoid defect is caused by an insertion of an intact T-DNA into the plant genome, the rhizoid defect of the mutant will co-segregate with the hygromycin resistance marker on the T-DNA in the F1 generation after crossing the mutant with wild type. In contrast, if the mutant defect is not caused by an intact T-DNA insertion, then the hygromycin resistance gene on the T-DNA will segregate independently of the gene responsible for the mutant phenotype. The location of intact T-DNA insertions in the plant genome can be easily identified using TAIL-PCR. Consequently, the genes responsible for the rhizoid defects of those mutant lines in which the rhizoid defect is caused by intact T-DNA insertion are easy to identify. Therefore, I analysed the co-segregation of the rhizoid defect with the hygromycin-

resistance marker on the T-DNA in the F1 generation after backcrossing each mutant with wild type, in order to identify those mutants for which the gene responsible for the rhizoid defect would be feasible to identify within the time frame of this project. Of the 120 (39.2 %) mutant lines with inherited rhizoid defect, 47 lines in total showed co-segregation of the rhizoid defect with the hygromycin resistance marker on the T-DNA (Table 3.2, Table 3.5). This is slightly higher than the co-segregation frequency of 29-35 % reported for Arabidopsis T-DNA mutant screens (Budziszewski *et al*., 2001; McElver *et al*., 2001). The gene responsible for the defective rhizoid phenotype of the mutant remained unresolved for 2 mutant lines due to the presence of multiple T-DNA insertions, whereas for 1 mutant line the sequence of the transcript likely to be affected was incomplete, and therefore the coding sequence of the gene could not be reliably defined. In total, the gene responsible for the rhizoid defective phenotype of the mutant was successfully identified for 44 T-DNA tagged backcrossed mutants using TAIL-PCR.

Table 3.2 Frequency of different rhizoid phenotypes observed in the screen for *M. polymorpha* mutants defective in rhizoid development. Inheritance of the mutant defect in the F1 after backcrossing with wild type, and co-segregation of the rhizoid defect with the T-DNA in the F1 are indicated. The rhizoid phenotype of the mutant lines was assessed from gemmae grown for 10 days under constant light on square plates containing Johnson's medium.

mutant phenotype	lines isolated	crossed with wild type	inherited	co-segregates
short rhizoids	132	103	87	28
very short rhizoids	35	13	13	8
curly rhizoids	13	9	9	2
few rhizoids	10	6	3	2
dorsal rhizoids	8	7	7	7
more ventral rhizoids	3	1	0	-
no rhizoids	2	0	-	-
bulges	1	1	1	0
total (%)	**204**	**140 (68.6)**	**120 (85.7)**	**47 (39.2)**

Many of the rhizoid defective mutants were challenging to grow on soil for subsequent backcrossing with wild type because of their defective rooting system and pleiotropic effects of the mutations. Furthermore, some of the genes defective in the mutants may play critical roles in the development of the sexual organs, gamete viability, fertilisation or progress through the sporophyte generation. Overall 86 of 103 female mutants (83.5 %) and 54 of 84 male mutants (64.3 %) were successfully crossed. Of the 204 mutants, 17 (8.3 %) mutants did not produce reproductive structures and therefore were not possible to cross with wild type. A further 47 (23 %) mutants were not successfully crossed with wild type despite multiple attempts. For these mutants, TAIL-PCR was carried out on the original mutant plant without co-segregation analysis. If there were more than one mutant line with a T-DNA inserted into the same gene, and if the respective lines had the

same rhizoid phenotype, I concluded that the lines represented independent mutant alleles for the same gene. I considered having more than one independent mutant allele for the same gene as a strong indication of that gene being involved in rhizoid development and the T-DNA being responsible for the rhizoid defect of the mutant despite the lack of co-segregation analysis. Using these criteria I identified 12 additional T-DNA tagged mutants. Therefore, in total 59 T-DNA tagged rhizoid defective mutants were identified in this screen.

Mutants with abnormal T-DNA insertion sequences

In total TAIL-PCR was carried out for 112 mutant lines. Of these, 104 lines had one or more simple T-DNA insertion that consisted of the T-DNA sequence between the left border and right border. Two lines had parts of the pCambia 1300 plasmid backbone inserted into the plant genome in addition to the T-DNA sequence. A further 6 mutants had tandem duplications of the T-DNA insertion. These findings suggest, that while in most T-DNA insertion lines a single copy of the T-DNA between the left border and right border was inserted into the plant genome, aberrant T-DNA insertions were present.

T-DNA copy number

The T-DNA used in this mutagenesis contains a plant selection marker gene that confers resistance to the antibiotic hygromycin. Therefore, the number of T-DNA insertions in each T-DNA mutant line can be estimated based on the ratio of

hygromycin resistant to hygromycin sensitive F1 plants from the cross between the mutant and wild type. In *M. polymorpha* the dominant generation is haploid, and thus 1:1 ratio of hygromycin resistant to hygromycin sensitive F1 plants indicates the presence of a single T-DNA insertion. A 3:1 ratio indicates that there are two T-DNA insertions and 7:1 ratio indicates that there are three T-DNA insertions. The majority of the mutants (87.5 %; 105 of 120 analysed) had a single intact T-DNA insertion based on 1:1 segregation ratio of hygromycin resistant to hygromycin sensitive plants in the F1 progeny, whereas 10 % had two T-DNA insertions and 2.5 % had three or more insertions (Table 3.3). Therefore, the average T-DNA copy number was 1.15 T-DNA insertions per line. This suggests that in the population of 150,000 T-DNA insertion lines screened the total number of independent T-DNA insertions can be estimated to be more than 172,500. The average T-DNA copy number observed here for *M. polymorpha* is lower than the 1.4-1.5 per line reported for Arabidopsis T-DNA insertion lines (Alonso *et al*., 2003; McElver *et al*., 2001).

Table 3.3 T-DNA copy number in the rhizoid defective *M. polymorpha* T-DNA insertion mutants backcrossed with wild type. The ratio of hygromycin sensitive to hygromycin resistant F1 plants was scored for 120 crosses in total.

T-DNA copy number			
inserts	**hyg s:hyg r**	**number of lines**	**% lines**
1	1:1	105	87.5
2	1:4	12	10.0
≥3	1:≥8	3	2.5

3.3.2. Twenty-five genes involved in *M. polymorpha* rhizoid development identified

The *M. polymorpha* rhizoid development genes identified based on the mutants isolated in this screen are listed in table 3.4. The list is sub-divided based on predicted roles of the genes inferred from the mutant phenotypes or sequence similarity with genes from other organisms. When possible, the rhizoid development genes were named after homologous genes in Arabidopsis, otherwise the genes were named as *FEW RHIZOIDS1* (*FRH1*) or *SHORT RHIZOIDS1-3* (*SRI1-3*) depending on the phenotype of the mutant. In total, 25 genes involved in *M. polymorpha* rhizoid development were identified. Of these, 16 genes were represented by multiple mutant alleles, or the mutant phenotype was complemented by introducing a wild type copy of the gene into the mutant background, validating that the gene identified is responsible for the rhizoid defect of the mutant. Of the 25 genes identified, only class I *RSL* genes have previously been described to be involved in rhizoid development based on reverse genetic studies in the moss *P. patens* (Menand *et al*., 2007). Therefore, this mutant screen identified 24 new genes involved in rhizoid development in bryophytes.

Table 3.4 Genes identified as involved in rhizoid development in *M. polymorpha* based on the mutants isolated in this screen. In each section, genes for which multiple mutant alleles were identified are on a darker background, while genes represented by a single T-DNA tagged mutant allele are on a lighter background.

RHIZOID PRECURSOR CELL DIFFERENTIATION		**closest Arabidopsis homolog**	**mutant phenotype**	**number of mutant alleles**
MpRSL1	bHLH transcription factor	At1G66470 (*RHD6*)	very few rhizoids	2
		At1G66470 (*RHD6*)	ectopic rhizoids	8
MpFRH1	miRNA	-	very few rhizoids	4
CELL WALL SYNTHESIS				
MpCSLD1	cellulose synthase-like class D	At3G03050 (*CSLD3*)	very short rhizoids	3
MpCSLD2	cellulose synthase-like class D	At3G03050 (*CSLD3*)	short rhizoids	5
MpXUT	xyloglucan-specific galacturonosyltransferase	At5G41250	very short rhizoids	1*
MpGMP	GDP-mannose pyrophosphorylase	At2G39770 (*GMP1*)	very short rhizoids	1
MpRHM1	rhamnose biosynthesis	At1G78570 (*RHM1*)	short rhizoids	1
MpTHE	CrRLK1 family receptor-like kinase	At5G54380 (*THE1*)	very short rhizoids	1
VESICLE TRANSPORT				
MpPI4Ka	1-phosphatidylinositol 4-kinase alpha	At1G49340	very short rhizoids	3
MpSRI1	Rab guanine nucleotide exchange factor, similar to *S. Cerevisiae RIC1*	At3G61480	short rhizoids	1*
MpSCD	Rab guanine nucleotide exchange factor	At1G49040 (*SCD1*)	short rhizoids	1*
MpSPI	WD-40 repeat protein	At1G03060 (*SPI*)	short rhizoids	2
MpXIA	Class XI myosin	At4G33200	short rhizoids	3
MpAP5M	AP-5 complex subunit mu	At2G20790	short rhizoids	1
MpSRI2	calcium binding EF-hand family protein, similar to *S. Cerevisiae PAN1*	At1G21630	very short rhizoids	1

*a second allele identified by G. Morieri or V. Jones.

Table 3.4 continued

OTHER/UNKNOWN FUNCTION				
MpALBA	alba-like DNA/RNA-binding protein	At1G76010	short rhizoids	4
MpFBA1	fructose-bisphosphate aldolase	At4G38970 (*FBA2*)	short rhizoids	4
MpGATA1	class A GATA zinc finger transcription factor	At5G25830 (*GATA12*)	short rhizoids	2
MpIRE	AGC-kinase	At5G62310 (*IRE*)	very short rhizoids	1**
MpPTI	serine/threonine kinase	At2G30740	short rhizoids	2
MpTMT	tonoplast monosaccharide transporter	At3G51490 (*TMT3*)	short rhizoids	2
MpWDL	predicted microtubule binding protein / TPX2 domain containing protein	At2G35880	curly rhizoids	1*
MpSRI3	unknown protein	At2G41830	short rhizoids	1
MpREN	Pleckstrin homology (PH) domain / RhoGAP domain-containing protein	At5G12150	curly rhizoids	1
MpXF	squalene monooxygenase	At1G58440	short rhizods	1

*a second allele identified by G. Morieri or V. Jones. **mutant complemented (Fig. A3.1 in the chapter 3 appendix)

Table 3.5 Inheritance of the mutant rhizoid defect and co-segregation of the rhizoid defect with the hygromycin resistance gene on the T-DNA. Frequencies of hygromycin resistant and hygromycin sensitive plants showing mutant and wild type phenotypes in F1 generation from a cross between T-DNA insertion mutant lines with wild type *M. polymorpha*. Probability (p) of obtaining the observed numbers of hygromycin sensitive and hygromycin resistant F1 plants with the estimated T-DNA copy number was determined using the Chi-square test.

			Mut		WT		total		HygS:HygR		T-DNA	
gene	**line name**	**mutant phenotype**	**HygR**	**HygS**	**HygR**	**HygS**	**HygR**	**HygS**	**ratio**	**p**	**insertions**	**E ratio**
MpALBA	ST37-4	short rhizoids	100	0	0	106	100	106	1: 0.9	0.676	1	1:1
MpALBA	ST37-8	short rhizoids	108	0	0	112	108	112	1: 1.0	0.787	1	1:1
MpALBA	ST49-13-2	short rhizoids	112	0	0	107	112	107	1: 1.0	0.735	1	1:1
MpAP5M	ST49-9	short rhizoids	101	0	0	107	101	107	1: 0.9	0.677	1	1:1
MpCSLD2	ST45-11	short rhizoids	110	0	0	99	110	99	1: 1.1	0.447	1	1:1
MpCSLD2	ST48-1	short rhizoids	133	0	0	149	133	149	1: 0.9	0.341	1	1:1
MpCSLD2	ST49-16	short rhizoids	141	0	0	134	141	134	1: 1.1	0.673	1	1:1
MpCSLD2	ST51-4	short rhizoids	104	0	0	99	104	99	1: 1.1	0.726	1	1:1
MpFBA1	ST36-5-3	short rhizoids	104	0	0	99	104	99	1: 1.1	0.726	1	1:1
MpFBA1	ST43-1	short rhizoids	128	0	0	116	128	116	1: 1.1	0.442	1	1:1
MpFBA1	ST48-4	short rhizoids	113	0	0	154	113	154	1: 0.7	0.012	1*	1:1
MpFBA1	ST51-5-2	short rhizoids	103	0	0	108	103	108	1: 1.0	0.731	1	1:1
MpFRH1	ST45-2	few rhizoids	131	0	0	125	131	125	1: 1.0	0.708	1	1:1
MpFRH1	ST49-10	few rhizoids	109	0	48	53	157	53	1: 3.0	0.936	2	1:3
MpGATA1	ST15-4	short rhizoids	106	0	0	102	106	102	1: 1.0	0.782	1	1:1
MpGATA1	ST43-2	short rhizoids	118	0	0	133	118	133	1: 0.9	0.344	1	1:1
MpGMP	ST40-1	very short rhizoids	101	0	0	98	101	98	1: 1.0	0.832	1	1:1
MpIRE	ST49-14	short rhizoids	131	0	0	143	131	143	1: 0.9	0.468	1	1:1

*deviation from the expected number of F1 plants showing wild type and mutant phenotypes based on the estimated T-DNA copy number.

Table 3.5 continued

			Mut		WT		total		HygS:HygR		T-DNA	
gene	**line name**	**mutant phenotype**	**HygR**	**HygS**	**HygR**	**HygS**	**HygR**	**HygS**	**ratio**	**p**	**insertions**	**E ratio**
MpPI4Kα	ST33-1	very short rhizoids	106	0	0	102	106	102	1: 1.0	0.782	1	1:1
MpPI4Kα	ST34-2	very short rhizoids	111	0	0	93	111	93	1: 1.2	0.208	1	1:1
MpPI4Kα	ST46-3	short rhizoids	96	0	0	110	96	110	1: 0.9	0.329	1	1:1
MpPTI	ST13-3	short rhizoids	114	0	0	122	114	122	1: 0.9	0.603	1	1:1
MpREN	ST25-4	curly rhizoids	94	0	0	118	94	118	1: 0.8	0.099	1	1:1
MpRHM1	ST49-17	short rhizoids	103	0	0	145	103	145	1: 0.7	0.008	1*	1:1
MpRSL1	ST13-1	dorsal rhizoids	64	0	97	17	161	17	1: 9.5	0.234	3	1:7
MpRSL1	ST19-15	dorsal rhizoids	82	0	77	44	159	44	1: 3.6	0.274	2	1:3
MpRSL1	ST21-3	dorsal rhizoids	117	0	0	151	117	151	1: 0.8	0.038	1*	1:1
MpRSL1	ST37-11	dorsal rhizoids	93	0	41	30	134	30	1: 4.5	0.047	2	1:3
MpRSL1	ST44-1	dorsal rhizoids	108	0	0	122	108	122	1: 0.9	0.356	1	1:1
MpRSL1	ST53-1	dorsal rhizoids	106	0	0	123	106	123	1: 0.9	0.261	1	1:1
MpRSL1	ST53-2	dorsal rhizoids	93	0	71	41	164	41	1: 4.0	0.098	2	1:3
MpSPI	ST17-11	short rhizoids	143	0	0	285	143	285	1: 0.5	0.000	1*	1:1
MpSPI	ST49-5	short rhizoids	111	0	0	133	111	133	1: 0.8	0.159	1	1:1
MpSRI2	ST36-1	very short rhizoids	97	0	0	115	97	115	1: 0.8	0.216	1	1:1
MpSRI3	ST49-12	short rhizoids	110	0	0	108	110	108	1: 1.0	0.892	1	1:1
MpTHE	ST14-3	very short rhizoids	119	0	0	123	119	123	1: 1.0	0.797	1	1:1
MpTMT	ST21-2	short rhizoids	105	0	1	125	106	125	1: 0.8	0.211	1	1:1
MpTMT	ST45-10	short rhizoids	108	0	0	104	108	104	1: 1.0	0.784	1	1:1
MpWDL	ST45-1	curly rhizoids	111	0	0	104	111	104	1: 1.1	0.633	1	1:1
MpXF	ST37-9	short rhizoids	120	0	0	164	120	164	1: 0.7	0.009	1*	1:1
MpXIA	ST19-7	short rhizoids	108	0	1	109	109	109	1: 1.0	1.000	1	1:1
MpXIA	ST37-2	short rhizoids	301	0	2	268	303	268	1: 1.1	0.143	1	1:1
MpXIA	ST49-8	short rhizoids	112	0	1	104	113	104	1: 1.1	0.541	1	1:1

*deviation from the expected number of F1 plants showing wild type and mutant phenotypes based on the estimated T-DNA copy number.

3.3.3. Twenty-four of the 25 *M. polymorpha* rhizoid development genes have predicted homologs in Arabidopsis

M. polymorpha and Arabidopsis proteins similar to the proteins encoded by the *M. polymorpha* rhizoid development genes were identified using OrthoFinder (Emms and Kelly, 2015). Arabidopsis homologs were identified for 24 of the 25 *M. polymorpha* rhizoid development genes (table 3.6). If more than 2 homologous Arabidopsis genes were predicted, phylogenetic analysis was carried out to further evaluate the similarity between the *M. polymorpha* genes and their predicted Arabidopsis homologs. Figures 3.2-3.17 contain the maximum likelihood phylogenetic trees constructed, together with images of mutant plants and gene models showing the intron-exon structures of the rhizoid development genes. When the proteins encoded by the genes analysed contained conserved domains, such as the basic helix-loop-helix or a kinase domain, the groups of homologous genes identified by OrthoFinder were large. In those cases the group of genes estimated as homologous was further refined based on the phylogenetic analysis and published literature on Arabidopsis gene families. From this point onwards, homologous genes refers to the genes identified by OrthoFinder, or the genes that grouped together in the phylogenetic analysis, in most cases constituting a gene family or a subfamily likely to have originated from a single ancestral gene. All the predicted Arabidopsis homologs of the *M. polymorpha* rhizoid development genes are listed in table A3.1 in the chapter 3 appendix. In conclusion, nearly all (24 of 25) the rhizoid development genes identified in this screen have predicted homologs in Arabidopsis.

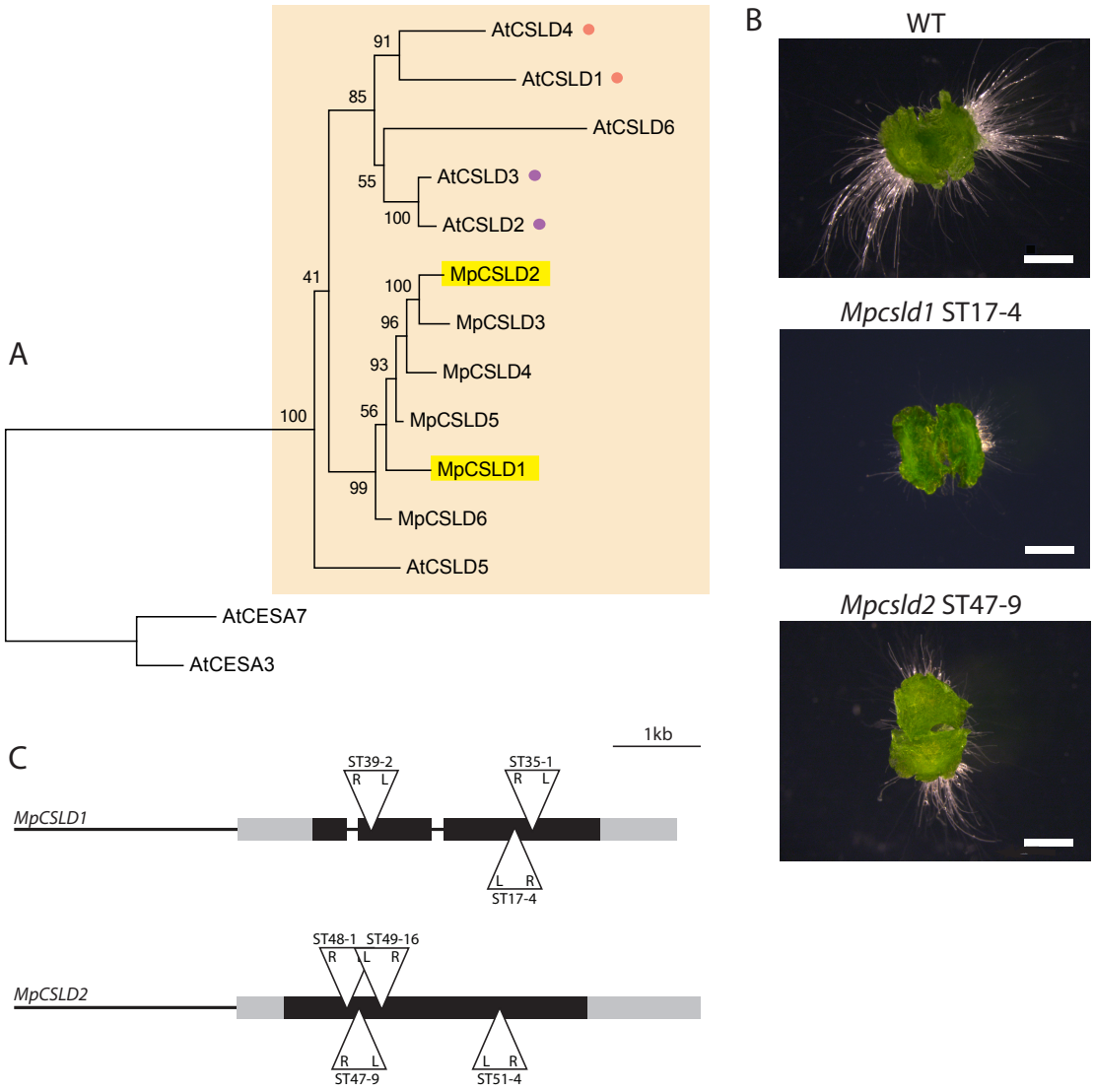

Figure 3.2 *CELLULOSE SYNTHASE-LIKE Class D* (*CSLD*) genes are required for rhizoid development in *M. polymorpha*. A) A phylogenetic tree of Arabidopsis and *M. polymorpha* Cellulose Synthase-like class D (CSLD) proteins. The tree was rooted using two Arabidopsis CELLULOSE SYNTHASE (CESA) proteins. Red dot: Arabidopsis genes that have enriched expression in pollen, purple dot: Arabidopsis genes with enriched expression in hair forming root epidermal cells (Arabidopsis eFP Browser 2.0). B) 10 day old gemmae of wild type, *Mpcsld1* mutant ST17-4 and *Mpcsld2* mutant ST47-9. Scale bar 2 mm. C) *MpCDLS1* and *MpCSLD2* gene models showing the location and orientation of the T-DNA insertion sites in the *Mpcsld1* mutants ST39-2, ST17-4 and ST35-1, and the *Mpcsld2* mutants ST48-1, ST47-9, ST49-16 and ST51-4. L and R stand for T-DNA left and right border, respectively.

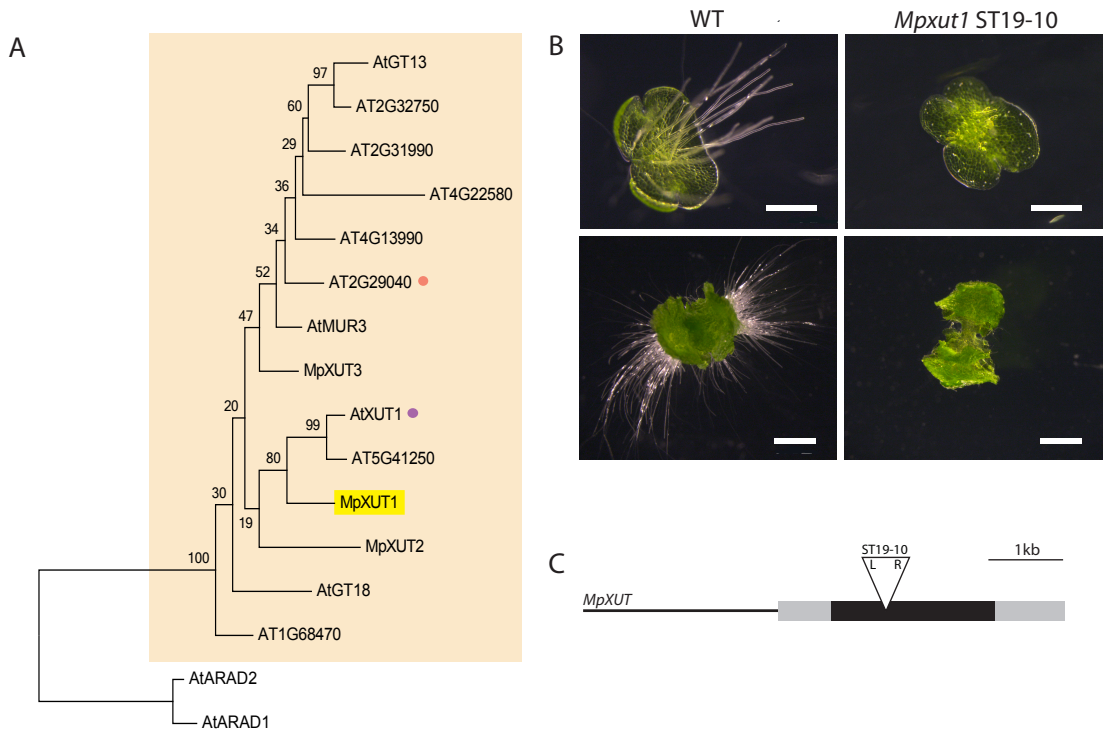

Figure 3.3 A putative xyloglucan-specific galacturonosyltransferase encoded by *MpXUT1* is required for rhizoid development. A) A phylogenetic tree of *M. polymorpha* and Arabidopsis XUT1-like proteins. The tree was rooted using two Arabidopsis arabinosyltransferases *ARAD1* and *ARAD2*. Red dot: Arabidopsis genes that have enriched expression in pollen, purple dot: Arabidopsis genes with enriched expression in hair forming root epidermal cells (Arabidopsis eFP Browser 2.0). B) 2 day old gemmae (top row, scale bar 500 µM) and 10 day old gemmae (bottom row, scale bar 2 mm) of wild type (left) and *Mpxut1* mutant ST19-10 (right). C) *MpXUT1* gene model indicating the location and orientation of the T-DNA insertion in the *Mpxut1* mutant ST19-10. L and R stand for T-DNA left and right border, respectively.

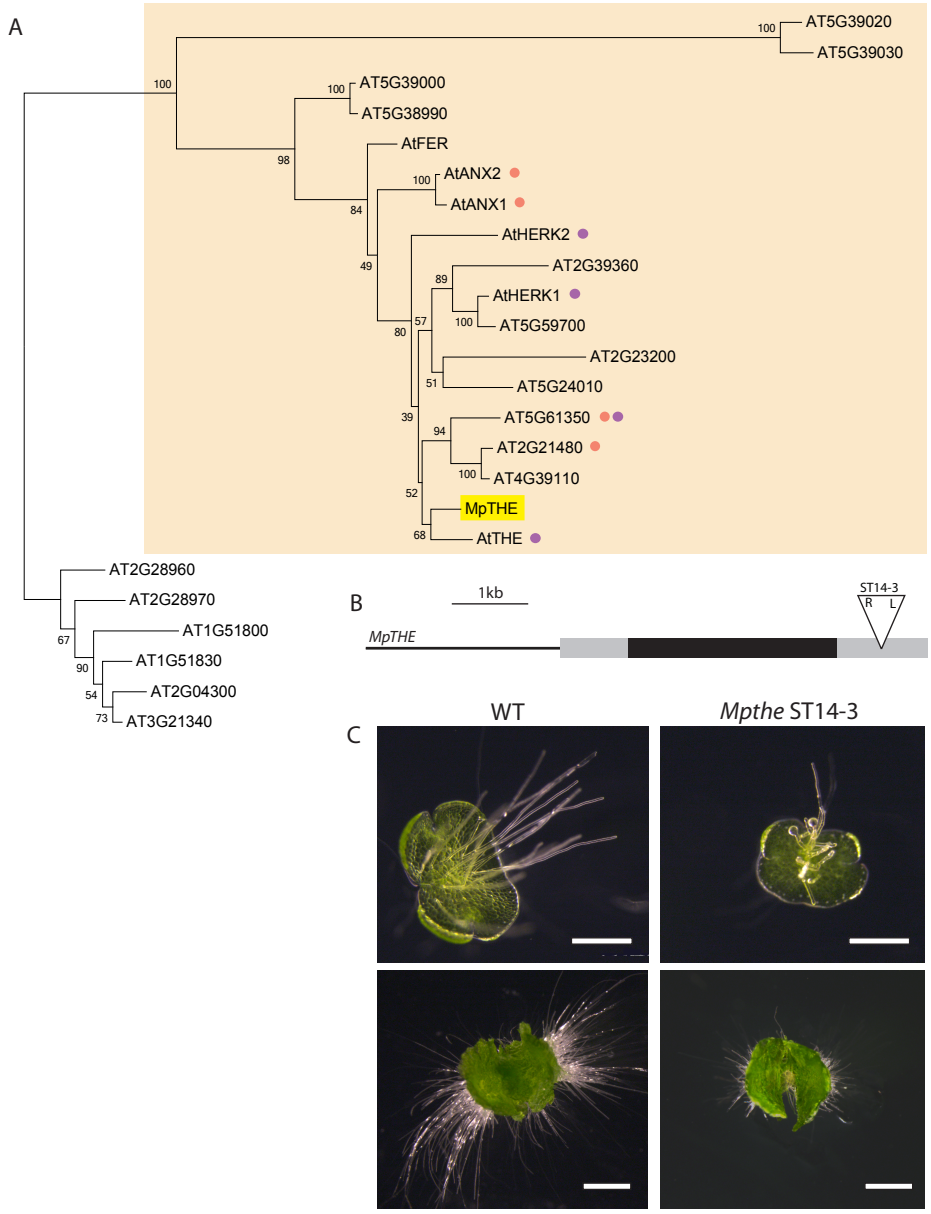

Figure 3.4 The *M. polymorpha* single-copy *Catharanthus roseus RLK1*-like (*CrRLK1L*) family receptor-like kinase *MpTHE* is required for rhizoid development. A) A phylogenetic tree of *M. polymorpha* and Arabidopsis CrRLK1-like proteins. The tree was rooted using the six most similar Arabidopsis receptor-like kinases. Red dot: Arabidopsis gene with enriched expression in pollen, purple dot: Arabidopsis gene with enriched expression in hair forming root epidermal cells (Arabidopsis eFP Browser 2.0). B) *MpTHE* gene model showing the location and orientation of the T-DNA insertion site in the *Mpthe* mutant ST14-3. L and R stand for T-DNA left and right border, respectively. C) 2 day old gemmae (top row, scale bar 500 µM) and 10 day old gemmae (bottom row, scale bar 2 mm) of wild type (left) and *Mpthe* mutant ST14-3 (right).

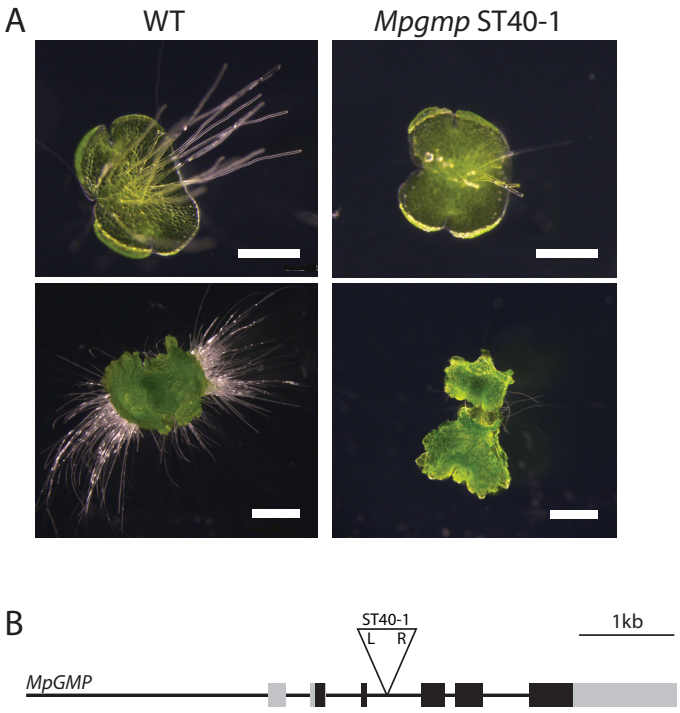

Figure 3.5 *MpGMP* is required for rhizoid development in *M. polymorpha*. A) 2 day old gemmae (top row, scale bar 500 µM) and 10 day old gemmae (bottom row, scale bar 2 mm) of wild type (left) and *Mpgmp* mutant ST40-1 (right). B) *MpGMP* gene model showing the location and orientation of the T-DNA insertion site in the *Mpgmp* mutant ST40-1. L and R stand for T-DNA left and right border, respectively. *MpGMP* has only two predicted Arabidopsis homologs that are very similar. Therefore, phylogeny construction was not carried out.

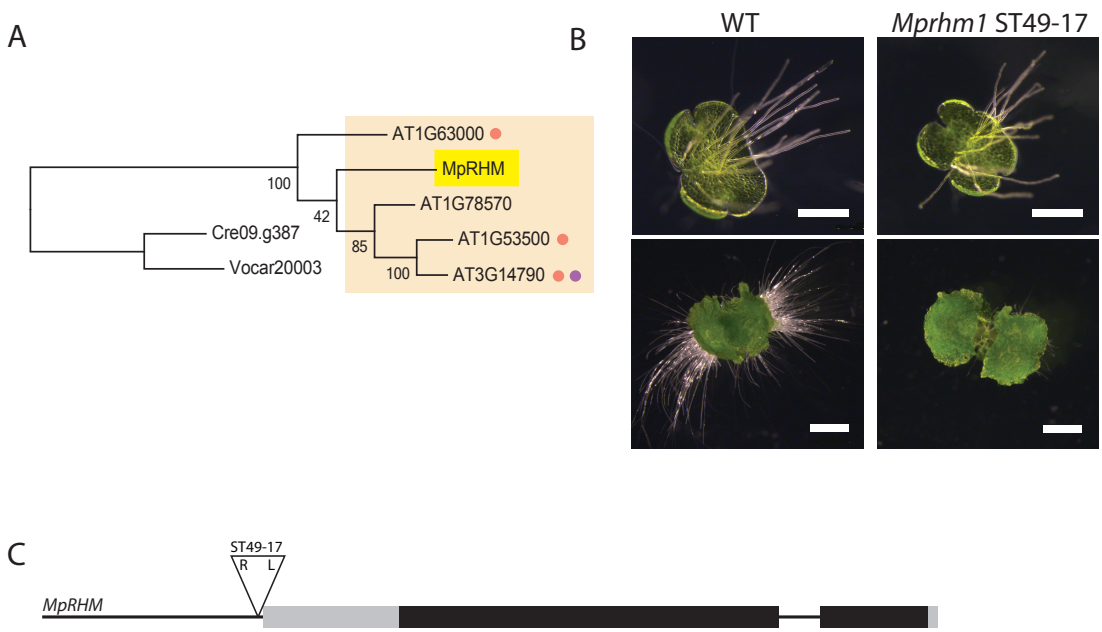

Figure 3.6 *MpRHM1* is required for rhizoid elongation in *M. polymorpha*. A) Phylogenetic tree of *M. polymorpha* and Arabidopsis RHM-like proteins. The tree was rooted using the RHM-like proteins from green algae. B) 2 day old gemmae (top row, scale bar 500 µM) and 10 day old gemmae (bottom row, scale bar 2 mm) of wild type (right) and *MpRHM1* mutant ST49-17 (left). C) *MpRHM1* gene model indicating the location and orientation of the T-DNA insertion in the *Mprhm1* mutant ST49-17. L and R stand for T-DNA left and right border, respectively.

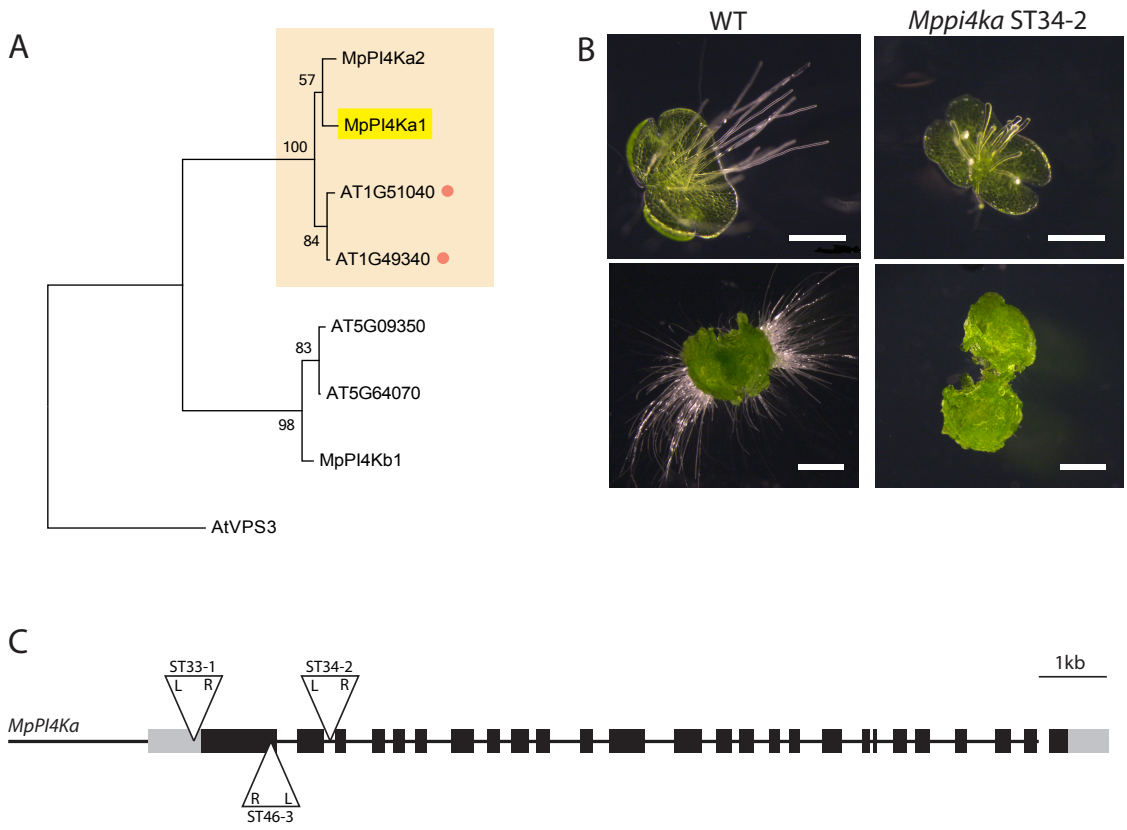

Figure 3.7 *MpPI4Kα1* is required for rhizoid elongation and regulation of rhizoid shape in *M. polymorpha*. A) Phylogenetic tree of *M. polymorpha* and Arabidopsis PI4Kα proteins. The tree was rooted using the Arabidopsis phosphatidylinositol 3-kinase VPS3. B) 2 day old gemmae (top row, scale bar 500 µM) and 10 day old gemmae (bottom row, scale bar 2 mm) of wild type (right) and *Mppi4kα* mutant ST34-2 (left). C) *MpPI4Kα1* gene model indicating the location and orientation of the T-DNA insertions in the *pi4kα* mutants ST33-1, ST46-3 and ST34-2. L and R stand for T-DNA left and right border, respectively.

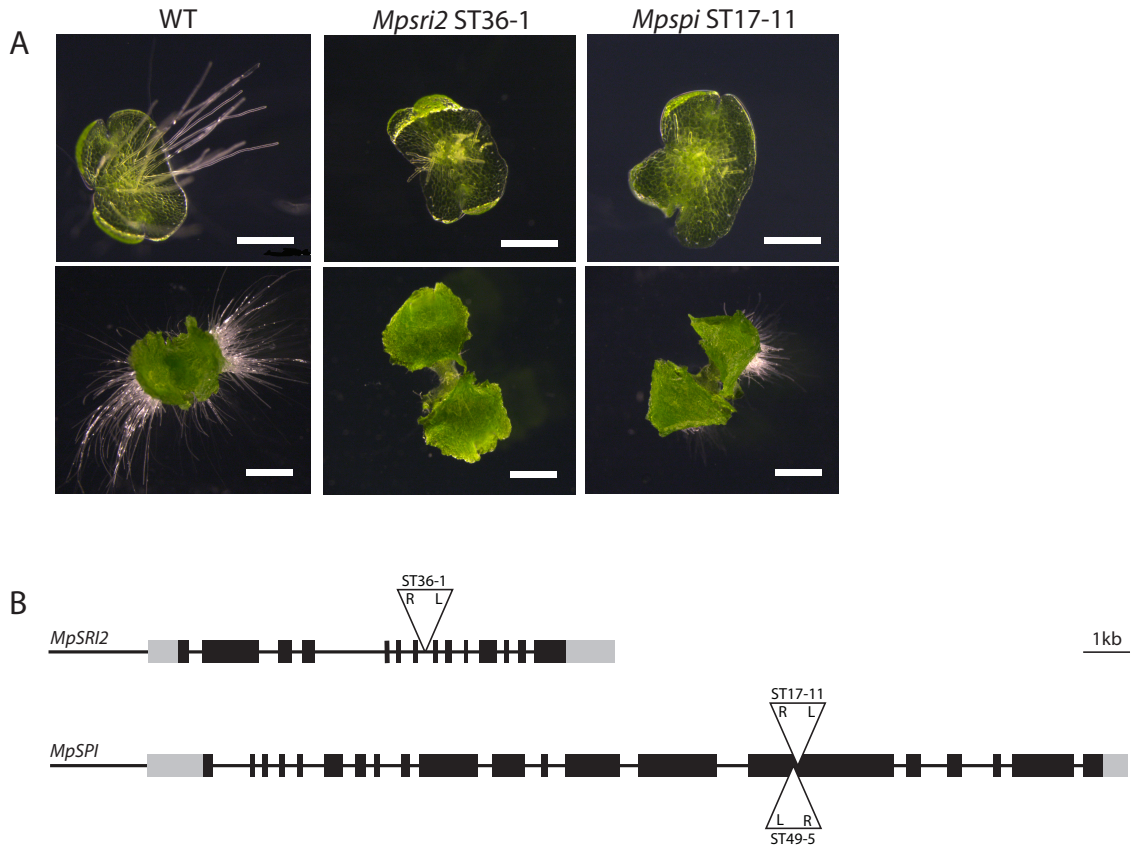

Figure 3.8 *MpSRI2* and *MpSPI* are required for rhizoid elongation in *M. polymorpha*. A) 2 day old gemmae (top row, scale bar 500 µM) and 10 day old gemmae (bottom row, scale bar 2 mm) of wild type (left), *Mpsri2* mutant ST36-1 (middle) and *Mpspi* mutant ST17-11 (right). B) *MpSRI2* and *MpSPI* gene models indicating the location and orientation of the T-DNA insertions in the *Mpsri2* mutant ST36-1 and *Mpspi* mutants ST17-11 and ST49-5. L and R stand for T-DNA left and right border, respectively. Both *MpSRI2* and *MpSPI* have two predicted Arabidopsis homologs that are very similar. Therefore, phylogeny construction was not carried out.

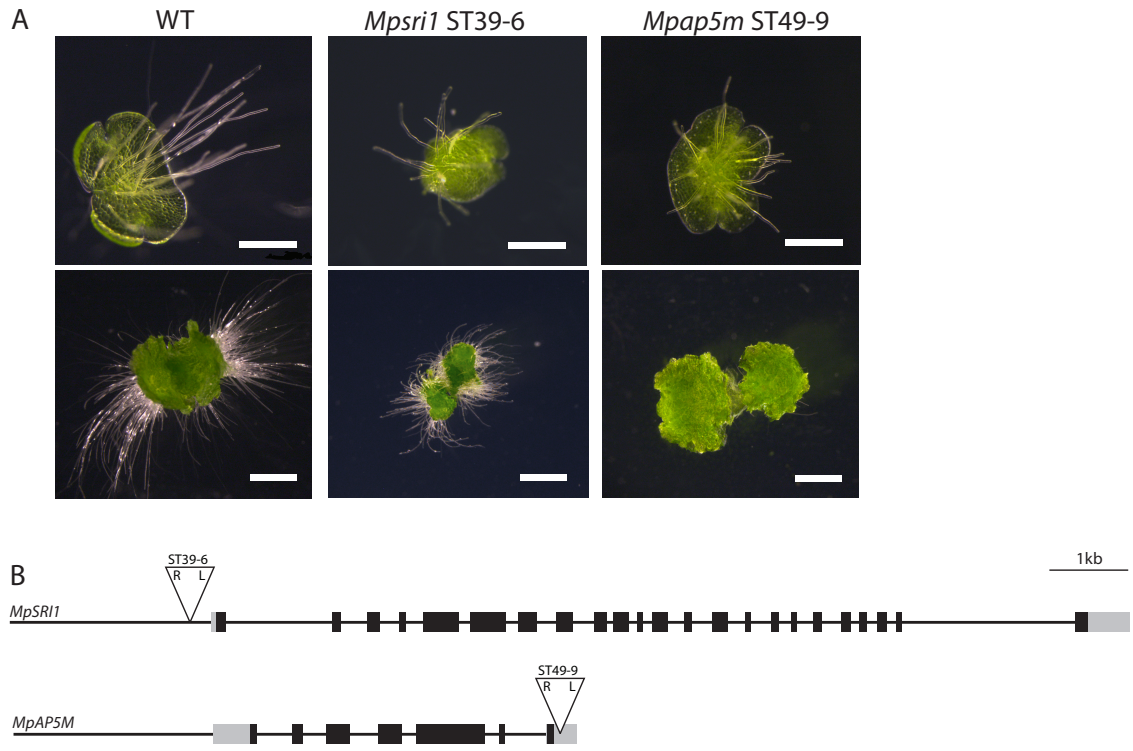

Figure 3.9 *MpSRI1* and *MpAP5M* are required for rhizoid elongation in *M. polymorpha*. A) 2 day old gemmae (top row, scale bar 500 µm) and 10 day old gemmae (bottom row, scale bar 2 mm) of wild type, *Mpsri1* mutant ST39-6 and *Mpap5m* mutant ST49-9 (from left to right). B) *MpSRI1* and *MpAP5M* gene models indicating the location and orientation of the T-DNA insertions in the *Mpsri1* mutant ST39-6 and *Mpap5m* mutant ST49-9. L and R stand for T-DNA left and right border, respectively. *MpSRI1* has only two very similar homologs in Arabidopsis, while *MpAP5M* has a single predicted Arabidopsis homolog. Therefore, phylogeny construction was not carried out.

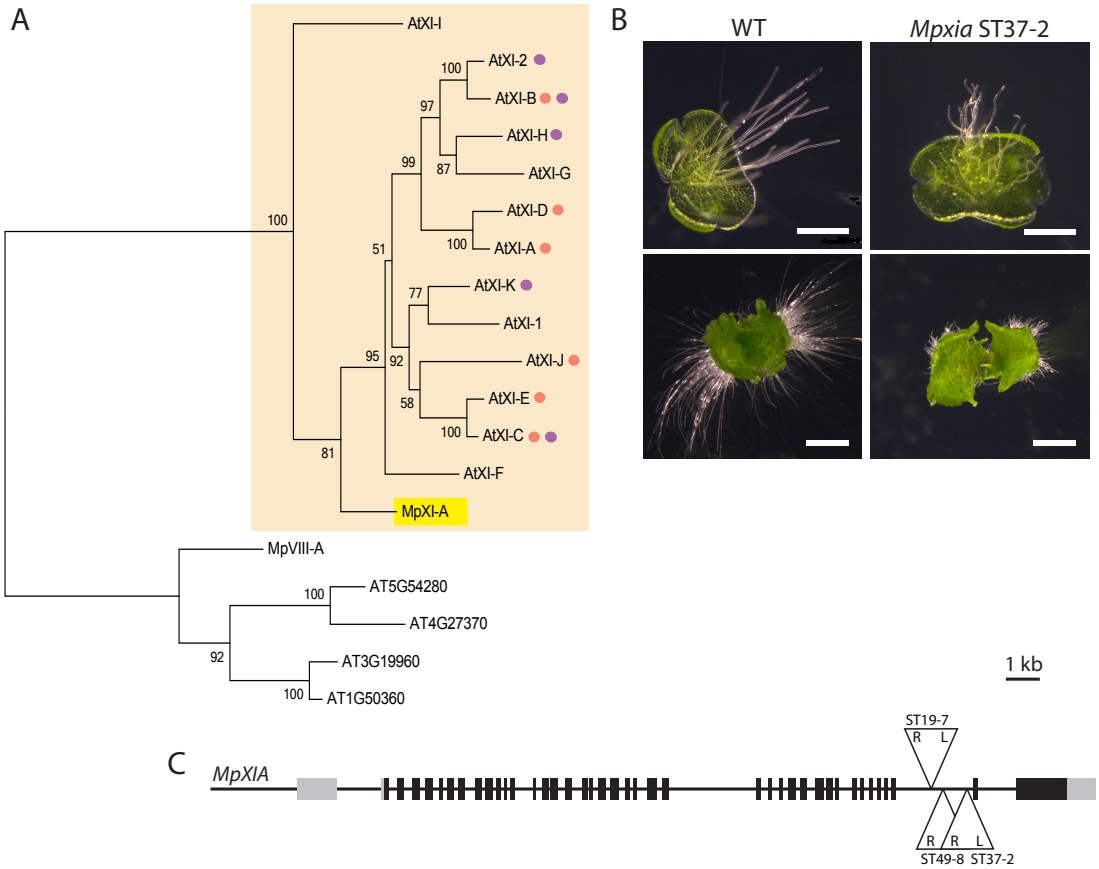

Figure 3.10 The *M. polymorpha* single-copy type XI myosin MpXIA is required for rhizoid development. A) A phylogenetic tree of *M. polymorpha* and Arabidopsis type XI myosin proteins. The tree is rooted using the Arabidopsis and *M. polymorpha* type VIII myosins. Red dot: Arabidopsis genes that have enriched expression in pollen, purple dot: Arabidopsis genes with enriched expression in hair forming root epidermal cells (Arabidopsis eFP Browser 2.0). B) 2 day old gemmae (top row, scale bar 500 µM) and 10 day old gemmae (bottom row, scale bar 2 mm) of wild type (right) and *Mpxia* mutant ST37-2 (left). C) *MpXIA* gene model indicating the location and orientation of the T-DNA insertion in the *Mpxia* mutants ST19-7, ST37-2 and ST49-8. L and R stand for T-DNA left and right border, respectively.

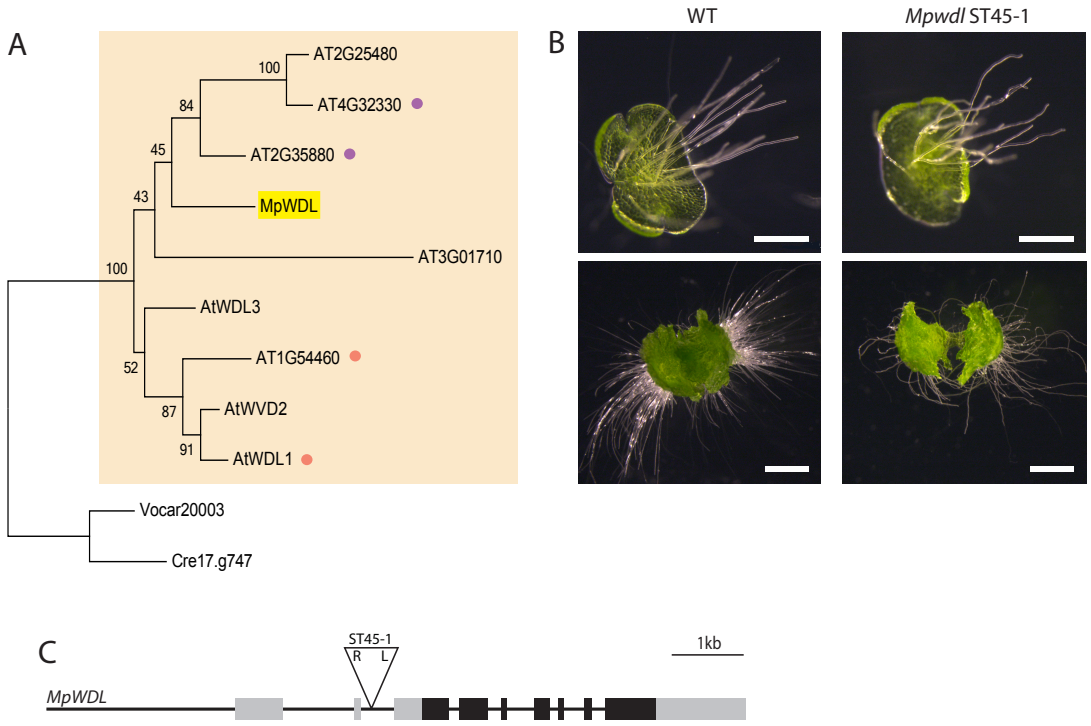

Figure 3.11 The *M. polymorpha* single-copy *WAVE DAMPENED-LIKE* family gene *MpWDL* is required for rhizoid development. A) A phylogenetic tree of *M. polymorpha* and Arabidopsis WDL family proteins. The tree is rooted using two TPX2-domain containing proteins from *C. reindhartii* and *V. Carteri*. Red dot: Arabidopsis genes that have enriched expression in pollen, purple dot: Arabidopsis genes with enriched expression in hair forming root epidermal cells (Arabidopsis eFP Browser 2.0). B) 2 day old gemmae (top row, scale bar 500 µM) and 10 day old gemmae (bottom row, scale bar 2 mm) of wild type (right) and *Mpwdl* mutant ST45-1 (left). C) *MpWDL* gene model indicating the location and orientation of the T-DNA insertion in the *Mpwdl* mutant ST45-1. L and R stand for T-DNA left and right border, respectively.

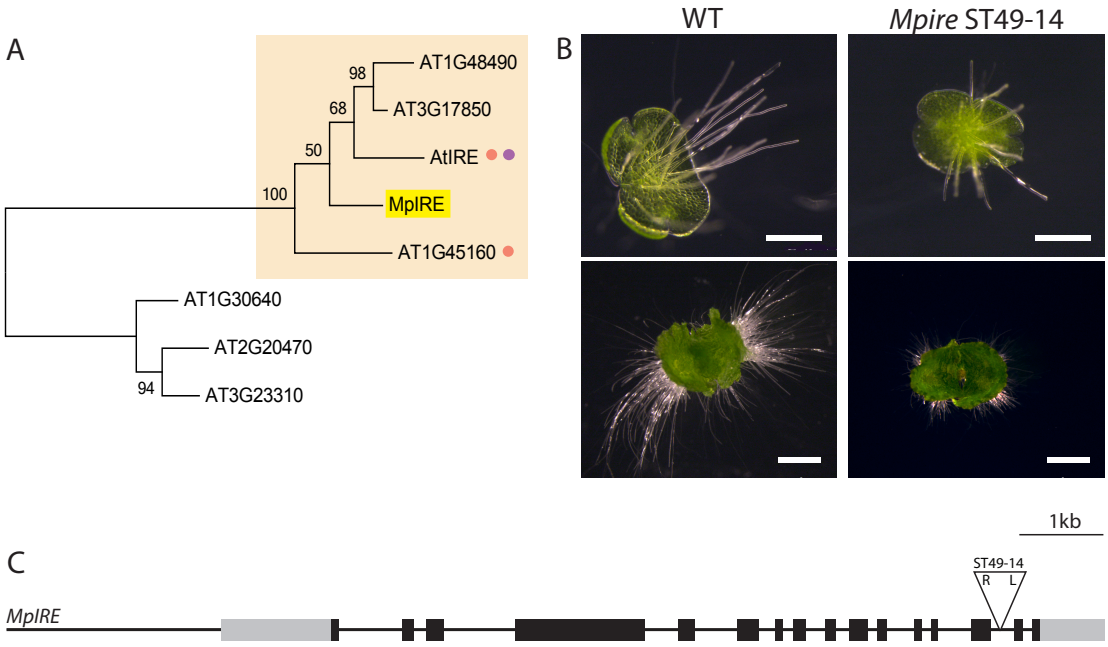

Figure 3.12 *MpIRE* is required for rhizoid elongation in M. polymorpha. A) A phylogenetic tree of Arabidopsis and *M. polymorpha* IRE-like AGC-kinases. The tree was rooted using three Arabidopsis NDR clade AGC-kinases most similar to the IRE clade kinases. Red dot: Arabidopsis gene with enriched expression in pollen, purple dot: Arabidopsis gene with enriched expression in hair forming root epidermal cells (Arabidopsis eFP Browser 2.0). B) 2 day old gemmae (top row, scale bar 500 µm) and 10 day old gemmae (bottom row, scale bar 2 mm) of wild type (left) and *Mpire* mutant ST49-14 (right). C) *MpIRE* gene model showing the location and orientation of the T-DNA insertion in the *Mpire* mutant ST49-14. L and R stand for T-DNA left and right border, respectively.

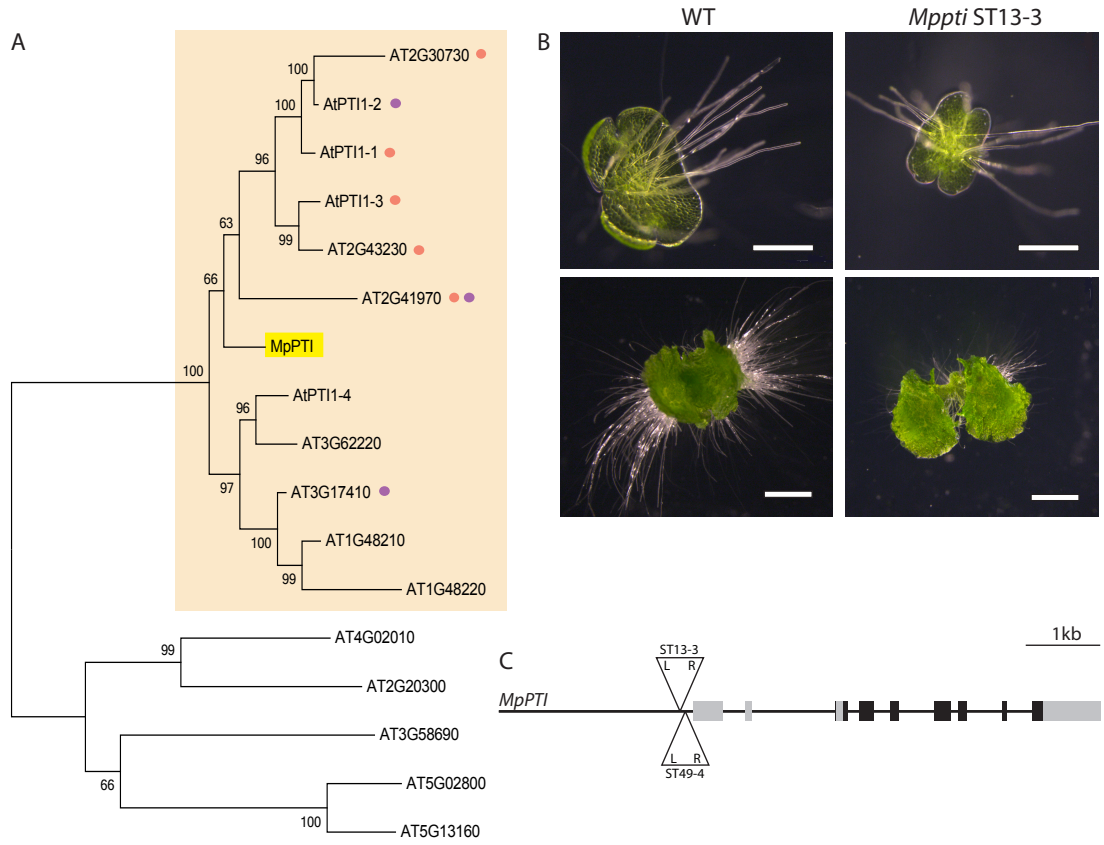

Figure 3.13 The *M. polymorpha* single-copy PTO-INTERACTING (PTI) kinase is required for rhizoid elongation. A) Phylogenetic tree of Arabidopsis and *M. polymorpha* PTI-like kinases. The tree was rooted using the five most similar kinases from Arabidopsis. Red dot: Arabidopsis gene with enriched expression in pollen, purple dot: Arabidopsis gene with enriched expression in hair forming root epidermal cells (Arabidopsis eFP Browser 2.0). B) 2 day old gemmae (top row, scale bar 500 µm) and 10 day old gemmae (bottom row, scale bar 2 mm) of wild type (left) and *Mppti* mutant ST13-3 (right). C) *MpPTI* gene model showing the location and orientation of the T-DNA insertions in the *Mppti* mutants ST13-4 and ST49-4. L and R stand for T-DNA left and right border, respectively.

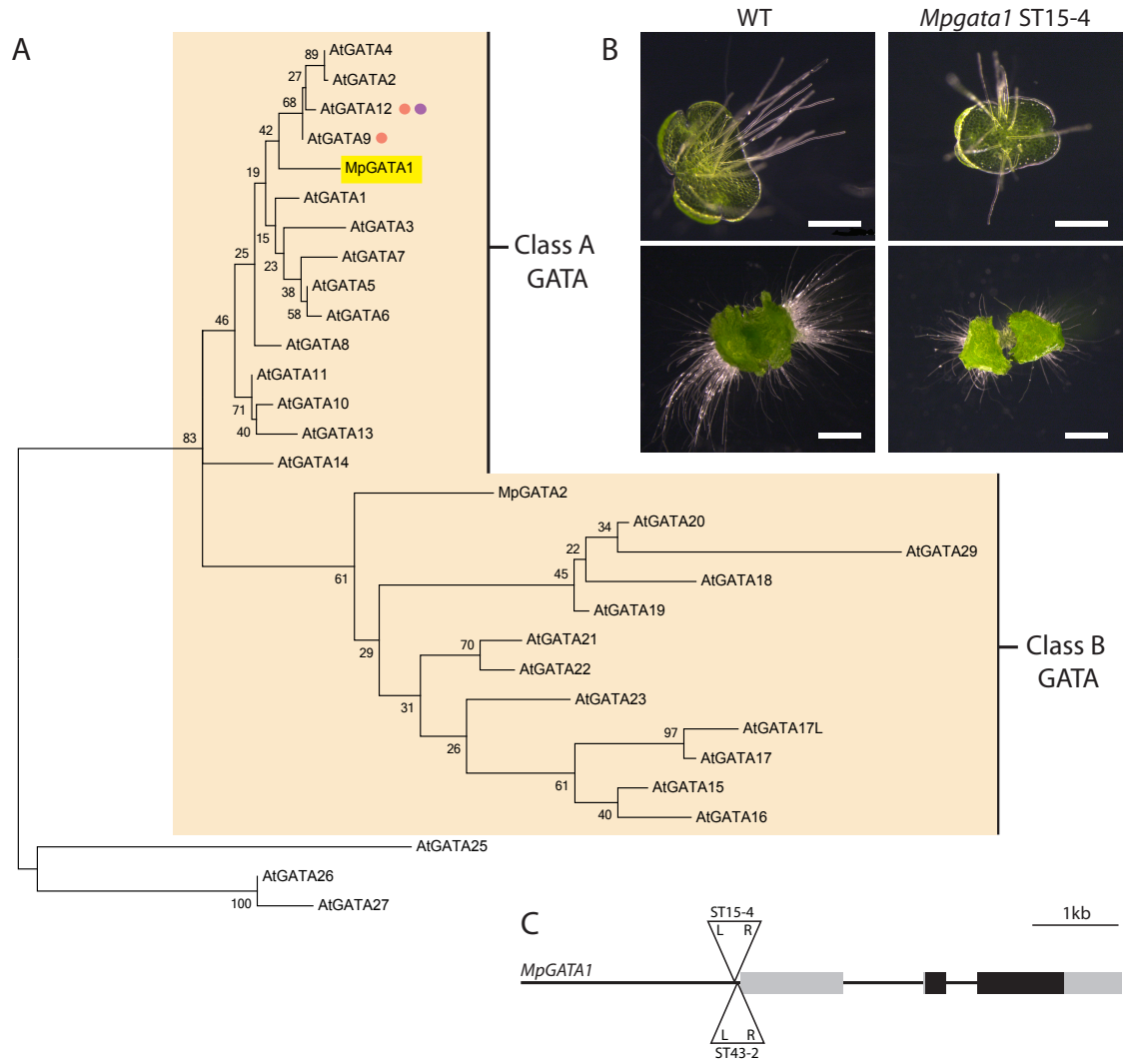

Figure 3.14 The *M. polymorpha* single-copy class A GATA transcription factor *MpGATA1* is required for rhizoid elongation. A) A phylogenetic tree of class A and class B GATA transcription factors in *M. polymorpha* and Arabidopsis. The tree was rooted using three Arabidopsis GATA transcription factors most similar to class A and class B GATA genes. Red dot: Arabidopsis gene with enriched expression in pollen, purple dot: Arabidopsis gene with enriched expression in hair forming root epidermal cells (Arabidopsis eFP Browser 2.0). The region of the tree for which *M. polymorpha* genes were identified is highlighted in orange. B) 2 day old gemmae (top row, scale bar 500 µm) and 10 day old gemmae (bottom row, scale bar 2 mm) of wild type (left) and *Mpgata1* mutant ST15-4 (right). C) *MpGATA1* gene model showing the location and orientation of the T-DNA insertions in the *Mpgata1* mutants ST15-4 and ST43-2. L and R stand for T-DNA left and right border, respectively.

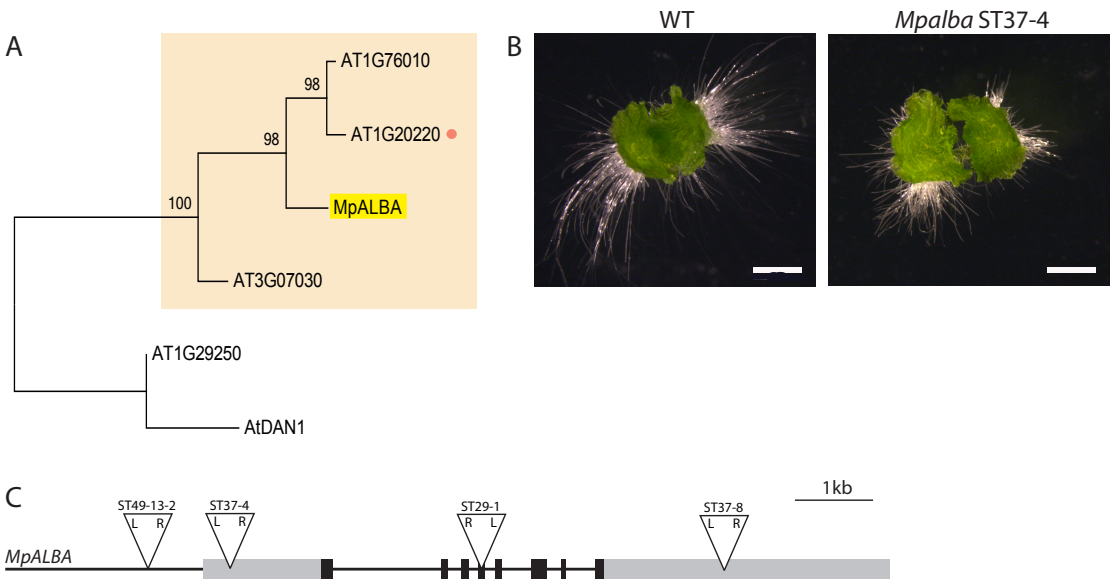

Figure 3.15 The *M. polymorpha* single-copy *ALBA*-like gene is required for rhizoid elongation. A) A phylogenetic tree of Arabidopsis and *M. polymorpha* ALBA-like proteins. Red dot: Arabidopsis gene with enriched expression in pollen (Arabidopsis eFP Browser 2.0). The tree was rooted using the two most similar Arabidopsis proteins. B) 2 day old gemmae (top row, scale bar 500 µM) and 10 day old gemmae (bottom row, scale bar 2 mm) of wild type (right) and *Mpalba* mutant ST37-4 (left). C) *MpALBA* gene model indicating the location and orientation of the T-DNA insertion in the *Mpalba* mutants ST49-13-2, ST37-4, ST29-1 and ST37-8. L and R stand for T-DNA left and right border, respectively.

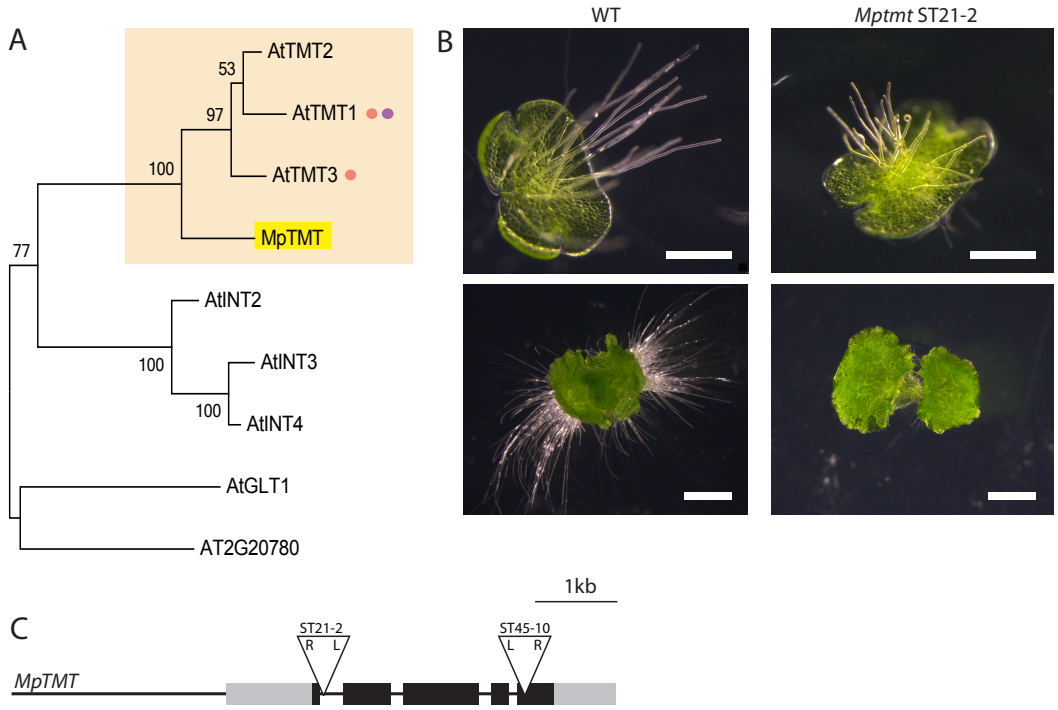

Figure 3.16 *The M. polymorpha TONOPLAST* MONOSACCHARIDE TRANSPORTER (*MpTMT*) is required for rhizoid development. A) Phylogenetic tree of *M. polymorpha* and Arabidopsis TMT proteins. The tree was rooted using the five most similar Arabidopsis genes; the inositol transporters AtINT2-4 and two putative glucose transporters AtGLT1 and At2G20780. Red dot: Arabidopsis gene with enriched expression in pollen (Arabidopsis eFP Browser 2.0). B) 2 day old gemmae (top row, scale bar 500 µM) and 10 day old gemmae (bottom row, scale bar 2 mm) of wild type (left) and *Mptmt* mutant ST21-2 (right). C) *MpTMT* gene model showing the location and orientation of T-DNA insertion sites in the *Mptmt* mutants ST21-1 and ST45-10. L and R stand for T-DNA left and right border, respectively.

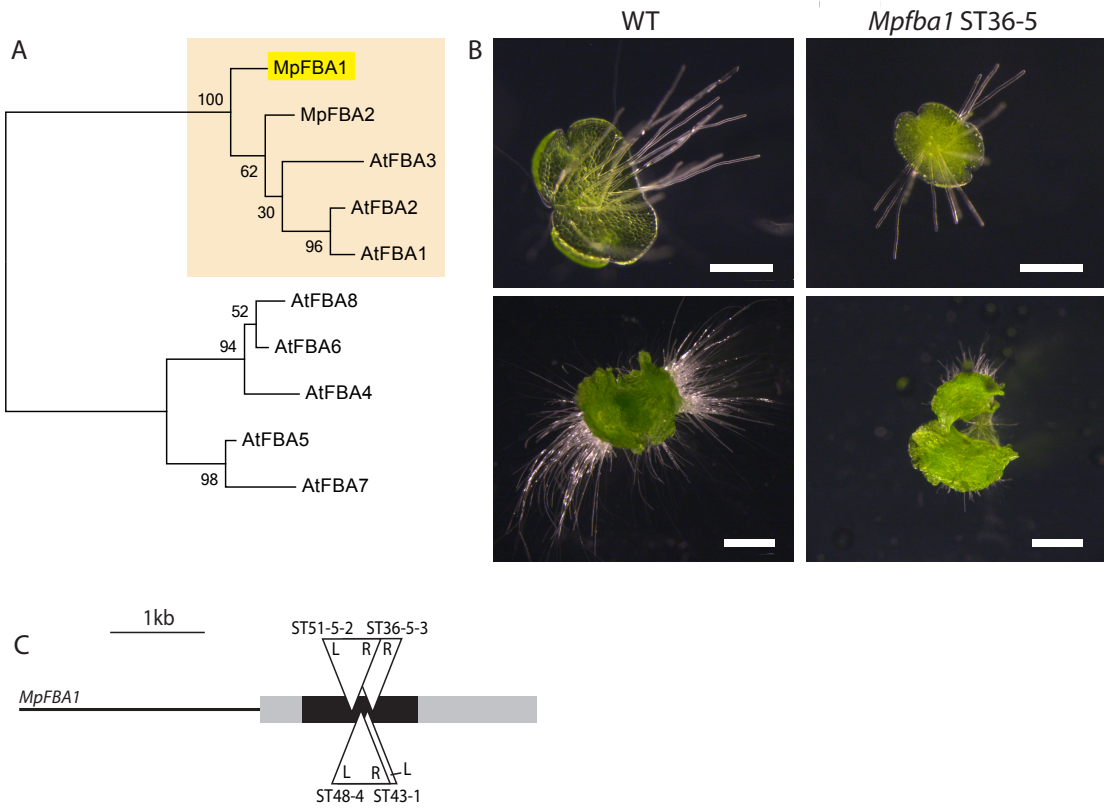

Figure 3.17 The *M. polymorpha* fructose-bisphoshpate aldolase *MpFBA1* is required for rhizoid development. A) Phylogenetic tree of *M. polymorpha* and Arabidopsis chloroplastic fructose bisphosphate aldolase proteins. The tree was rooted using the Arabidopsis cytosolic fructose bisphosphate aldolases. B) 2 day old gemmae (top row, scale bar 500 µM) and 10 day old gemmae (bottom row, scale bar 2 mm) of wild type (right) and *Mpfba1* mutant ST36-5 (left). C) *MpFBA1* gene model indicating the location and orientation of the T-DNA insertions in the *Mpfba1* mutants ST51-5-2, ST36-5-3, ST43-1 and ST48-4. L and R stand for T-DNA left and right border, respectively

3.3.4. Many Arabidopsis multicopy genes are present as a single gene in *M. polymorpha*

Of the 24 rhizoid development genes with predicted Arabidopsis homologs, 16 were present as single-copy genes in *M. polymorpha*, while only 2 genes (*SCD* and *AP5M*) were single-copy genes in Arabidopsis (Table 3.6). The most striking example was the *Catharanthus roseus RLK1-like* (*CrRLK1L)* family of receptor-like kinases, which have 17 members in Arabidopsis, whereas *M. polymorpha* has a single *CrRLK1L* family gene (Table 3.6, Fig. 3.4). Similarly, *M. polymorpha* has a single class A *GATA* transcription factor gene, while the Arabidopsis genome encodes for 14 class A *GATA* transcription factors (Table 3.6, Fig. 3.14). Genes involved in vesicle transport were often present as 1-2 copies in Arabidopsis, whereas the copy number of the Arabidopsis genes belonging to the other functional categories was in most cases more than 2. This finding suggests the presence of selective constrains that suppress the copy number of vesicle transport associated genes. Taken together, these findings indicate that many genes involved in filamentous rooting cell development are likely to have undergone gene duplications in the lineage leading to flowering plants. Alternatively, the gene copy number may have become reduced in the liverwort lineage.

Table 3.6 Number of predicted Arabidopsis homologs, their expression pattern and published root hair defective mutant phenotypes of the *M. polymorpha* rhizoid development genes. Homologous genes were identified using OrthoFinder (Emms and Kelly, 2015) and phylogenetic analysis. The expression data was obtained from the Arabidopsis eFP Browser 2.0. Details of the publications describing the root hair defective mutant phenotypes are provided in table A3.2 in the chapter 3 appendix.

				in Arabidopsis	
RHIZOID PRECURSOR CELL DIFFERENTIATION		**similar genes in *M. Polymorpha***	**similar genes in Arabidopsis**	**root hair enriched expression**	**root hair defective mutant phenotype**
MpRSL1	bHLH transcription factor	1	2	yes	yes
MpFRH1	miRNA	1	-	-	
CELL WALL SYNTHESIS					
MpCSLD1	cellulose synthase-like class D	6	6	yes	yes
MpCSLD2	cellulose synthase-like class D	6	6	yes	yes
MpXUT	xyloglucan-specific galacturonosyltransferase	3	11	yes	yes
MpGMP	GDP-mannose pyrophosphorylase	1	2		seedling lethal
MpRHM1	rhamnose biosynthesis	2	4	yes	yes
MpTHE	CrRLK1 family receptor-like kinase	1	17	yes	yes
VESICLE TRANSPORT					
MpPI4Ka	1-phosphatidylinositol 4-kinase alpha	2	2		
MpSRI1	Rab guanine nucleotide exchange factor, similar to *S. Cerevisiae RIC1*	1	2	yes	
MpSCD	Rab guanine nucleotide exchange factor	1	1	yes	yes
MpSPI	WD-40 repeat protein	1	2	yes	yes
MpXIA	Class XI myosin	1	13	yes	yes
MpAP5M	AP-5 complex subunit mu	1	1	yes	
MpSRI2	calcium binding EF-hand family protein, similar to *S. Cerevisiae PAN1*	2	2	yes	

Table 3.6 continued

				in Arabidopsis	
OTHER/UNKNOWN FUNCTION		**similar genes in *M. Polymorpha***	**similar genes in Arabidopsis**	**root hair enriched expression**	**root hair defective mutant phenotype**
MpALBA	alba-like DNA/RNA-binding protein	1	3		
MpFBA1	fructose-bisphosphate aldolase	2	3		
MpGATA1	class A GATA zinc finger transcription factor	1	14	yes	
MpIRE	AGC-kinase	1	4	yes	yes
MpPTI	serine/threonine kinase	1	11	yes	
MpTMT	tonoplast monosaccharide transporter	1	3	yes	
MpWDL	predicted microtubule binding protein / TPX2 domain containing protein	1	8	yes	
MpSRI3	unknown protein	2	4		
MpREN	Pleckstrin homology (PH) domain / RhoGAP domain-containing protein	1	2		
MpXF	squalene monooxygenase	1	3		yes

3.3.5. Many of the *M. polymorpha* rhizoid development genes are likely to have a conserved role in filamentous rooting cell development

The expression pattern of all the Arabidopsis homologs of the *M. polymorpha* rhizoid development genes recorded on the Arabidopsis eFP Browser 2.0 was determined. All homologous groups that contained one or more genes with root hair cell enriched expression in the root epidermis are presented on table 3.6. Of the 24 groups of homologous genes, members of 17 groups displayed root hair enriched expression. Furthermore, in most cases the groups also contained genes highly expressed in pollen. Therefore, many of the Arabidopsis homologs of the *M. polymorpha* rhizoid development genes have enriched expression in the two tip growing cell types, suggesting these genes are likely to have roles in tip growth.

I searched the literature for the mutant phenotypes of the Arabidopsis homologs of the *M. polymorpha* rhizoid development genes. Eleven of the 24 groups of Arabidopsis genes have been shown to be required for root hair development based on their root hair defective mutant phenotypes (Table 3.6, Table A3.2). Therefore, many similar genes are required for filamentous rooting cell development in liverworts and flowering plants. Furthermore, 7 groups contained one or more genes that have root hair enriched expression, but no published root hair defective mutant phenotype (Table 3.6). Analysis of loss-of-function mutants, and potentially generating double and triple knock-outs for genes predicted to function redundantly, will determine if these genes have a role in root hair development.

3.3.6. Similar genes are required for cell wall synthesis and cell wall integrity during the elongation of rhizoids and root hairs

During tip growth, new cell wall materials are continuously synthesised and secreted at the apex of the elongating cell. The plant cell wall consists of cellulose microfibrils that are cross-linked together by non-covalently bound hemicellulose, and embedded in a pectin matrix (reviewed in Cosgrove, 2005). The identity of the genes I discovered to be involved in *M. polymorpha* rhizoid development from my mutant screen suggest many similar genes are required for cell wall synthesis and integrity in root hairs and rhizoids.

CSLD genes are required for the development of tip growing cells in M. polymorpha, Arabidopsis and rice

In Arabidopsis, primary cell wall cellulose microfibrils are synthesised by (1->4)-beta-glucan synthases belonging to the CELLULOSE SYNTHASE (CESA) family (Cosgrove, 2005). In addition to the CESA family genes, the Arabidopsis genome contains seven families of similar cellulose synthase-like (*CSL*) genes, of which cellulose synthase-like D (*CSLD*) family genes are thought to be involved in synthesis of nonmicrofibrillar (1->4)-beta-glucan (Yin *et al*., 2009; Park *et al*., 2011). Two cellulose synthase-like D (*CSLD*) family genes were identified to be involved in *M. polymorpha* rhizoid development (Fig. 3.2). Three mutants with very short rhizoids had a T-DNA insertion within the coding sequence of a predicted *CSLD* gene, named *MpCSLD1*. A further five mutants with a milder rhizoid elongation defect were identified with a T-DNA insertion in a second *CSLD* family gene named *MpCSLD2*.

Both *M. polymorpha* and Arabidopsis genomes contain six predicted *CSLD* genes. In phylogenetic analysis the *M. polymorpha CSLD* genes form a strongly supported clade with Arabidopsis *CSLD1-4* and *CSLD6*, while *AtCSLD5* is sister to all *M. polymorpha* and Arabidopsis *CSLD* genes (Fig. 3.2). Four of the six Arabidopsis *CSLD*s have been described as playing a role in tip-growth; *AtCSLD3* and *AtCSLD2* are required for root hair elongation, while *AtCSLD1* and *AtCSLD4* are required for pollen tube growth (Bernal *et al*., 2008; Favery *et al*., 2001; Wang *et al*., 2001). In addition, a *CSLD* family gene has been described to be involved in root hair elongation in rice (Kim *et al.,* 2007). These results suggest *CSLD* family genes are required for the development of tip growing cells in *M. polymorpha*, Arabidopsis and rice. The *M. polymorpha csld1* mutant rhizoid tips are often brown, indicative of cell rupture (Fig. 3.18). Similarly, the Arabidopsis *csld3* mutant root hairs burst at their tips soon after the bulge stage, whereas the *Atcsld2* mutant most root hairs burst later during the elongation phase (Bernal *et al*., 2008; Favery *et al*., 2001). Together, these findings indicate that *CSLD* genes are required for correct cell wall deposition and cell wall integrity during tip growth in both *M. polymorpha* and *Arabidopsis*, suggesting that the function of *CSLD* genes as a part of the tip growth machinery is likely to be ancient and conserved across land plants.

A predicted xyloglucan-specific galacturonosyltransferase is required for filamentous rooting cell development in both M. polymorpha and Arabidopsis

Cellulose microfibrils are cross-linked together by branched hemicellulose chains in plant cell walls. Xyloglucan is a constituent of the hemicellulose fraction of

land plant cell walls. Family GT47 glycosyltransferase XYLOGLUCAN-SPECIFIC GALACTURONOSYLTRANSFERASE 1 (*XUT1)* is required for root hair development in Arabidopsis (Pena *et al*., 2012). *AtXUT1* catalyses the addition of galacturonic acid to xyloglucan generating acidic xyloglucan (Pena *et al.,* 2012). Similarly, a *M. polymorpha* mutant line with a T-DNA insertion within the coding sequence of a predicted family GT47 glycosyltransferase gene similar to the *AtXUT1* had very short, uneven rhizoids (Fig. 3.3). In *M. polymorpha*, there are a further two genes similar to *MpXUT1*, while there are 10 *MpXUT1*-like genes in Arabidopsis. *MpXUT1* is most similar to two Arabidopsis genes, At5g41250 and *AtXUT1*, however overall the topology of the phylogenetic tree is poorly resolved indicating high sequence similarity between the *MpXUT1*-like Arabidopsis genes (Fig. 3.3). The Arabidopsis *xut1* mutant is defective in root hair elongation (Pena *et al.,* 2012) and the expression of the wild type gene is enriched in root hair forming cells of the root (Arabidopsis eFP Browser 2.0). Moreover, the *Atxut1* mutant growth defect is restricted to root hair cells suggesting a tip growth specific function (Pena *et al*., 2012). Pena *et al*. (2012) postulated that the short root hair phenotype of the *Atxut1* mutant could result from reduced extensibility of the cell wall restricting cell elongation. In contrast, the rhizoid tips of *M. polymorpha xut1* mutant often burst during the elongation phase, suggesting *MpXUT1* function is required for rhizoid cell wall integrity during tip growth (Fig. 3.18). These findings suggest that a glycosyltransferase similar to *AtXUT1* and *MpXUT1* is required for cell elongation in both root hairs and rhizoids. However, if MpXUT1 and AtXUT1 are functionally conserved, the way in which the function of these genes alters the physical properties of the cell wall needs to be re-evaluated.

Catharanthus roseus RLK1-like family proteins are required for cell wall integrity in M. polymorpha and Arabidopsis

In Arabidopsis, several members of the *Catharanthus roseus RLK1-like* (*CrRLK1L*) family of receptor-like kinases have been implicated in regulation of cell wall integrity and tip growth (Boisson-Dernier *et al*., 2009; Miyazaki *et al*., 2009; Duan *et al*., 2010). Similarly, a T-DNA insertion at the 3'UTR of a predicted *M. polymorpha Catharanthus roseus CrRLK1L* family gene *MpTHESEUS (THE)* resulted in strongly defective rhizoid elongation and bursting of most rhizoids during the early elongation phase (Fig. 3.18) suggesting that *MpTHE* is required for cell wall integrity in elongating rhizoids. Arabidopsis has 17 *CrRLK1L* family genes, whereas the *M. polymorpha* genome contains a single *CrRLK1L* gene most similar to Arabidopsis *THESEUS* (Fig. 3.4) (Cheung and Wu, 2011). *CrRLK1L* family genes encode plasma membrane receptor-like kinases that contain an extracellular ligand-binding domain and an intracellular kinase domain (Cheung and Wu, 2011). Typically, binding of a ligand to the extracellular ligand-binding domain of receptor-like kinases alters the activity of the intracellular kinase domain and doing so triggers an intracellular signaling cascade. The downstream signaling pathway from many CrRLK1 subfamily receptor-like kinases functions through activation of ROS production by NADPH oxidases (Duan *et al.,* 2010; Boisson-Dernier *et al*., 2013; Kessler *et al*., 2015). Treatment of Arabidopsis roots with ROS inhibits root hair elongation, while treatment with ROS scavengers ascorbic acid and MCLA results in bursting of growing root hairs (Monshausen *et al*., 2007). These findings suggest ROS promote rigidification of the cell wall during tip growth. During tip growth, co-ordinated relaxation and rigidification of the cell wall must take place to allow extension of

the existing wall with newly deposited cell wall materials without bursting. Therefore, *MpTHE* may be involved in coupling cell wall integrity with NADPH oxidase activity at the tips of growing rhizoids, resulting in regulation of ROS production and appropriate levels of cell wall relaxation and rigidification during rhizoid elongation. To test this hypothesis, we could test if treatment with ROS is sufficient to rescue the *Mpthe* mutant rhizoid integrity defect.

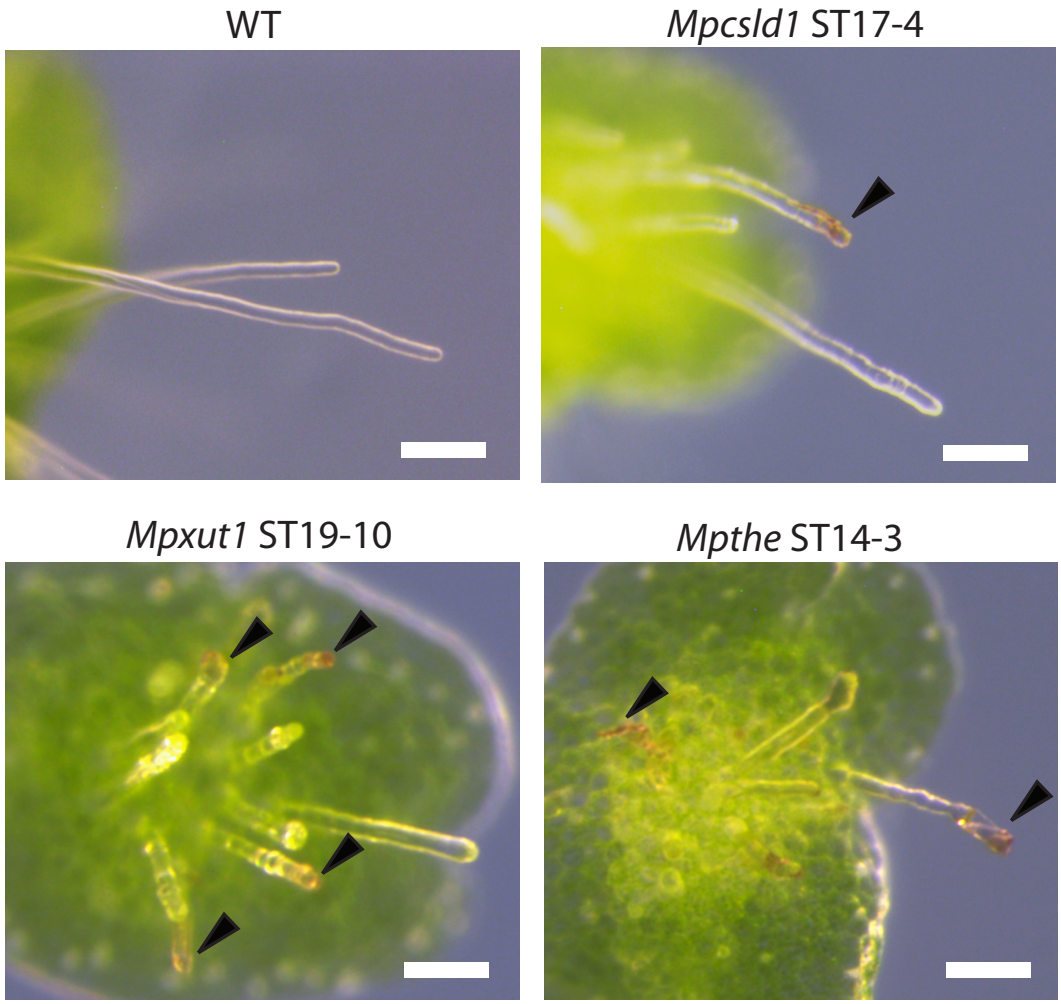

Figure 3.18 *MpCSLD1*, *MpXUT1* and *MpTHE* are required for cell wall integrity in elongating rhizoids. Rhizoid tips on 2 day old gemmae of wild type, *Mpcsld1*, *Mpxut1* and *Mpthe* mutant. The arrows indicate brown rhizoid tips indicative of cell wall rupture. Scale bar 100 µm.

In addition to the genes identified to be required for cell wall integrity based on the burst rhizoids of the mutants, further genes likely to be involved in rhizoid cell wall synthesis were identified based on their sequence similarity with Arabidopsis cell wall biosynthetic genes.

T-DNA insertion in the *M. polymorpha* gene similar to the Arabidopsis *GDP-MANNOSE PYROPHOSPHORYLASE1* (*GMP1)* resulted in short rhizoids (Fig. 3.5). The Arabidopsis GMP1 catalyses a reaction that produces GDP-D-mannose (Lukowitz *et al*., 2001). GDP-D-mannose is a precursor of GDP-L-fucose and ascorbic acid. Both GDP-D-mannose and GDP-L-fucose provide a source of mannosyl and fucosyl residues that are incorporated into the hemicellulosic fraction of the primary cell wall. In addition, GDP-D-mannose forms the core of the glycan side chain added to many cell wall proteins through N-glycosylation (Pattison and Amtmann, 2009). These findings suggest that the *MpGMP* function is required for rhizoid elongation in *M. polymorpha*, possibly through generating mannose residues for N-glycosylation or to be incorporated to the cell wall hemicellulose.

Rhamnose is a constituent of the plant cell wall pectin matrix. T-DNA insertion in a *M. polymorpha* gene similar to the Arabidopsis *RHAMNOSE BIOSYNTHESIS1-3* (*RHM1-3*) genes resulted in a strong reduction in rhizoid elongation (Fig. 3.6). Similarly, the Arabidopsis *rhm1* mutant has short root hairs and altered cell wall pectin composition (Diet *et al*., 2006; Ringli *et al*., 2008). All three closely related Arabidopsis RHM proteins function in rhamnose biosynthesis (Watt *et al*., 2004; Oka *et al*., 2007). Therefore, the *M. polymorpha RHM1* gene is also likely to be involved in rhamnose biosynthesis. The rhamnose component of

the pectin matrix may be important for the elasticity of the cell walls, enabling cell expansion during the elongation of root hairs and rhizoids.

3.3.7. Rhizoid elongation requires genes associated with actin cytoskeleton dynamics and vesicle transport machinery

During tip growth, newly synthesised cell wall materials and cell wall proteins are continuously transported to the growing apex of the cell in exocytic vesicles, while excess materials are recycled back from the apex through the endocytic vesicle transport pathway (Brandizzi and Wasteneys 2013). The actin cytoskeleton plays an important role in directing vesicle trafficking in plant cells (Rounds and Bezanilla, 2013). Consequently, the factors involved in modifying of the actin cytoskeleton are functionally linked with vesicle trafficking.

Seven genes likely to be involved in vesicle trafficking and actin cytoskeleton modification were found to be required for *M. polymorpha* rhizoid development (Table 3.6). Loss-of-function mutations in Arabidopsis genes similar to 3 of these genes (*MpSCD*, *MpSPI* and *MpXIA*) have been reported to result in defective root hair elongation (Table 3.6, Table A3.2). Genes similar to the remaining 4 vesicle trafficking associated genes (*MpPI4Kα*, *MpSRI1*, *MpSRI2* and *MpAP5M*) are present across land plants, however mutants for plant similar genes have not been described in published literature. Therefore, the rhizoid defective mutants identified here provide the first indication of the role of these genes in developmental processes in plants.

3.3.8. The *M. polymorpha* rhizoid defective mutants identify 14 genes with a novel role in filamentous rooting cell development

I discovered 14 genes required for rhizoid development in *M. polymorpha*, for which the closest Arabidopsis homologs have not previously been shown to be involved in root hair development. For example, T-DNA insertion in a gene encoding for a predicted microtubule associated protein similar to Arabidopsis WAVE DAMPENED LIKE (WDL) family proteins (Fig. 3.11) resulted in the development of curly rhizoids. In Arabidopsis, two *WDL* clade genes *WVD1* and *WDL2* have been shown to be involved in regulation of microtubule organisation (Perrin *et al*., 2007). Treatment with drugs that interfere with microtubule stability results in curling of root hairs in Arabidopsis (Bibikova *et al*., 1999) and *M. polymorpha* (Clement Champion, unpublished data). Therefore, the curly rhizoid phenotype of the *M. polymorpha wdl* mutant is consistent with the hypothesis *MpWDL* regulates microtubule dynamics in rhizoids. The Arabidopsis *WDL* clade genes have not yet been shown to be required for root hair development. However, some of the Arabidopsis *WDL* family genes show strongly enriched expression in root hair cells. Therefore, it is likely that *WDL* genes also function in root hair development in flowering plants.

3.3.9. The first mutants with defects in six previously uncharacterised plant genes define genes required for rhizoid development

This screen identified mutations in 6 genes (*MpALBA, MpAP5M, MpPI4Kα, MpSRI1, MpSRI2, and MpSRI3*) that are present in the genomes of land plants but for which neither function nor mutant phenotypes have previously been described. For example, ALBA proteins are required for rhizoid elongation; *Mpalba* mutants develop short rhizoids (Fig. 3.15). *ALBA*-like genes encode for nucleic acid binding proteins that are present across archaea and eukaryotes (Aravind *et al*., 2003). Archaeal ALBA proteins have been shown to bind both DNA and RNA, and are thought to function in epigenetic regulation and RNA metabolism (Guo *et al*., 2003; Marsh *et al*., 2005). Further characterisation of the mutant phenotypes combined with functional characterisation of the genes will provide insight into the mechanism of function of these genes in plants.

3.3.10 Technical considerations

Gain-of-function mutants

T-DNA screens in Arabidopsis have been described to produce loss-of-function mutants in nearly all cases. In addition to likely loss-of-function mutants, I identified several putative gain-of-function mutants. Two mutants that lack rhizoids or rhizoid precursor cells were identified with a T-DNA insertion within the coding sequence of the *M. polymorpha* basic helix-loop-helix transcription factor Mp*RSL1.* A further 7 mutants, isolated based on ectopic rhizoid initiation on the upper dorsal

side of the thallus, had a T-DNA insertion in the promoter of *MpRSL1*. As the phenotype of the mutants with a T-DNA insertion in the *MpRSL1* promoter was opposite to those with a T-DNA insertion within the coding sequence of the gene, I hypothesised the promoter insertion mutants are *MpRSL1* gain-of-function mutants. Consistent with this hypothesis, the steady state transcript level of *MpRSL1* was found to be strongly elevated in the promoter insertion mutants (described in chapter 4). All *MpRSL1* gain-of-function mutants had the right border of the T-DNA insertion facing towards the coding sequence of the gene. The T-DNA insertion sequence near the right border contains a 35S-promoter driving the expression of a hygromycin resistance gene (Fig. 3.19). We hypothesise that the 35S-promoter does not have a strictly defined orientation in *M. polymorpha*, and therefore is sufficient to activate the expression of genes both upstream and downstream of it.



Figure 3.19 pCambia1300 T-DNA insert sequence. The pCambia1300 T-DNA sequence contains a gene for the plant selection marker hygromycin driven by the Cauliflower mosaic virus 35S-promoter.

Coverage of the screen

Assuming that the T-DNA is inserted in a random site in the genome, the probability of obtaining a T-DNA insertion in a given gene is given by the equation $P = 1 - (1 - \frac{y}{x})^n$ in which *P* is the probability, *y* is the size of the gene (in kb), *x* is the size of the genome (in kb) and *n* is the number of independent T-DNA insertions in the population screened (Krysan *et al*., 1999). The size of the *M. polymorpha* genome has been estimated to be 280 Mbp (Okada *et al*., 2000). The total number of independent T-DNA insertions in the population of 150,000 T-DNA transformed plants screened was estimated to be 172,500. The probability of obtaining a T-DNA insertion in a gene is dependent on the size of that gene. Therefore, with 172,500 T-DNA insertions in the population of plants screened, the probability of obtaining at least one T-DNA insertion in a given gene is 91.5 % for each 4 kb gene, but drops down to 70.8 % for 2 kb genes and 50 % for 1 kb genes. In addition, it is worth keeping in mind that previous studies on Arabidopsis T-DNA insertion lines suggest T-DNA insertion sites are not randomly distributed in the genome (Szabados *et al*., 2002; Krysan *et al*., 2002; Alonso *et al*., 2003; Li *et al*., 2006). Instead, the insertion events are positively correlated with the gene density of the chromosomal region, while T-DNA insertions on the centromeric, telomeric and interspersed regions or ribosomal RNA genes were relatively rare (Szabados *et al*., 2002; Krysan *et al*., 2002; Alonso *et al*, 2003). Furthermore, within the gene rich regions, the T-DNA is preferentially inserted within promoter regions or at transcription start and termination sites (Szabados *et al*., 2002; Alonso *et al*., 2003; Pan *et al.*, 2005; Li *et al.*, 2006). Despite these limitations, the mutant screen described here together

with the further 186,000 T-DNA insertion lines generated and screened by colleagues V. Jones and G. Morieri is likely to have resulted in good coverage of the genome.

3.4. Conclusion

Based on the *M. polymorpha* rhizoid developmental genes identified here, the role of many genes involved in cell wall biosynthesis in tip growing cells is likely to be conserved between liverworts and vascular plants. Cellulose synthase-like class D genes, *XUT1*-like predicted xyloglucan-specific galacturonosyltransferase, *CrRLK1L* family receptor-like kinase and *RHM-like* gene are required for both rhizoid development in *M. polymorpha* and root hair development in Arabidopsis. However, the composition of the cell wall in liverworts is thought to be markedly different from that of vascular plants (reviewed in Sarkar *et al*., 2009). Therefore, these findings may suggest that the last common ancestor of liverworts and vascular plants had tip growing cells whose development required *CSLD, XUT1*-like, *CrRLK1L* and *RHM*-like genes and the role of these genes has remained conserved, while other factors that define the composition of the cell wall have diverged between the two lineages.

A diversity of genes involved in the organisation of the actin cytoskeleton and endocytic vesicle trafficking are required for rhizoid development in *M. polymorpha*. A subset of these genes have characterised Arabidopsis homologs, all of which are required for root hair development. Therefore, many similar components with the endocytic vesicle transport machinery are required for tip growth in both liverworts and flowering plants. Although the transport of cell wall materials to the apex of the elongating cell through the exocytic pathway is also likely to be important during tip growth, no mutants for genes associated with

exocytosis were identified in this screen. This suggests perturbations of the exocytic pathway may be lethal.

Many flowering plant gene families or subfamilies were found to be present as single-copy genes in *M. polymorpha*. Furthermore, many similar genes were found to be required for tip growth in both liverworts and flowering plants, suggesting that multiple aspects of the tip growth machinery are conserved between flowering plants and liverworts. Therefore, characterisation of the rhizoid defective *M. polymorpha* mutants described here is likely to provide useful insights into the function of the members of those multi-copy gene families in flowering plants.

The screen of 150,000 *M. polymorpha* T-DNA insertion lines described here, together with the 185,000 lines screened by colleagues V. Jones and G. Morieri, is likely to have resulted good coverage of the *M. polymorpha* genome. However, many Arabidopsis gene families are represented by a single-copy gene in *M. polymorpha*. Consequently, as T-DNA insertions in most cases induce complete loss of gene function, this low level of redundancy observed in the *M. polymorpha* genome is likely to lead to loss-of-function mutations in subset of rhizoid developmental genes being lethal. Therefore, further mutant screens using point mutation inducing mutagens that more commonly produce weak mutant alleles, would most likely result in identification of additional genes involved in *M. polymorpha* rhizoid development.

Chapter 4

The *M. polymoprha* class I *RSL* gene *MpRSL1* is a positive regulator of rhizoid precursor cell differentiation

4.1. Summary

Virtually all land plants have filamentous rooting cells; root hairs that develop from the epidermal cells of the axial roots in the diploid sporophyte generation or rhizoids that develop from the epidermal cells of the haploid gametophyte generation. Here I demonstrate that an ancient genetic mechanism controls the development of root hairs and rhizoids. Loss-of-function mutation in the liverwort *Marchantia polymorpha* class I RSL gene *MpRSL1* resulted in loss of rhizoids and rhizoid precursor cells. Conversely, T-DNA insertion within the *MpRSL1* promoter resulted in elevated *MpRSL1* expression and ectopic rhizoid differentiation from dorsal thallus epidermal cells. Therefore, *MpRSL1* is necessary and sufficient for rhizoid precursor cell differentiation from epidermal cells. As class I *RSL* genes have previously been shown to be required for root hair differentiation in flowering plants, these findings suggest the class I *RSL* gene mechanism is ancient and most likely to have originated before the liverwort and flowering plant lineages diverged more than 440 Mya. Furthermore, the function of *MpRSL1* is not restricted to rhizoid development, but *MpRSL1* is also required for the development of mucilage papillae and gemmae. The first step in each of these *MpRSL1* regulated processes is outgrowth of a single epidermal cell. This may reflect the ancestral function of class I *RSL* genes, or alternatively class I *RSL* genes may have evolved these novel developmental roles in the liverwort lineage.

4.2. Introduction

Evolution of transcription factor networks that regulate the development of an organisms body plan underpins the evolution of morphological complexity in living organisms. Increased morphological complexity is likely to have played a crucial role when the ancestors of first land plants evolved from streptophyte algae and colonised land more than 470 million years ago. One of the morphological innovations that co-occurred when plants colonised the land was the evolution of specialised rooting cells that enabled anchorage and nutrient acquisition.

An ancient genetic mechanism regulates the development of filamentous rooting cells in land plants. The basic helix-loop-helix transcription factors encoded by class I *RSL* genes (*ROOT HAIR DEFECTIVE SIX-LIKE*) function as positive regulators of root hair development on the diploid sporophyte generation of *Arabidopsis* and other flowering plants (Menand *et al*., 2007; Dolan lab, unpublished data). Similarly, class I *RSL* genes positively regulate rhizoid differentiation on the haploid leafy gametophore of the moss *Physcomitrella patens* (Menand *et al*., 2007; Jang *et al*., 2011). Furthermore, constitutive over-expression of the two *P. patens* class I *RSL* genes converts most of the developing leafy gametophore tissue into rhizoids, indicating that in moss class I *RSL* gene expression is sufficient to promote rhizoid initiation from cells that do not produce rhizoids in the wild type (Jang *et al*., 2011). In addition to rhizoid development, the *P. patens* class I *RSL* genes are also required for the development of caulonema: a second type of tip growing cells with rooting functions that form at the filamentous protonema stage of the moss life-cycle (Menand *et al*., 2007). These findings indicate that the role of class I *RSL* genes as

positive regulators of filamentous rooting cell development is conserved between moss and flowering plants, and likely to have originated before the two lineages diverged more than 443 Mya.

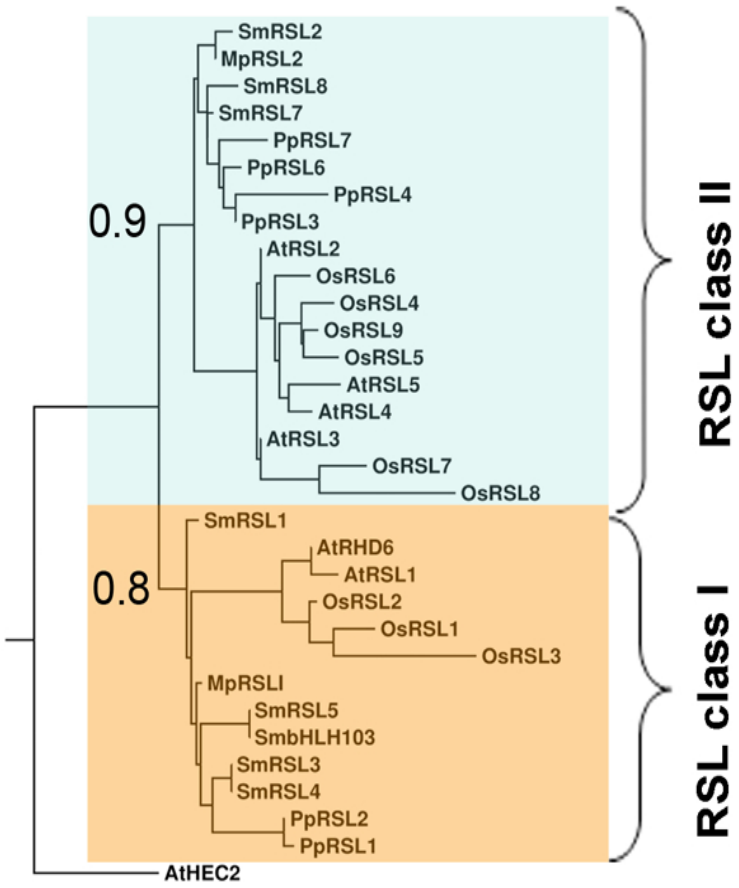

Figure 4.1 *M. polymorpha* has a single class I *RSL* gene. Maximum likelihood tree of RSL proteins from the liverwort *Marchantia polymorpha* (Mp), the moss *Physcomitrella patens* (Pp), the lycophyte *Selaginella moellendorffii* (Sm), the dicot *Arabidopsis thaliana* (At) and the monocot *Oryza sativa* (Os). The tree was rooted using Arabidopsis basic helix-loop-helix transcription factor AtHEC2. (Helene Proust, unpublished data)

The liverwort *M. polymorpha* has a single class I *RSL* gene (Fig. 4.1). In this chapter I describe the function of the *M. polymorpha* class I *RSL* gene *MpRSL1* as a positive regulator of rhizoid development based on the characterisation of the *Mprsl1* loss-of-function and gain-of-function mutants isolated in the screen for *M. polymorpha* mutants with defective rhizoid development (described in chapter 3). Characterisation of *M. polymorpha* mutants defective in class I *RSL* gene function reveals novel developmental roles for class I *RSL* genes in the liverwort lineage. These novel roles may give an indication of the ancestral function of the class I *RSL* gene mechanism in the common ancestor of land plants.

4.3. Results

4.3.1. The class I *RSL* gene *MpRSL1* is required for rhizoid development in *M. polymorpha*

Two rhizoidless *M. polymorpha* T-DNA insertion lines (ST44-8 and ST46-1) were identified in the screen for mutants defective in rhizoid development (chapter 3). I carried out TAIL-PCR to identify the T-DNA insertion sites in these mutants. There was a T-DNA insertion within the coding sequence of *MpRSL1, M. polymorpha* single-copy class I *RSL* gene, in each of the two rhizoidless mutants (Fig. 4.2B). T-DNA insertion within the coding sequence of a gene is likely to disrupt the coding sequence and result in loss-of-function mutation. The two putative *MpRSL1* loss-of-function mutants were named *Mprsl1-1* and *Mprsl1-2*. The *Mprsl1-1* T-DNA insertion is at the end of the second exon, whereas in *Mprsl1-2* the T-DNA is inserted in the intron between the second and third exons.

I carried out qRT-PCR analysis to measure the levels of *MpRSL1* expression in the two putative *Mprsl1* loss-of-function mutants. Steady state levels of *MpRSL1* mRNA were similar to wild type in *Mprsl1-1*, while no *MpRSL1* transcript was detected in *Mprsl1-2* (Fig 4.2A). The primers used amplify across the second intron of *MpRSL1*, in which *Mprsl1-2* has a T-DNA insertion. This suggests that a T-DNA insertion in the second intron of *MpRSL1* in *Mprsl1-2* mutant results in defective splicing therefore disrupting the coding sequence of the gene. As the phenotypes of *Mprsl1-1* and *Mprsl1-2* lines are identical, it is likely that the transcript produced in *Mprsl1-1* is also non-functional and both mutants are loss-of-function mutants.

Together, these findings suggest that *MpRSL1* function is required for rhizoid development in *M. polymorpha*.

MpRSL1 is required for rhizoid precursor cell differentiation

As no rhizoids were observed in the *Mprsl1* loss-of-function mutants, I hypothesised that *MpRSL1* may be involved in the differentiation of the cells that give rise to rhizoids. In *M. polymorpha*, rhizoid precursor cells are most easily observed on young gemmae. Gemmae are disc-shaped asexual reproductive propagules that initiate rhizoids early in their development on both dorsal and ventral sides (Taren, 1958; Ishizaki *et al*., 2012). In wild type *M. polymorpha*, the rhizoid precursor cells on gemmae can be distinguished as larger lighter cells in the mid region of the young gemmae, while non-rhizoid precursor cells are smaller and darker green (Fig. 4.3A) (Vashishta *et al*., 2011). In contrast, *Mprsl1* mutant gemmae had no clearly differentiated rhizoid precursor cells (Fig. 4.3B). These findings suggest that *MpRSL1* is required for differentiation of cells that give rise to rhizoids.

4.3.2. *MpRSL1* is a positive regulator of rhizoid precursor cell differentiation

In mature fully differentiated wild type *M. polymorpha* thallus, rhizoid growth is restricted to the lower ventral side of the thallus. Eight T-DNA insertion lines that grew rhizoids ectopically on the upper dorsal side of their thallus were isolated in the rhizoid mutant screen described in chapter 3. Seven of the eight dorsal rhizoid mutant lines were identified to have a T-DNA insertion within the

promoter of *MpRSL1* using TAIL-PCR (Fig. 4.2). The remaining dorsal rhizoid mutant was found to be allelic to the *MpRSL1* promoter insertion mutants based on an allelic cross. Thus, all the dorsal rhizoid mutants identified in this screen had a T-DNA insertion within the promoter of *MpRSL1*.

As the phenotype of the mutants with a T-DNA insertion in the *MpRSL1* promoter was opposite to that of the putative *Mprsl1* loss-of-function mutants, I hypothesised that the promoter insertion mutants would harbor gain-of-function mutations that confer elevated levels of *MpRSL1* expression. To test this hypothesis, I carried out qRT-PCR analysis on three lines with a single T-DNA insertion on the *MpRSL1* promoter (ST21-3, ST44-1 and ST53-1). As predicted, the steady state levels of *MpRSL1* mRNA were highly elevated in all the three dorsal rhizoid mutant lines (Fig. 4.2). Therefore, T-DNA insertion within the *MpRSL1* promoter resulted in elevated expression of *MpRSL1* and ectopic rhizoid growth. This indicates the dorsal rhizoid mutants are *MpRSL1* gain-of-function mutants, and therefore from now on denoted as $MpRSL1^{GOF}$.

The $MpRSL1^{GOF}$ lines initiate rhizoids ectopically on the dorsal side of the mature thallus, suggesting *MpRSL1* can promote differentiation of dorsal thallus epidermal cells into rhizoid precursor cells. As these dorsal epidermal cells do not differentiate as rhizoids in wild type, these data suggest that *MpRSL1* is a positive regulator of rhizoid precursor cell differentiation. Moreover, elevated *MpRSL1* expression is sufficient to induce ectopic rhizoid precursor cell differentiation in cells that do not typically give rise to rhizoids.

To demonstrate that ectopic rhizoid differentiation in the dorsal rhizoid mutants results from an intact T-DNA insertion, and to estimate the T-DNA copy number in each dorsal rhizoid mutant line, these mutants were backcrossed with wild type. The frequencies of hygromycin resistant and hygromycin sensitive F1 plants showing wild type and dorsal rhizoid phenotypes were scored (Table 4.1). In each of the crosses, all the F1 plants showing the dorsal rhizoid phenotype were hygromycin resistant, i.e. the hygromycin resistance gene on the T-DNA co-segregated with the dorsal rhizoid phenotype in the F1. Therefore, the dorsal rhizoid phenotype in all these mutants resulted from an insertion of an intact T-DNA sequence.

Table 4.1 The dorsal rhizoid phenotype of the *MpRSL1* gain-of-function mutants co-segregates with the hygromycin resistance on the T-DNA in the F1. Frequencies of hygromycin resistant and hygromycin sensitive F1 plants from a cross between the different *MpRSL1*^{GOF} lines and wild type. Probability (p) of obtaining the observed numbers of F1 plants showing mutant and wild type phenotype with the estimated T-DNA copy number was tested using the Chi-square test.

	Mut		WT		total		HygS:HygR	T-DNA	Expected	
line name	HygR	HygS	HygR	HygS	HygR	HygS	ratio	insertions	ratio	p
ST13-1	64	0	97	17	161	17	1: 9.5	3	1:7	0.234
ST19-15	82	0	77	44	159	44	1: 3.6	2	1:3	0.274
ST21-3	117	0	0	151	117	151	1: 0.8	1*	1:1	0.038
ST37-11	93	0	41	30	134	30	1: 4.5	2*	1:3	0.047
ST44-1	108	0	0	122	108	122	1: 0.9	1	1:1	0.356
ST53-1	106	0	0	123	106	123	1: 0.9	1	1:1	0.261
ST53-2	93	0	71	41	164	41	1: 4.0	2	1:3	0.098

*deviation from the expected number of F1 plants showing wild type and mutant phenotypes based on the estimated T-DNA copy number.

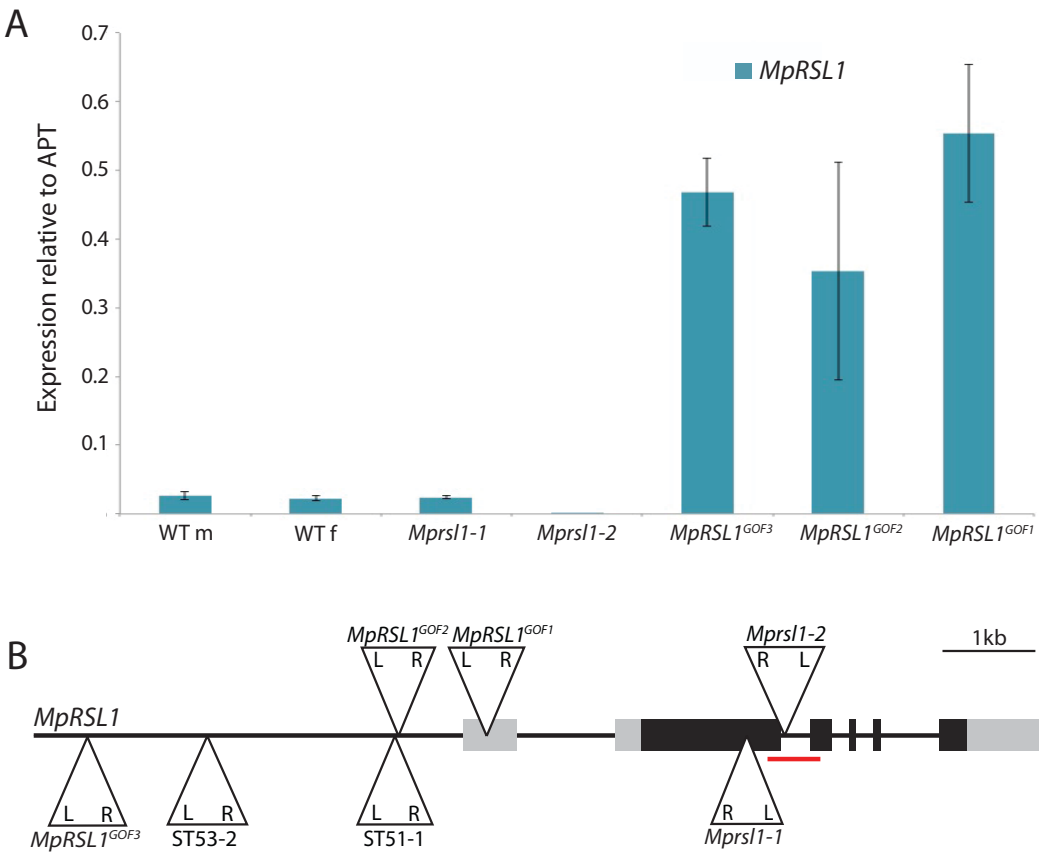

C

Distance from T-DNA right border to *MpRSL* ATG	
MpRSL^{GOF1}/ST53-1	1601bp
MpRSL^{GOF2}/ST44-1	2542bp
ST51-1	2594bp
ST53-2	4605bp
MpRSL^{GOF3}/ST21-3	5842bp
ST13-1	32730bp
ST19-15	34473bp

Figure 4.2 T-DNA insertions within the *MpRSL1* promoter resulted in elevated Mp*RSL1* expression. A) *MpRSL1* expression in 15 day old wild type *M. polymorpha* gemmae, and gemmae of mutants with T-DNA insertion within the *MpRSL1* coding sequence (*Mprsl1-1 and Mprsl1-2*) or on the *MpRSL1* promoter (*MpRSL1*^{GOF1}, *MpRSL1*^{GOF2}, *MpRSL1*^{GOF3}). Expression of *MpRSL1* quantified relative to *MpAPT*. The error bars indicate ± s.d. B) T-DNA insertion sites identified in the *MpRSL1* locus. L and R stand for T-DNA left and right border, respectively. The region amplified by the qRT-PCR primers is indicated in red. C) Ectopic rhizoid mutant T-DNA insertion sites within the *MpRSL1* promoter. Distance presented in basepairs from the T-DNA insertion right border to the beginning of the *MpRSL1* coding sequence.

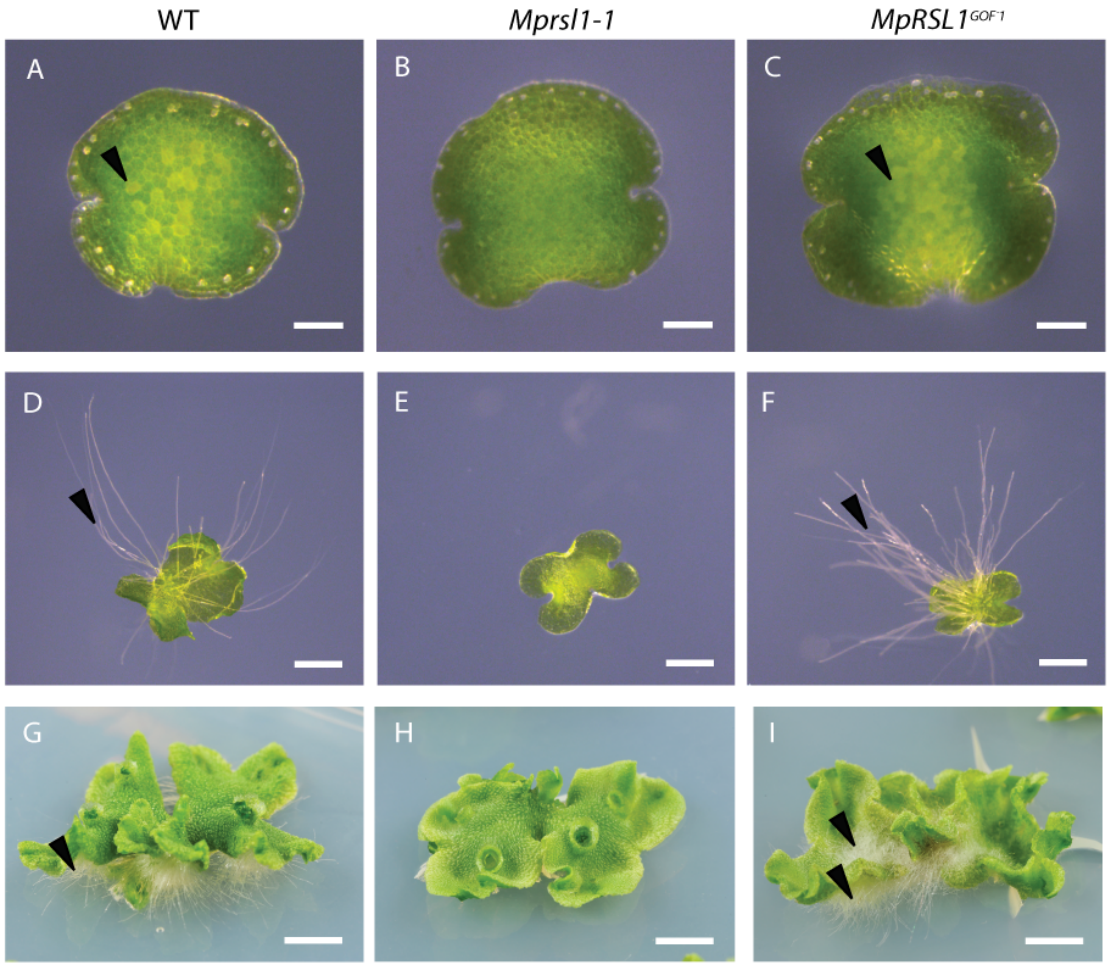

Figure 4.3 *M. polymorpha* wild type (A, D and G), *MpRSL1* loss-of-function (B, E and H) and gain-of-function mutant phenotypes (C, F and I). A-C) Young gemmae 5 hours after plating. Arrows indicate rhizoid precursor cells. Scale bar 100 µM. D-F) Four day old gemmae. Arrows indicate rhizoids. Scale bar 1 mm. G-I) 28 day old gemmae with fully differentiated thallus (G-I). Arrows indicate rhizoids. Scale bar 5 mm.

The three *MpRSL1*^{GOF} lines with a single T-DNA insertion (ST21-3, ST44-1 and ST53-1) were crossed with each other to confirm that the same gene is responsible for the dorsal rhizoid phenotype in these lines. After more than 100 individual F1 plants from each cross were observed, 100 % of the resulting F1 plants showed the dorsal rhizoid phenotype, indicating that ST21-3, ST44-1 and ST53-1 are allelic (Table 4.2).

Table 4.2 *MpRSL1*^{GOF} lines are allelic. Allelic crosses between the *MpRSL1*^{GOF} mutant lines ST21-3, ST44-1 and ST53-1 indicate that the same gene is responsible for the dorsal rhizoid phenotype in these mutants.

cross	F1 plants assayed	F1 with dorsal rhizoids	% F1 with dorsal rhizoids
ST44-1 x ST53-1	125	125	100%
ST44-1 x ST21-3	112	112	100%

The 35S-promoter on the T-DNA is likely to be responsible for the elevated MpRSL1 expression in the gain-of-function mutants

T-DNA insertion up to 34.5kb away from the beginning of the *MpRSL1* coding sequence was found to be sufficient to give the dorsal rhizoid phenotype observed in the *MpRSL1* gain-of-function mutants (Fig. 4.2). The T-DNA insertion right border was facing towards *MpRSL1* coding sequence in each of the seven dorsal rhizoid mutants. This suggests that the T-DNA right border sequence may be involved in the activation of the expression of nearby gene. The next transcript on the same genome scaffold is approximately 36 kb upstream of *MpRSL1*, suggesting that a T-DNA insertion right border towards the *MpRSL1* anywhere within the DNA sequence between the two genes is likely to be sufficient to activate *MpRSL1* expression. The 35S-promoter is next to the right border on the T-DNA but the promoter is facing towards the T-DNA left border. This suggests that the 35S-promoter directionality may not be strictly defined in *M. polymorpha*, and so in addition to the hygromycin resistance gene, the *M. polymorpha* gene next to the right border of the T-DNA insert may become over-expressed in T-DNA transformed plants.

4.3.3. *MpRSL1* function is not restricted to rhizoid development

The *MpRSL1* loss-of-function mutant phenotype is not strongly pleiotropic; most aspects of thallus growth in the *Mprsl1* mutants are similar to the wild type. This suggests *MpRSL1* has a specific regulatory function and it is not involved in basic cell growth processes. However, several other developmental processes were

found to be defective in the *Mprsl1* loss-of-function mutants suggesting that the function of *MpRSL1* is not restricted to rhizoid development.

MpRSL1 is required for gemmae development

In wild type *M. polymorpha,* cup-like structures called gemma cups form on the dorsal side of fully differentiated thalli (Fig 4.4). Disc-shaped gemmae develop inside the gemma cups, from which they are washed away by rain droplets or get pushed out when more gemmae are produced at the bottom of the gemma cup (Barner and Land, 1908; Taren, 1958). The gemmae cups of the *Mprsl1* loss-of-function mutants have no or very few gemmae (Fig. 4.4). In contrast, the *MpRSL1* gain-of-function mutants have gemmae cups full of gemmae. These findings suggest functional *MpRSL1* is required for gemmae development.

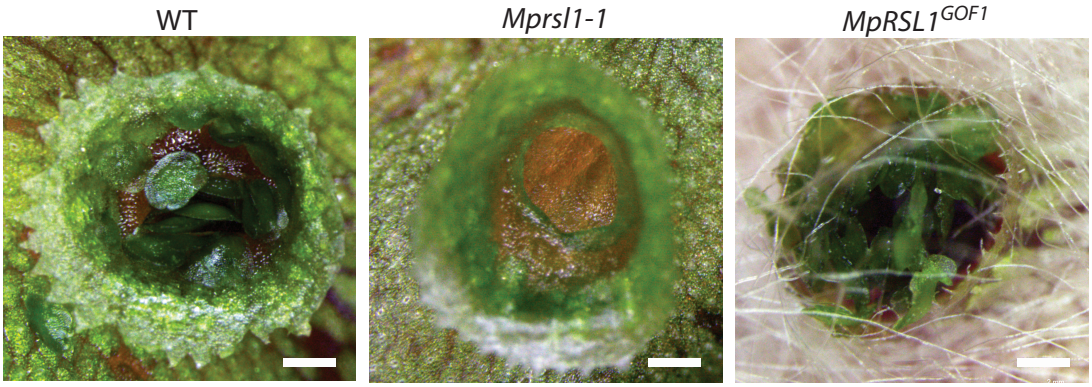

Figure 4.4 *MpRSL1* is required for gemma development. Gemma cups of wild type (A), *Mprsl1-1* (B) and *MpRSL1*^{GOF1} (C). Scale bar 800 µM.

MpRSL1 is required for the development of epidermal papillae

In wild type *M. polymorpha* gemmae, small tubular outgrowths of epidermal cells form near the meristem located in a notch between the expanding gemma lobes (Fig. 4.5A). The *Mprsl1* loss-of-function mutants lack these epidermal papillae (Fig. 4.5B). These findings suggest *MpRSL1* function is required for epidermal papilla development.

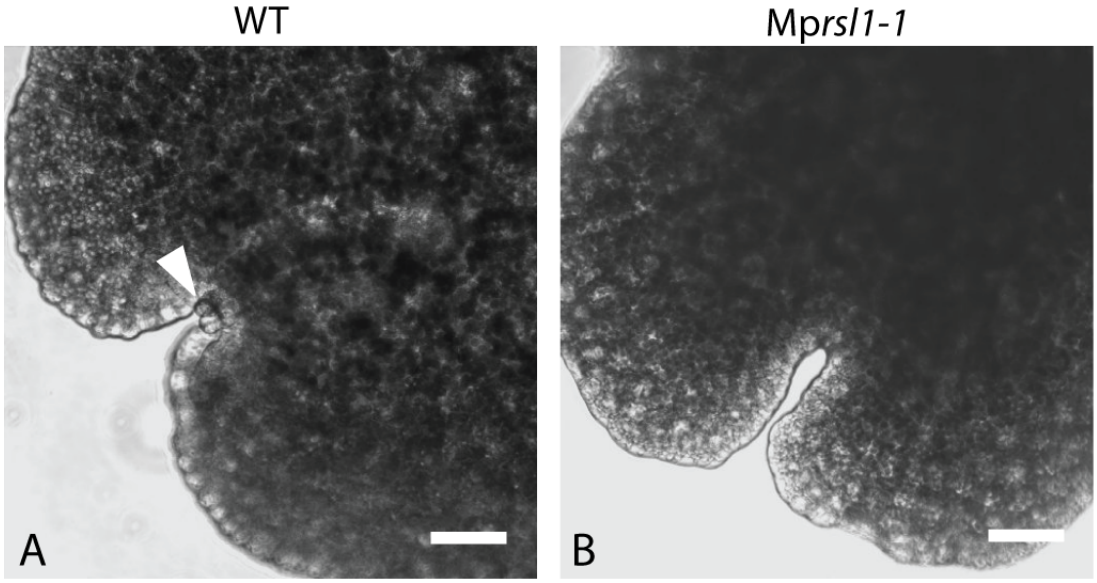

Figure 4.5 *MpRSL1* is required for the development of epidermal papillae. High magnification brightfield images showing the meristematic region of 1 day old gemma of wild type *M. polymorpha* (A) and *MpRSL1* loss-of-function mutant *Mprsl1-1* (B). The arrow is indicating the papillae. Scale bar 50 µm.

MpRSL1 is likely to be required for the induction of reproductive development or the formation of sexual reproductive structures

In *M. polymorpha*, the reproductive phase of the life-cycle commences by differentiation of the thallus apical meristem into a gametophore stalk. The gametophore stalk will elongate upwards, during which the gametophore apical

part will mature and begin to form the male or female gametes. The *Mprsl1* loss-of-function mutants were never observed to grow the gametophore stalk or any reproductive structures despite extended periods under inducing conditions. The induction of reproduction was recovered by introducing a functional copy of *MpRSL1* in the *Mprsl1* mutant background (Helene Proust, unpublished data). This suggests *MpRSL1* is likely to be required for the induction of the reproductive phase or during the earliest stages of gametophore development.

4.4. Discussion

Class I *RSL* genes have previously been shown to function as positive regulators of filamentous rooting cell development (root hairs, rhizoids and caulonema) in the angiosperm *A. thaliana* and the moss *Physcomitrella patens* (Menand *et al*., 2007; Jang *et al*., 2011; Dolan lab, unpublished data). Here, I have shown that a class I *RSL* gene also positively regulates rhizoid development in a member of another early diverging group of land plants, liverworts. In the liverwort *M. polymorpha*, the single copy class I *RSL* gene *MpRSL1* is required for development of rhizoid precursor cells and rhizoids. Furthermore, elevated expression of *MpRSL1* was sufficient to trigger rhizoid precursor cell differentiation in cells that do not give rise to rhizoids in the wild type. Thus, the role of Class I *RSL* genes as positive regulators of filamentous rooting cell development is conserved between the members of early diverging groups of land plants, liverwort *M. polymorpha* and moss *P. patens,* as well as many flowering plants, and is thus likely to be conserved across all land plants. These findings suggest that the *RSL* mechanism for filamentous rooting cell differentiation is likely to have been present in the early land plants, at the time when the bryophyte and vascular plant lineages diverged.

In addition to defective rhizoid precursor cell development, the *M. polymorpha* class I *RSL* gene mutants are defective in the early stages of gemmae development. In wild type *M. polymorpha*, gemma development begins with outgrowth of an epidermal cell at the bottom of the gemma cup (Barnes and Land, 1908; Vashishta *et al*., 2011). This epidermal cell then divides at its apical region,

and the newly formed apical cell continues to divide giving rise to the disc-shaped gemma. In *Mprsl1* loss-of-function mutants the cells at the bottom of gemmae cups only very rarely form outgrowths. Further investigation of the *Mprsl1* loss-of-function mutant gemma cups showed that the *Mprsl1* mutant is missing mucilage producing papillae that form at the bottom of the wild type gemmae cups (Helene Proust, unpublished data; Barnes and Land, 1908; Taren, 1958). These data suggest *MpRSL1* is required for epidermal cell outgrowth during the earliest stages of gemmae and mucilage papilla development at the base of the gemmae cups. Moreover, *MpRSL1* was found to be required for the development of tubular epidermal outgrowths that form near meristematic region in gemmae. Based on preliminary observations, these outgrowths are also present near the meristematic regions of mature fully differentiated wild type *M. polymorpha* thalli (Victor Jones, unpublished data). Similar tubular outgrowths interpreted as mucilage papillae have been described in the liverwort *Marchasta areolata* (Campbell, 1954). Therefore, it seems likely that the epidermal outgrowths observed here are also mucilage papillae. Furthermore, the *Mprsl1* loss-of-function mutants were unable to induce the growth of these sexual reproductive structures even after extensive periods under inductive conditions, suggesting that *MpRSL1* function is likely to be required during the early steps of the gametophore development. Taken together, these results suggest that the role of *MpRSL1* is not restricted to rhizoid development, but *MpRSL1* function is required for a range of processes, all of which involve formation of an epidermal cell outgrowth.

The first step of all the processes identified to require *MpRSL1* function is expansion of an epidermal cell to form a tubular outgrowth, which then most likely elongates by tip growth. Therefore, *MpRSL1* is likely to directly or indirectly regulate genes involved in the physiological processes required for differentiation of epidermal cells into tip growing cells, as well as genes that function in the tip growth machinery. These processes have been most extensively characterised in Arabidopsis root hair development, where they involve changes in the organisation of the cytoskeleton and localisation of cellular organelles, establishment of cytoplasmic Ca^{2+} gradient and stimulation of proton efflux at the site of the future outgrowth, which results in acidification of the apoplast and leads to increased cell wall elasticity (reviewed in Datta *et al*., 2011).

The role of the moss *Physcomitrella patens* Class I *RSL* genes has previously been described to be limited to regulating the development of filamentous rooting cells; rhizoids and caulonema (Menand, *et al.*, 2007; Jang *et al*., 2011). Similarly to *M. polymorpha*, during its haploid gametophyte generation *P. patens* develops mucilage papillae in on its leafy gametophore (Eklund *et al*., 2010). Further investigation into whether the development of these mucilage papillae is defective in the *P. patens* class I *RSL* gene loss-of-function mutant will provide insight on the ancestral function of the class I *RSL* genes in early land plants and their algal ancestors. If the class I *RSL* genes are required for mucilage papilla development in *P. patens*, it would suggest that this role originated before the divergence of the liverwort and moss lineages, and therefore is also ancient. If so, the class I *RSL* genes may have first acquired their role as positive regulators of epidermal cell

outgrowth, and then later been recruited to control filamentous rooting cell development in the early ancestor of land plants. Alternatively, the ancestral role of class I *RSL* genes may have been to control the development filamentous rooting cells, and during the evolution of the liverwort body plan the class I *RSL* genes may have become re-utilised in multiple processes that involve outgrowth of an epidermal cell, such as outgrowth of rhizoids, gemmae, mucilage papillae and reproductive structures.

Chapter 5

FEW RHIZOIDS1 is a novel negative regulator of *MpRSL1* and rhizoid precursor cell differentiation

5.1. Summary

Factors that regulate temporal and spatial expression of developmental regulators are crucial for establishing patterns of cell and tissue differentiation in living organisms. The basic helix-loop-helix transcription factor encoded by the liverwort *M. polymorpha* class I *RSL* gene *MpRSL1* functions as a positive regulator of rhizoid, gemma and mucilage papilla differentiation. Here, I describe the identification of *FEW RHIZOIDS1 (MpFRH1)*, a novel liverwort specific micro RNA that functions as a negative regulator of *MpRSL1.* Similar to the *Mprsl1* loss-of-function mutants, elevated *MpFRH1* expression results in very few rhizoid precursor cells and therefore few rhizoids, gemmae and mucilage papillae. The *MpRSL1* transcript has a MpFRH1 miRNA target site and *FRH1* gain-of-function lines have reduced levels of the *MpRSL1* transcript. These data suggest that *Mp*FRH1 miRNA targets the *MpRSL1* transcript. Furthermore, *MpRSL1* positively regulates *MpFRH1* expression, suggesting that *MpFRH1* may provide a negative feedback mechanism that temporally or spatially regulates *MpRSL1* transcript levels. The MpFHR1 miRNA target site on class I *RSL* gene transcripts is conserved in the two major liverwort lineages Jugermanniales and Marchantiales that diverged in the Early Devonian period approximately 370 Mya. Therefore, the MpFRH1 miRNA may have originated early in the evolution of the liverwort lineage.

5.2. Introduction

During the development of multicellular organisms, the expression of developmental regulators needs to be temporally and spatially regulated in order to establish the organisms' body plan. These developmental regulators are often transcription factors that regulate the expression of genes required for the differentiation of cells and tissues. The basic helix-loop-helix transcription factors encoded by class I *RSL* genes promote epidermal cell differentiation to form an outgrowth during rhizoid development in bryophytes, and during root hair development in angiosperms (Menand *et al*., 2007, Chapter 4). Thus, the role of the Class I *RSL* genes as positive regulators of filamentous rooting cell development is conserved between liverworts and angiosperms. Furthermore, in *M. polymorpha* and *P. patens* class I *RSL* gene expression was found to be sufficient to induce rhizoid development when ectopically expressed in epidermal cells that in wild type plants do not give rise to rhizoids (Chapter 4, Jang *et al*., 2011). These findings indicate the class I *RSL* genes can function as molecular switches, whose expression is sufficient to turn on the differentiation into a tip-growing cell in any epidermal cell.

A forward genetic screen for rhizoid defective liverwort *M. polymorpha* mutants did not identify any genes similar to the genes that regulate the patterning of root hair differentiation or class I *RSL* gene expression in flowering plants (Chapter 3). Instead, T-DNA insertions in a previously uncharacterised locus *FEW RHIZOIDS1* (*MpFRH1*) resulted in defective rhizoid precursor cell differentiation. This suggests, that novel regulators of class I *RSL* gene expression are involved in

the regulation of rhizoid precursor cell differentiation in liverworts. In this chapter, I describe the identification and characterisation of *MpFRH1*; a novel liverwort specific negative regulator of the class I *RSL* gene *MpRSL1*.

5.3. Results

5.3.1. Identification of a novel regulator of rhizoid precursor cell differentiation

In the screen for mutants defective in rhizoid development I identified six mutants that developed few rhizoid precursor cells and consequently developed few rhizoids. I carried out TAIL-PCR to identify the T-DNA insertion site in these mutants. Four of the six mutants had a T-DNA insertion within a 1190 bp region of the *M. polymorpha* genome scaffold 2431 (Fig. 5.1), suggesting that this genomic region is very likely to be involved in rhizoid precursor cell differentiation.

In the *MpRSL1* gain-of-function mutants, a T-DNA insertion in the *MpRSL1* promoter was found to result in elevated expression of *MpRSL1* (Chapter 4). No transcript in the *M. polymorpha* transcriptome overlapped with the T-DNA insertion site in the four few rhizoid mutants. Therefore, I hypothesised that the T-DNA insertions in these mutants may have altered the expression level of a nearby transcript, as was observed in the *MpRSL1* gain-of-function mutants. To test this hypothesis, I carried out qRT-PCR analysis to determine the steady state transcript levels of all genes transcribed near the T-DNA insertion sites in the few rhizoid mutants. To identify the genes transcribed from this genomic region, I aligned the 15 kb genomic sequence around the T-DNA insertion sites with *M. polymorpha* transcriptome sequences. Four transcripts mapped to this 15 kb genomic region. None of the transcripts shared sequence similarity or conserved domains with previously known genes. The steady state levels of two short 341 bp and 476 bp transcripts were strongly elevated in the few rhizoid mutants compared to wild

type, while the levels of other transcripts mapping to this genomic region were the same as wild type (data not shown). This suggested the two short transcripts present in the transcriptome were partial fragments of a longer transcript. Therefore, I performed 3' and 5' RACE-PCR that verified that the two small transcripts were indeed fragments of a larger intron-less 1.2kb polyadenylated transcript. This transcript maps next to the right border of the T-DNA insertions and is over-expressed in the few rhizoid mutants (Fig. 5.1). Therefore, the transcript was named as *FEW RHIZOIDS1 (FRH1)*.

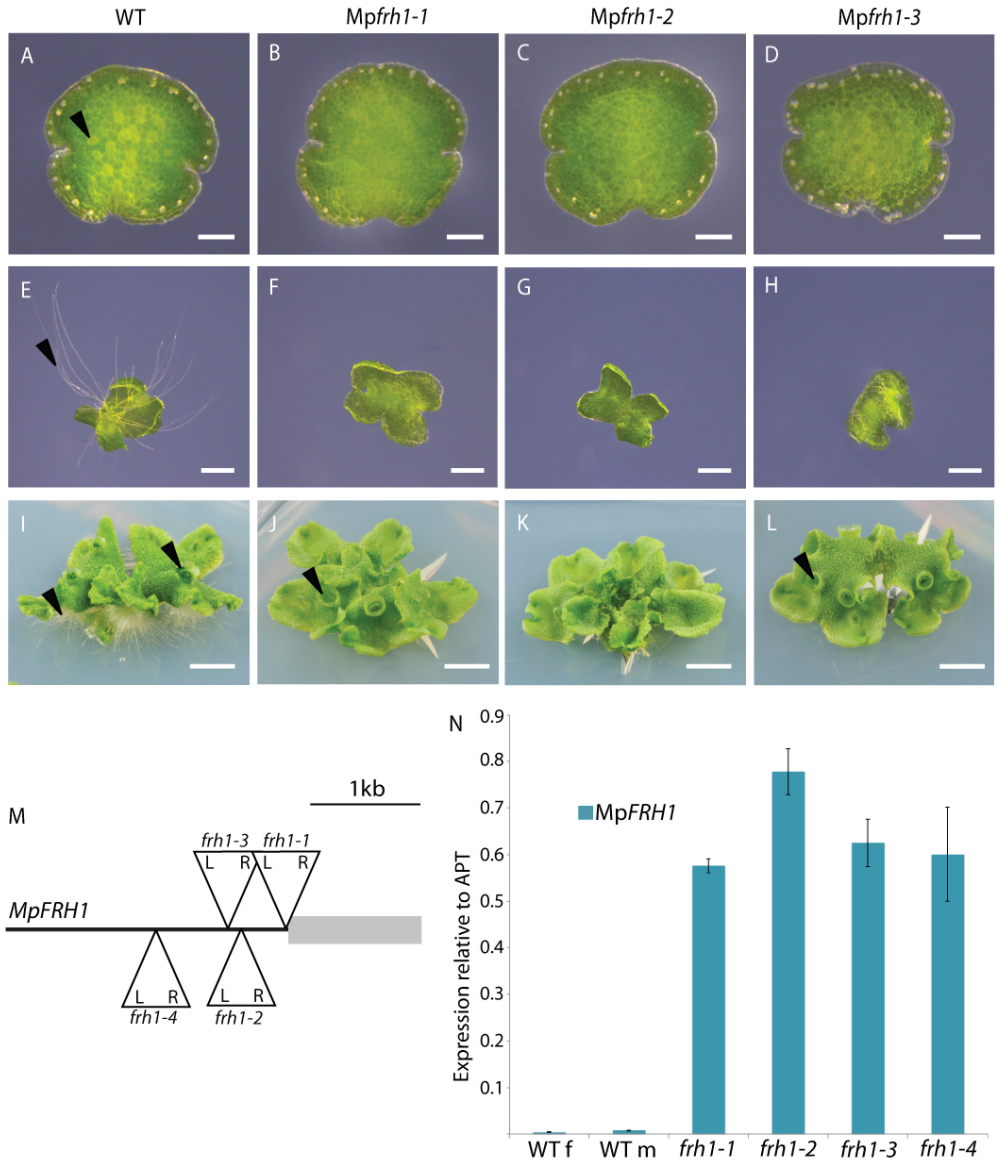

Figure 5.1 T-DNA insertion within the *MpFRH1* promoter results in elevated steady state levels of Mp*FRH1* mRNA and defective rhizoid precursor cell differentiation. A-L) Phenotype of wild type *M. polymorpha* and the *few rhizoids1* (*Mpfrh1*) mutants. A-D) One day old gemmae (scale bar 100 µm), E-H) four day old gemmae (scale bar 1 mm), I-L) 28 day old gemmae (scale bar 5 mm) of wild type (A, E, I) and the *few rhizoids1* mutants *Mpfrh1-1* (N, F, J), *Mpfrh1-2* (C, G, K) and *Mpfrh1-3* (D, H, J). The arrows indicate rhizoid precursor cells (in A-D) rhizoids (in E-L) and gemma cups (in I-L). M) Location and orientation of the T-DNA insertion sites within the *MpFRH1* locus. L and R stand for T-DNA left and right border, respectively. N) qRT-PCR analysis of steady state *MpFRH1* mRNA levels in 15 day-old gemmae of wild type and the *Mpfrh1* mutants. The *MpFRH1* transcript level was normalised against *MpAPT*. The error bars indicate ± s.d.

The few rhizoid phenotype of Mpfrh1-2 and Mpfrh1-3 is inherited and co-segregates with the hygromycin resistance marker on the T-DNA

Two of the four *Mpfrh1* mutant alleles (*Mpfrh1-2* and *Mpfrh1-3)* were successfully backcrossed with wild type and the phenotypes of individuals from the F1 generation were analysed to assess inheritance and co-segregation of the mutant phenotype with the hygromycin resistance marker on the T-DNA. The few rhizoid phenotype of both mutants showed Mendelian inheritance in the F1 generation, i.e. the observed ratio of plants with few rhizoids and plants with wild type phenotype was 1:1 (Table 5.1). Furthermore, for both *Mpfrh1-2* and *Mpfrh1-3,* the few rhizoid phenotype of the mutant co-segregated with the hygromycin resistance marker gene on the T-DNA in the F1 generation, indicating that the T-DNA insertion in the *MpFRH1* locus is responsible for the few rhizoid phenotype of the mutants (Table 5.1). Based on the ratios of hygromycin resistant to hygromycin sensitive F1 plants, *Mpfrh1-3* has a single T-DNA insertion, while *Mpfrh1-2* has two T-DNA insertions; one in the *MpFRH1* locus and a second unlinked T-DNA insertion.

Table 5.1 The few rhizoid phenotype of the *Mpfrh1* mutants *Mpfrh1-2* and *Mpfrh1-3* co-segregates with the hygromycin resistance on the T-DNA in the F1 generation after backcrossing with wild type. Frequencies of hygromycin resistant and hygromycin sensitive plants showing mutant and wild type phenotypes in F1 generation from a cross between *Mpfrh1-2 and Mpfrh1-3* with wild type *M. polymorpha*. Probability (p) of obtaining the observed numbers of hygromycin sensitive and hygromycin resistant F1 plants with the estimated T-DNA copy number was determined using the Chi-square test.

	mutant		WT		total		HygS:HygR	T-DNA	Expected	
line name	HygR	HygS	HygR	HygS	HygR	HygS	ratio	insertions	ratio	p
Mp*frh1-2*	109	0	48	53	157	53	1: 3.0	2	1:3	0.936
Mp*frh1-3*	131	0	0	125	131	125	1: 1.0	1	1:1	0.708

The Mpfrh1 mutant lines are defective in reproductive development

Mpfrh1-2 and *Mpfrh1-3* rarely produced reproductive structures in conditions where wild type plants develop reproductive structures. However, when reproductive structures did develop their morphology was similar to those of wild type. The few rhizoid phenotype of *Mpfrh1-1* was consistently observed to be stronger than that of *Mpfrh1-2* and *Mpfrh1-3.* Furthermore, *Mpfrh1-1* never successfully induced the development of any reproductive structures, and thus this line was not backcrossed with the wild type. This suggests that *Mpfrh1-1* is a stronger allele than *Mpfrh1-2* and *Mpfrh1-3.* Together, these findings suggest that *MpFRH1* is involved in the transition to reproductive development, or in the early stages of the development of reproductive structures.

The *Mpfrh1-4* mutant thallus was slow growing and misshapen, while the other three *Mpfrh1* mutant alleles were similar to wild type in overall thallus morphology. All other aspects of the *Mpfrh1-4* phenotype were similar to the other three *Mpfrh1* mutant lines. This suggests that in addition the T-DNA insertion in the *MpFRH1* locus, *Mpfrh1-4* is likely to have a second unlinked mutation responsible for the slow growth phenotype. Consistent with this hypothesis, a second T-DNA insertion was identified in *Mpfrh1-4* using TAIL-PCR. Therefore, *Mpfrh1-4* was excluded from further analysis. Furthermore, due to its poor growth *Mpfrh1-4* was not successfully backcrossed with wild type.

5.3.2. *MpFRH1* negatively regulates the development of rhizoid precursor cells and rhizoids

As the previously uncharacterised 1.2 kb *MpFRH1* transcript was over-expressed in the *Mpfrh1* mutants, I hypothesised that this elevated expression of *MpFRH1* is responsible for the few rhizoid phenotype of the *Mpfrh1* mutants. To test this hypothesis, I expressed the *MpFRH1* transcript under the control of the strong constitutive rice actin promoter in wild type *M. polymorpha*. Expression level of *MpFRH1* was assessed in eight transformed lines; four lines with very few rhizoids and four lines showing wild type phenotype. Strong over expression of *MpFRH1* was detected in the lines with few rhizoids, while wild type levels of *MpFRH1* expression was observed in the transformed lines with wild type phenotype (Fig. 5.2). Therefore, over-expression of the 1.2 kb *MpFRH1* transcript in the wild type is sufficient to reproduce the phenotype of the few rhizoid mutants. This suggests that the *Mpfrh1* mutants are gain-of-function mutants, in which elevated expression of *MpFRH1* results in reduced number of rhizoid precursor cells and rhizoids. Thus, the *MpFRH1* mutants were re-named as $MpFRH1^{GOF1}$, $MpFRH1^{GOF2}$, $MpFRH1^{GOF3}$ *and* $MpFRH1^{GOF4}$. Taken together, these findings indicate that *MpFRH1* is a negative regulator of rhizoid precursor cell differentiation.

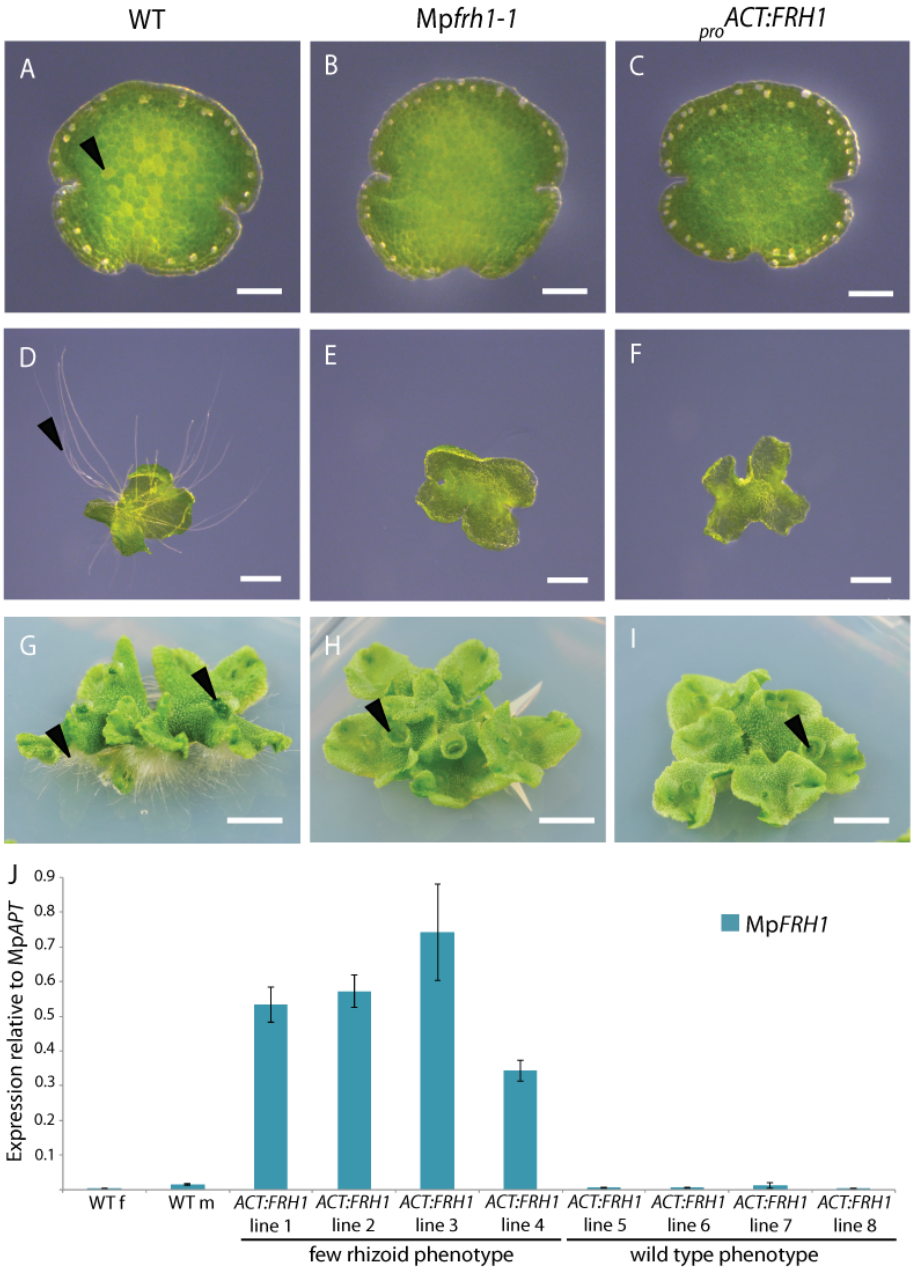

Figure 5.2 Over-expression of *MpFRH1* behind the strong constitutive rice actin promoter in the wild type *M. polymorpha* is sufficient to reproduce the few rhizoid phenotype of the *Mpfrh1* mutants. A-I) Phenotype of wild type *M. polymorpha*, T-DNA insertion mutant *Mpfrh1-1* and a plant transformed with *proACT:FRH1*. One day old gemmae (A-C, scale bar 100 µm), four day old gemmae (D-F, scale bar 1 mm) and 28 day old gemmae (G-I, scale bar 5 mm) of wild type (A, D, G), *Mpfrh1-1* (B, E, H), *proACT:FRH1* (G, H, I). The arrows indicate rhizoid precursor cells (in A-C), rhizoids (in D-I) and gemma cups (in G-I). J) qRT-PCR analysis of steady state *MpFRH1* transcript levels in 15 days old gemmae of wild type and eight lines transformed with *proACT:FRH1*. The error bars indicate ± s.d.

5.3.3. *MpFRH1* negatively regulates the development of epidermal papillae and gemmae

In addition to having defective rhizoid precursor cell differentiation, the *MpFRH1* gain-of-function mutants were also affected in other developmental processes. *MpFRH1*^{GOF} mutants lack small tubular epidermal papillae that form near meristematic regions in wild type *M. polymorpha* gemmae (Fig. 5.3). Furthermore, *MpFRH1*^{GOF} and $_{pro}$*ACT:FRH1* lines often have empty gemma cups, while wild type *M. polymorpha* gemma cups were always full of gemmae as soon as the opening of the gemma cup was visible (Fig. 5.2). Together, these findings suggest *MpFRH1* negatively regulates the development of gemmae and epidermal papillae.

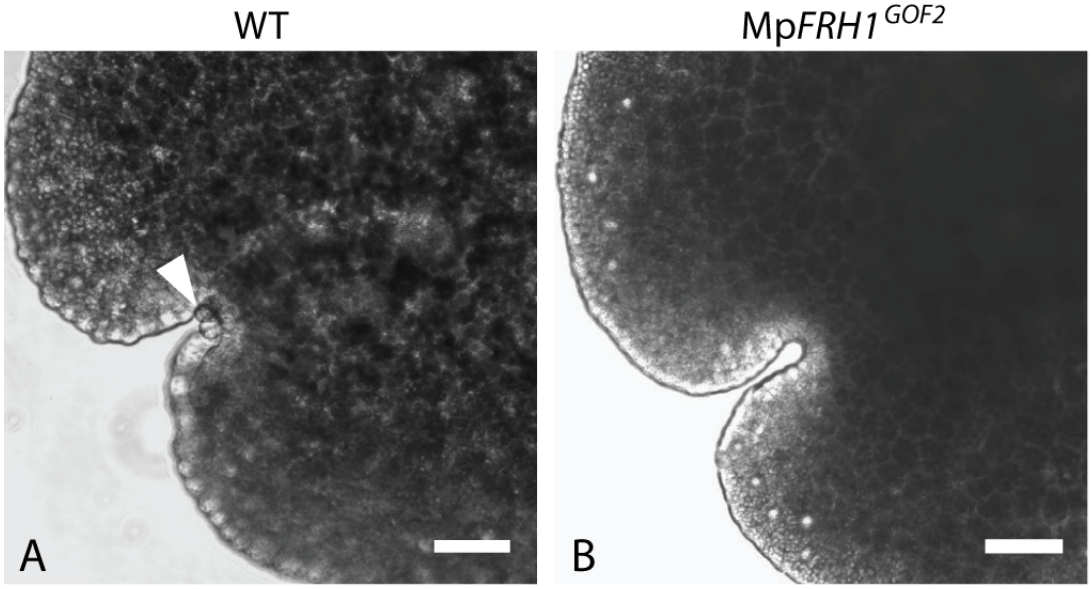

Figure 5.3 *MpFRH1* negatively regulates the development of epidermal papillae. High-magnification brightfield microscopy images of 1 day old wild type (A) and *MpFRH1*^{GOF2} (B) gemmae meristematic region. Scale bar 50 µm.

5.3.4. *MpFRH1* negatively regulates *MpRSL1* transcript levels

The phenotypes of the lines with elevated *MpFRH1* levels (*MpFRH1*^{GOF} mutants and *proACT:FRH1* plants) resemble those of the *Mprsl1* loss-of-function mutant. Young gemmae of the *MpFRH1* gain-of-function mutants and *proACT:FRH1* plants lack rhizoid precursor cells like *Mprsl1* mutants (Fig. 5.2). Gemma cups of the *MpFRH1*^{GOF} mutants and *proACT:FRH1* plants were often empty and gemmae did not develop, as observed in *Mprsl1* loss of function mutants (Fig. 5.2). Moreover, like the *Mprsl1* mutants, *MpFRH1*^{GOF} plants lack the epidermal papillae near the meristematic regions of growing gemmae (Fig. 5.3). However, rhizoid precursor cell differentiation and gemmae development in the lines with elevated *MpFRH1* expression were not entirely defective, because later in development some plants formed small number of rhizoids and gemmae, especially in the older parts of the thallus and under drought stress. The similarity of the *Mprsl1* loss-of-function and *MpFRH1* gain-of-function mutant phenotypes suggest that *MpFRH1* and *MpRSL1* may function in the same pathway.

As the *Mprsl1* loss-of-function and the *MpFRH1* gain-of-function mutant phenotypes were similar, I hypothesised that *MpFRH1* may function as a negative regulator of *MpRSL1*. To test this hypothesis, I carried out qRT-PCR analysis to check the steady state levels of *MpRSL1* transcript in *MpFRH1*^{GOF} mutants and plants over-expressing *MpFRH1* behind the rice actin promoter. The steady state level of *MpRSL1* mRNA was reduced in both *MpFRH1*^{GOF} and *proACT:FRH1* lines, suggesting that elevated levels of *MpFRH1* result in reduced levels of *MpRSL1* transcript (Fig. 5.4). This suggests *MpFRH1* negatively regulates *MpRSL1* transcript level.

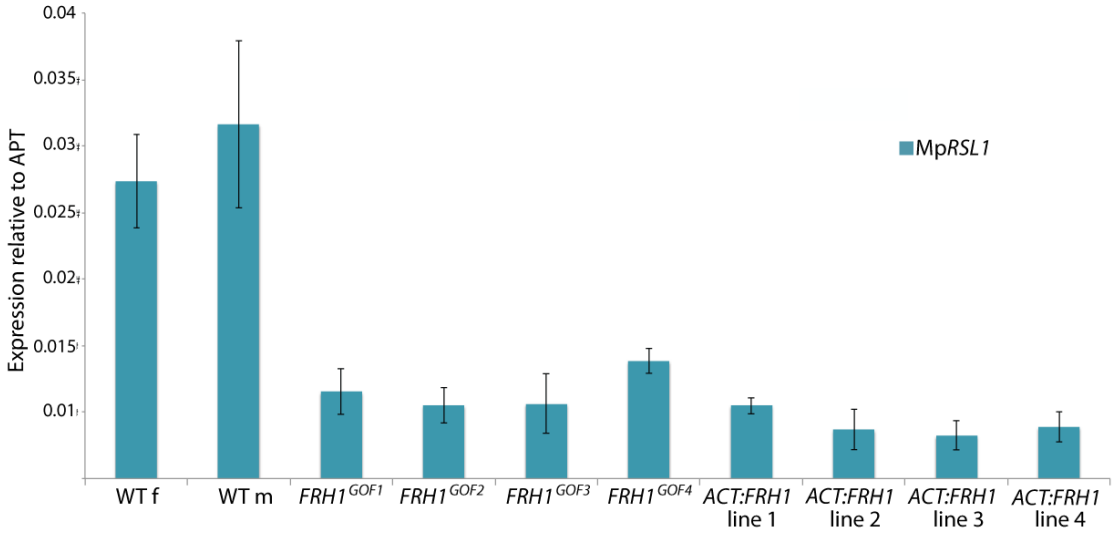

Figure 5.4 *MpFRH1* negatively regulates *MpRSL1* transcript level. qRT-PCR quantification of steady state *MpRSL1* transcript levels in 15 day old wild type gemmae, and gemmae of the four *MpFRH1*^{GOF} mutant lines as well as in four *proACT:FRH1* lines with a strong few rhizoid phenotype. *MpRSL1* transcript levels were normalised against *MpAPT*. The error bars indicate ± s.d.

5.3.5. *MpRSL1* positively regulates *MpFRH1* transcript level

To identify if *MpRSL1* also regulates *MpFRH1* transcript level, I carried out a qRT-PCR analysis to measure steady state levels of *MpFRH1* transcript in the *Mprsl1* loss-of-function and gain-of-function mutants. *MpFRH1* transcript level was lower in the *Mprsl1* loss-of-function mutants than in wild type, and higher in the *MpRSL1* gain-of-function mutants that have elevated levels of *MpRSL1* expression (Fig. 5.5). These results suggest that *MpRSL1* positively regulates *MpFRH1* transcript levels. However, functional *MpRSL1* is not required for *MpFRH1* expression, as a low level of *MpFRH1* mRNA is retained in the *Mprsl1* loss-of-function mutant background. This suggests that other mechanisms contribute to the regulation of *MpFRH1* expression.

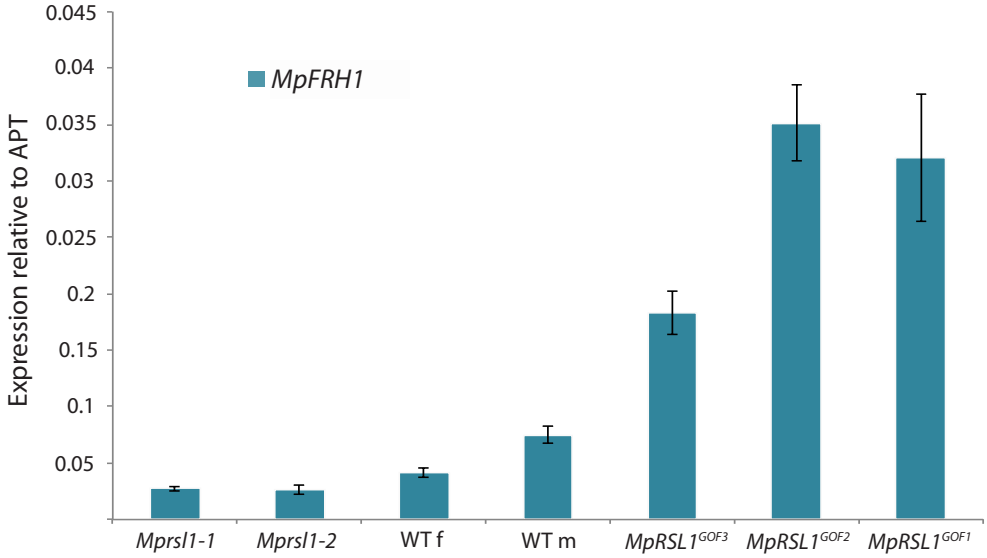

Figure 5.5 *MpRSL1* positively regulates *MpFRH1* transcript level. qRT-PCR quantification of steady state *MpFRH1* transcript levels in 15 day old gemmae of wild type *M. polymorpha*, *Mprsl1* loss-of-function mutants *Mprsl1-1* and *Mprsl1-2*, and *MpRSL1* gain-of-function mutants $MpRSL1^{GOF1}$, $MpRSL1^{GOF2}$ and $MpRSL1^{GOF3}$. *MpFRH1* transcript levels were normalised against *MpAPT*. The error bars indicate ± s.d.

5.3.6. *MpFRH1* functions as RNA

Intriguingly, the 1.2 kb *MpFRH1* transcript sequence does not contain any long open reading frames or show sequence similarity with Arabidopsis proteins. However, there are three putative small open reading frames of 150 bp, 144 bp and 216 bp on the transcript. Based on SignalIP 4.0 prediction (Nordahl Petersen *et al*., 2011), none of these small open reading frames contain endoplasmic reticulum targeting signal peptides commonly found in small secreted peptides. Thus, it is unlikely that *MpFRH1* functions as a small secreted peptide. To test if these small open reading frames are sufficient to reproduce the few rhizoid phenotype, I over-expressed the three putative small open reading frames (ORF1 to ORF3) behind the strong constitutive rice actin promoter in wild type *M. polymorpha*. Transformed plants over-expressing ORF2 and ORF3 were wild type in phenotype (Fig. 5.6, Table 5.2). Over-expression of ORF1 resulted in a few rhizoid phenotype identical to that of plants over-expressing the full-length *MpFRH1* transcript (Fig. 5.6, Table 5.2). These results suggest the 150 bp sequence within the ORF1 is required and sufficient to give rise to the few rhizoid phenotype of the $MpFRH1^{GOF}$ lines.

The question remained whether *MpFRH1* functions as RNA or whether its function requires translation of a small peptide encoded by ORF1. Over-expression of the full-length *MpFRH1* transcript, in which the ATG start codon of the putative ORF1 coding sequence was mutated into ATC (which should not initiate translation), behind the rice actin promoter in the wild type *M. polymorpha* was sufficient to reproduce the few rhizoid phenotype. Combined with the lack of endoplasmic

reticulum targeting signal these results indicate that *MpFRH1* functions as RNA (Fig. 5.6, Table 5.2).

Table 5.2 Frequencies of different phenotypes observed in sporelings transformed with modified versions of the *MpFRH1* transcript sequence driven by the strong constitutive rice actin promoter. The phenotypes of the transformant sporelings were scored four weeks after the initial transformation by co-cultivation with *Agrobacterium*.

	rhizoids	**few rhizoids**	**no/very few rhizoids**	**total**
proACT:MpFRH1	4	11	88	103
proACT:MpFRH1-ORF1	18	32	59	109
proACT:MpFRH1-ORF2	102	6	0	108
proACT:MpFRH1-ORF3	106	3	0	109
proACT:MpFRH1-noATG	7	14	83	104

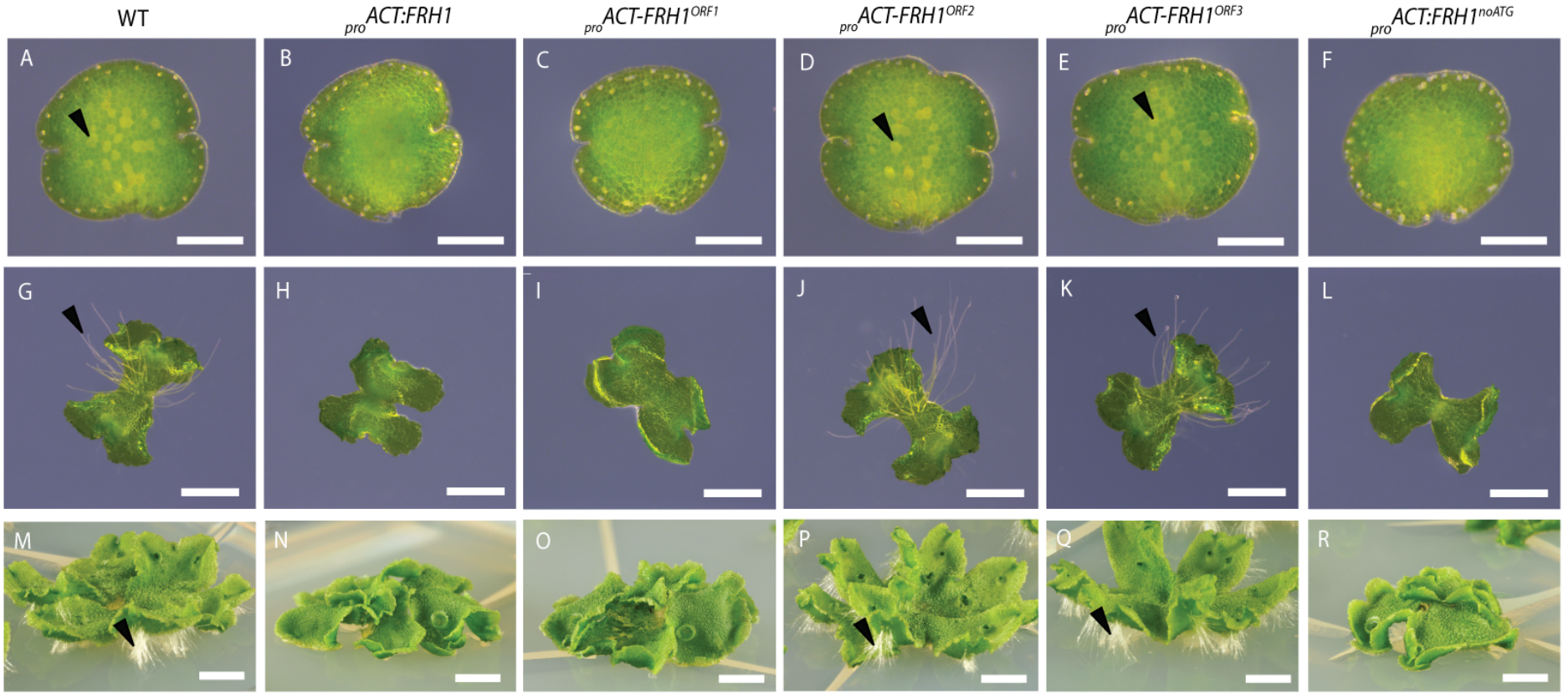

Figure 5.6 *MpFRH1* functions as RNA. One day old gemmae (A-F, scale bar 100 µm), four day old gemmae (F-L, scale bar 1 mm) and 28 day old gemmae (M-R, scale bar 5 mm) of wild type (A, G, M), $_{pro}$*ACT:FRH1* (B, H, N), $_{pro}$*ACT:FRH1*^{ORF1} (C, I, O), $_{pro}$*ACT:FRH1*^{ORF2}*(D, J, P),* $_{pro}$*ACT:FRH1*^{ORF3} *(E, K, Q) and* $_{pro}$*ACT:FRH1*^{noATG} (F, L, R). The arrows indicate rhizoid precursor cells (in A-F) and rhizoids (in G-R).

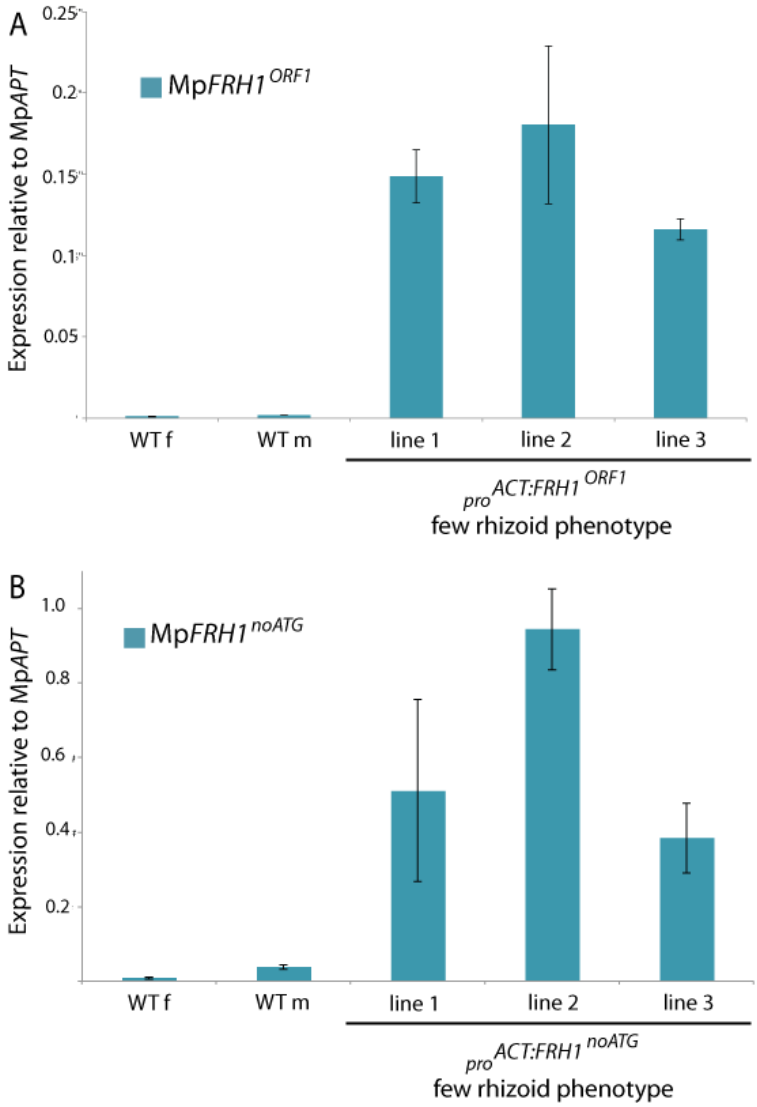

Figure 5.7 Expression levels of *MpFRH1*^{ORF1} and *MpFRH1*^{noATG} in 15 day old gemmae of wild type *M. polymorpha* and three lines transformed with $_{pro}$*ACT:FRH1*^{ORF1} (A) or $_{pro}$*ACT:FRH1*^{noATG} (B). The transformant lines analysed were selected based on their strong few rhizoid phenotype. *MpFRH1*^{ORF1} and *MpFRH1*^{noATG} levels were normalised against *MpAPT*. The error bars indicate ± s.d.

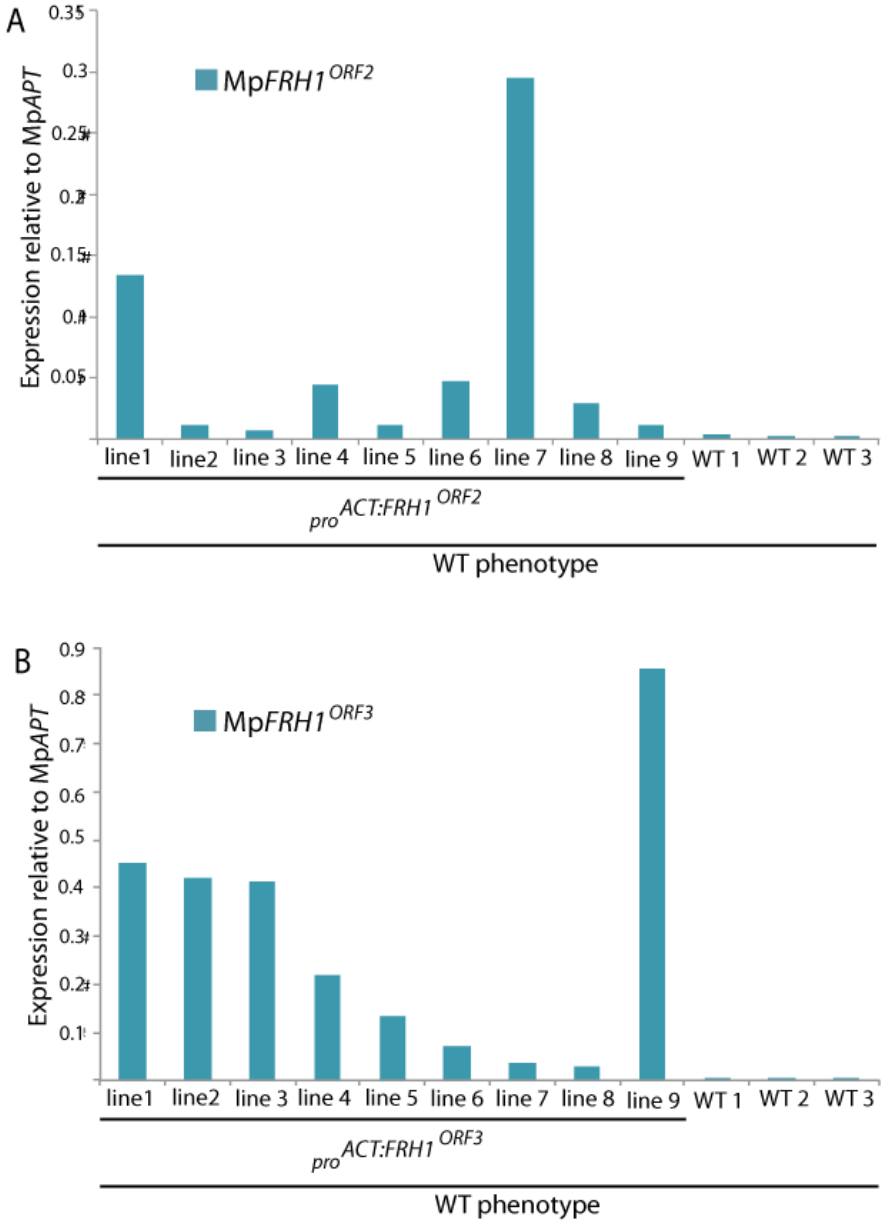

Figure 5.8 Expression levels of *MpFRH1*^{ORF2} and *MpFRH1*^{ORF3} in 15 day old gemmae of wild type and nine lines transformed with $_{pro}$*ACT:FRH1*^{ORF2} (A) or $_{pro}$*ACT:FRH1*^{ORF3} (B). All lines had a wild type phenotype. *MpFRH1*^{ORF2} and *MpFRH1*^{ORF3} levels were normalised against *MpAPT*.

5.3.7. *MpFRH1* is a pri-miRNA gene that gives rise to a 21 bp MpFRH1 miRNA

MicroRNAs (miRNAs) are 21-24 bp small RNAs that negatively regulate the expression of their target genes (reviewed in Mallory and Vaucheret, 2006; Voinnet, 2009; Rogers and Chen, 2013). miRNAs are produced from longer polyadenylated primary miRNA (pri-miRNA) transcripts with distinct secondary structure, and are transcribed by RNA polymerase II (Pol II) (Jones-Rhoades and Bartel, 2004; Kim *et al*., 2011). The *MpFRH1* transcript was found to be polyadenylated using 3' RACE-PCR. Consistent with *MpFRH1* giving rise to a RNA Pol II transcribed pri-miRNA transcript, the Softberry TSSP promoter prediction (Solovyev & Shahmuradov, 2003) analysis identified a TATA-box sequence, characteristic of pol II transcribed genes, on the *MpFRH1* promoter. To achieve its secondary structure, the pri-miRNA transcript folds back into an imperfectly basepaired double stranded hairpin, and the miRNA is produced from the stem of this hairpin (Kurihara and Watanabe, 2004). RNA folding prediction of the sequence contained within the $MpFRH1^{ORF1}$ was carried out using RNAfold (Gruber *et al*., 2008). Based on this RNA folding prediction, the 150 bp sequence contained within ORF1 folds into a hairpin structure (Fig. 5.9). As *MpFRH1* was found to be a Pol II transcribed transcript that functions as RNA, and the 150 bp sequence sufficient to reproduce the *MpFRH1* gain-of-function phenotype folds into a hairpin loop, I hypothesised that *MpFRH1* might be a micro RNA primary precursor (pri-miRNA) gene that gives rise to a micro RNA (miRNA).

During miRNA processing in Arabidopsis, the stem of the pri-miRNA hairpin loop is typically cut twice by DICER-LIKE1 (DCL1), resulting in a 21 bp double stranded RNA duplex that contains a miRNA strand, and a complementary miRNA* strand (Kurihara and Watanabe, 2004; Kurihara *et al*., 2006; Qi *et al*., 2005). The miRNA strand becomes incorporated into ARGONAUTE1 (AGO1) containing RNA induced silencing complex (RISC), in which the miRNA guides AGO1 mediated cleavage of the miRNAs target mRNA transcripts through base pairing with the partially complementary target site sequence on its target mRNAs (Vaucheret *et al*., 2004; Baumberger and Baulcombe, 2005; Qi *et al*., 2005). In contrast, the miRNA* strand becomes degraded.

Small RNA sequencing data of *M. polymorpha*, and a related liverwort species *M. paleacea*, was produced and kindly shared with us by Mario Arteaga-Vazquez (University of Veracruz, Mexico). Consistent with the hypothesis that *MpFRH1* gives rise to a miRNA, a 21 bp predicted miRNA (UGUGUGAGAAGAGGCCAAUGU) and a complementary miRNA* (AUUGGUCUCUUCACGCACAAA) sequence, corresponding to the stem of the predicted *MpFRH1* RNA hairpin loop, were present in small RNA sequencing data from both *M. polymorpha,* (Fig. 5.9) and *M. paleacea*. Two basepair overhangs characteristic to DCL1 processed Arabidopsis miRNA duplexes (Rogers and Chen, 2013) can be observed between the MpFRH1 miRNA and miRNA* sequences (Fig. 5.9). Together, these findings suggest *MpFRH1* is a pri-miRNA gene that gives rise to a 21 bp MpFRH1 miRNA.

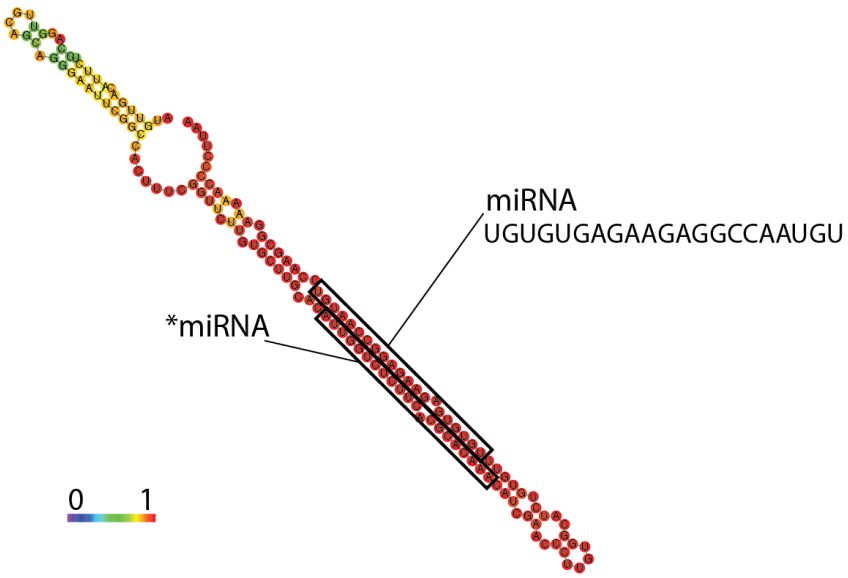

Figure 5.9 The 150 bp sequence sufficient for the MpFRH1 gain-of-function phenotype folds into a hairpin. RNA folding prediction of the 150 bp sequence sufficient to reproduce the few rhizoid phenotype when over-expressed in the wild type carried out by RNAfold (Gruber *et al*., 2008). The colours represent base-pairing probabilities. The small RNA sequences corresponding to MpFRH1 miRNA and the complementary *miRNA present in the *M. polymorpha* small RNA sequencing data are indicated.

The mature MpFRH1 miRNA is present in wild type and MpFRH1^{GOF} M. polymorpha

Stem-loop PCR was carried out to verify the MpFRH1 miRNA. In stem-loop PCR, the mature miRNA is first reverse transcribed using a primer specific to the miRNA sequence fused to a stem-loop sequence that contains a universal primer-binding site. PCR is then carried out to amplify the reverse transcribed miRNA using the universal primer and a primer specific to the miRNA sequence. A 60 bp fragment that corresponds to the expected size of the MpFRH1 miRNA and a fused stem-loop sequence was amplified from small RNA enriched RNA extracted from 15

day old gemmae of wild type, *MpFRH1*^{GOF1}, *MpFRH1*^{GOF2} and *MpFRH1*^{GOF3} *M. polymorpha* (Fig. 5.10). The 60 bp MpFRH1 miRNA band was stronger in the *MpFRH1* gain-of-function mutant samples, suggesting that elevated levels of the *MpFRH1* pri-miRNA gene in these mutants give rise to elevated levels of mature MpFRH1 miRNA.

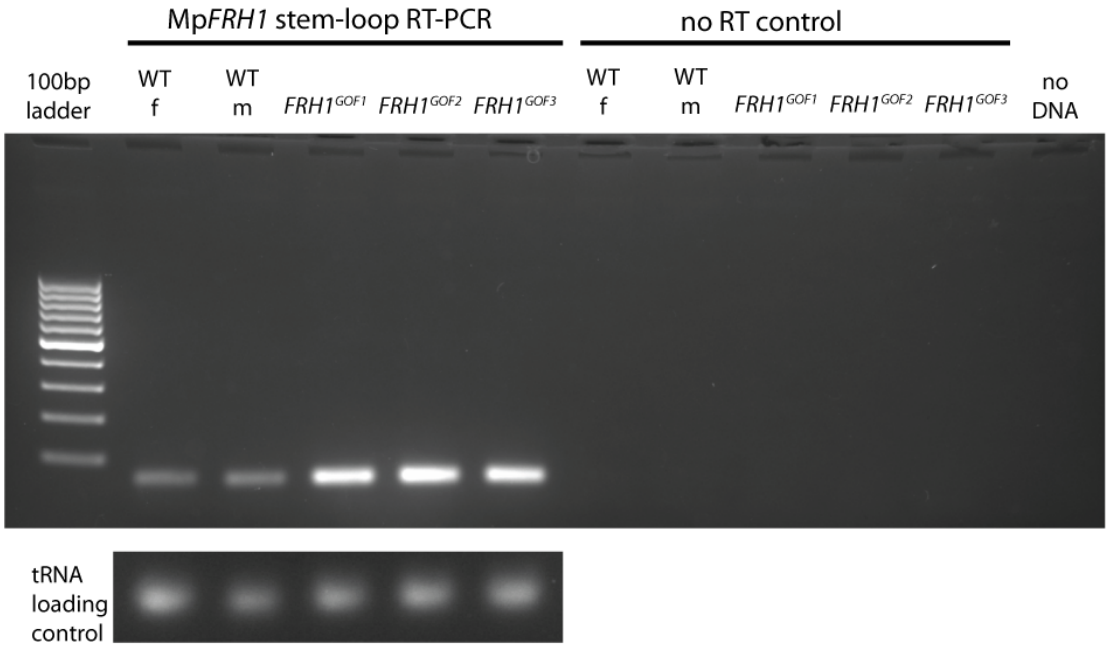

Figure 5.10 Stem-loop PCR detection of the MpFRH1 miRNA. RNA extracted from 15 day old wild type and *MpFRH1*$^{GOF1-3}$ plants was used as a template for the stem-loop PCR amplification. Amplification products after 28 PCR cycles were visualised on a EtBr stained 2 % agarose gel. The tRNA band was used as a loading control.

5.3.8. MpFRH1 miRNA targets *MpRSL1*

MpFRH1 miRNA target prediction was carried out by Mario Arteaga-Vazquez (University of Veracruz, Mexico). Potential targets of the MpFRH1 miRNA were predicted based on sequence similarity between the miRNA sequence and sequences in a *M. polymorpha* gametophyte transcriptome (Dolan lab, unpublished data). Seven predicted targets of MpFRH1 miRNA were identified (Table 5.3). Consistent with the reduced *MpRSL1* transcript levels observed in the lines with elevated MpFRH1 miRNA levels, *MpRSL1* was one of the predicted MpFRH1 miRNA targets. qRT-PCR analysis of the expression levels of the predicted additional MpFRH1 miRNA targets in wild type and in the *MpFRH1*^{GOF} lines will indicate if the other predicted Mp*FRH1* targets are regulated by the MpFRH1 miRNA. However, since the phenotypes of the *Mprsl1* loss-of-function mutants and *MpFRH1*^{GOF} lines are similar, the reduced level of MpRSL1 protein in *MpFRH1*^{GOF} lines is likely sufficient to explain the *MpFRH1*^{GOF} phenotype.

Table 5.3 Predicted targets of MpFRH1 miRNA in *M. polymorpha*. Lower scores indicate a more likely target based on sequence similarity between the miRNA and the target transcript.

Gene	Arabidopsis ortholog	score
foie gras domain containing protein	AT5G65950	2.5
ribosomal protein S16	AT4G34620 (SSR16)	3.5
basic helix-loop-helix (bHLH) family protein MpRSL1	**AT5G37800 (RHD6)**	**4**
basic helix-loop-helix (bHLH) family protein	AT4G37850	4
GDP-D-mannose 4,6-dehydratase	AT5G66280 (GMD1)	4
nucleotide-rhamnose synthase/epimerase-reductase)	AT1G63000	4
SAUR-like	AT3G43120 (SAUR39)	4

Two of the seven predicted *M. polymorpha* FRH1 miRNA targets, a predicted ortholog of *MpRSL1* and At5g65950 (an uncharacterised foie gras domain containing protein), were also predicted targets of *FRH1* in *M. paleacea* (Mario Arteaga-Vazquez, University of Veracruz, Mexico). The sequence of the FRH1 miRNA and its predicted target site on the class I *RSL* gene transcript is 100% conserved between *M. polymorpha* and *M. paleacea*. These findings suggest the function of FRH1 miRNA is likely to be conserved between *M. polymorpha* and *M. paleacea*.

5.3.9. The FRH1 miRNA target site on class I *RSL* gene transcripts is conserved across liverworts

The FRH1 miRNA was found to be conserved between *M. polymorpha* and a closely related liverwort species *M. paleacea* (Mario Arteaga-Vazquez). To assess the extend of the conservation of the FRH1 miRNA binding site, the presence of the MpFRH1 miRNA binding site on class I *RSL* gene transcripts from different liverwort species was analysed. The extant liverwort species fall into three major lineages: Marchantiopsida, Jugermanniopsida and Haplomitriopsida (Forrest *et al*., 2006). The FRH1 miRNA binding site is 100 % conserved in all eight liverwort species for which class I *RSL* gene transcript sequence data was available through the 1000 plants project (https://www.bioinfodata.org/Blast4OneKP, Fig. 5.11, a longer region of the alignment is provided in the chapter 5 appendix figure A5.1). These eight liverwort species belong to the Marchantiopsida and Jugermanniopsida lineages (sequence data for Haplomitriopsida class I *RSL* gene transcripts was not available). The Marchantiopsida and Jugermanniopsida lineages have been estimated to have

diverged in the Late Devonian period approximately 373 Mya (Heinrichs *et al.*, 2007). Therefore, the MpFRH1 miRNA binding site on liverwort class I *RSL* genes is likely to have evolved before the divergence of the two lineages. This suggests the MpFRH1 miRNA may also be ancient and conserved within the liverwort lineage.

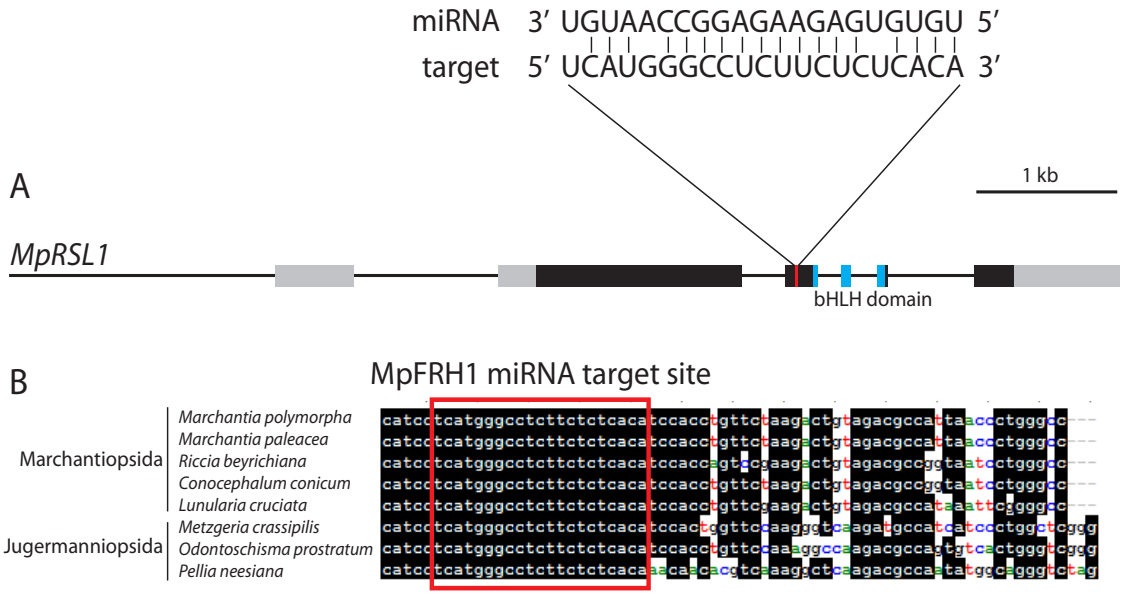

Figure 5.11 FRH1 miRNA target site conservation. A) *MpRSL1* gene model showing the location of the MpFRH1 miRNA target site. B) Nucleotide alignment of class I *RSL* gene transcripts from different liverwort species showing the conservation of the FRH1 miRNA target site.

In contrast, class I *RSL* genes from Arabidopsis, the lycophyte *S. Kraussiana* and the moss *P. patens* lack the *MpFRH1* binding site sequence. This suggests, that in these lineages class I *RSL* genes are either not regulated by FRH1-like miRNAs, or that both the miRNA sequence and the binding site of the miRNA on the class I *RSL* genes have diverged and therefore are not similar to *MpFRH1*.

5.3.10. The *MpFRH1* promoter is expressed in rhizoid precursor cells, rhizoids and epidermal papillae

To visualise the *MpFRH1* promoter expression pattern, I combined the 3.5 kb genomic sequence upstream of *MpFRH1* including a predicted TATA-box sequence, with three copies of yellow fluorescent protein fused to a nuclear localisation signal (3xYFP-NLS). *MpFRH1* transcript level was higher in the *MpRSL1* gain-of-function mutants than in wild type. As the *MpRSL1* gain-of-function mutants have more rhizoids and rhizoid precursor cells than wild type, I hypothesised that *MpFRH1* expression is associated with rhizoid precursor cell fate. The chloroplasts in wild type *M. polymorpha* rhizoid precursor cells shrink and lose their chlorophyll autofluorescence early in rhizoid precursor cell differentiation. Consequently, rhizoid precursor cells can be distinguished from non-rhizoid precursor cells based on their strongly reduced red chlorophyll autofluorescence even before rhizoid elongation takes place. As expected, high levels of *MpFRH1* promoter activity were observed in the rhizoid precursor cells (Fig. 5.12). The YFP signal persisted in elongating rhizoids, either due to perdurance of the promoter activity or due to slow degradation of the yellow fluorescent protein (Fig. 5.12).

Rhizoid precursor cells are larger than non-rhizoid precursor cells, and also have larger nuclei. To verify that the stronger YFP-signal in the rhizoid precursor cells of *proFRH1:3xYFP-NLS* gemmae is a result of differential expression of the promoter between rhizoid precursor cells and non-rhizoid precursor cells, and not simply due to different size of the nuclei between the two cell types, the pattern of 3xYFP-NLS expression driven by the ubiquitously expressed 3.5 kb *M. polymorpha*

INCOMPLETE ROOT HAIR ELONGATION (*MpIRE*) promoter was analysed as a control. *MpIRE* promoter expression was detected evenly in both rhizoid precursor cells and non-rhizoid precursor cells (Fig. 5.13). These results suggest that the stronger *proFRH1:3xYFP-NLS* signal detected in rhizoid precursor cells truly results from stronger *MpFRH1* promoter activity in these cells than in surrounding cells.

Strong *MpFRH1* promoter activity was also observed in tubular structures that form near the gemmae meristematic region of 1 day old gemmae (Fig. 5.11). These tubular structures correspond to the putative mucilage papillae that are missing in the *Mprsl1* mutants and *MpFRH1* gain-of-function lines. However, many mucilage papillae without YFP signal were observed, suggesting that *MpFRH1* may be expressed during a specific mucilage papilla developmental stage.

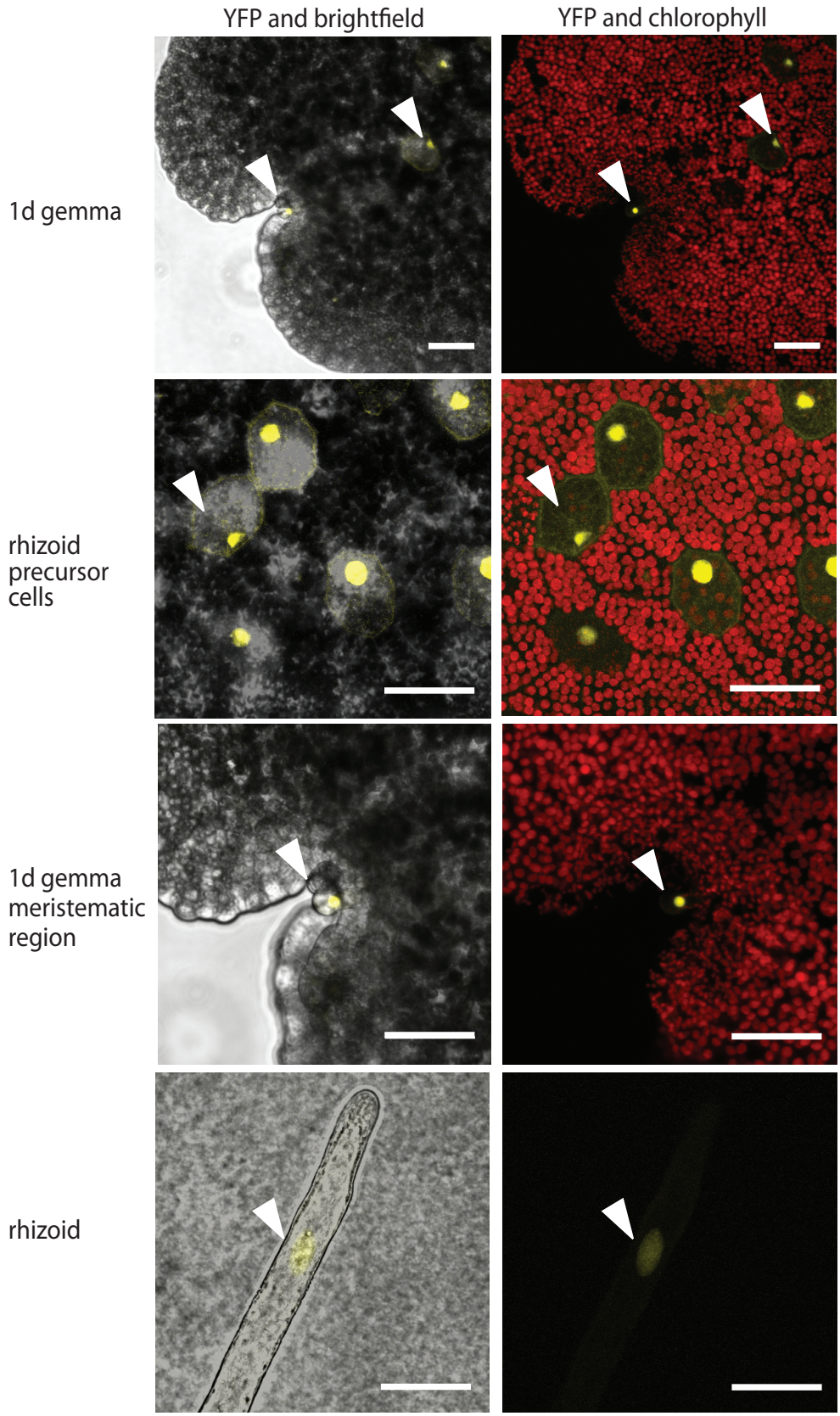

Figure 5.12 *MpFRH1* promoter expression pattern. Pattern of $_{promoter}$*MpFRH1:3xYFP-NLS* expression in 1 day old gemmae. The arrows indicate rhizoid precursor cells, epidermal papillae and rhizoids. Scale bar 50 µm.

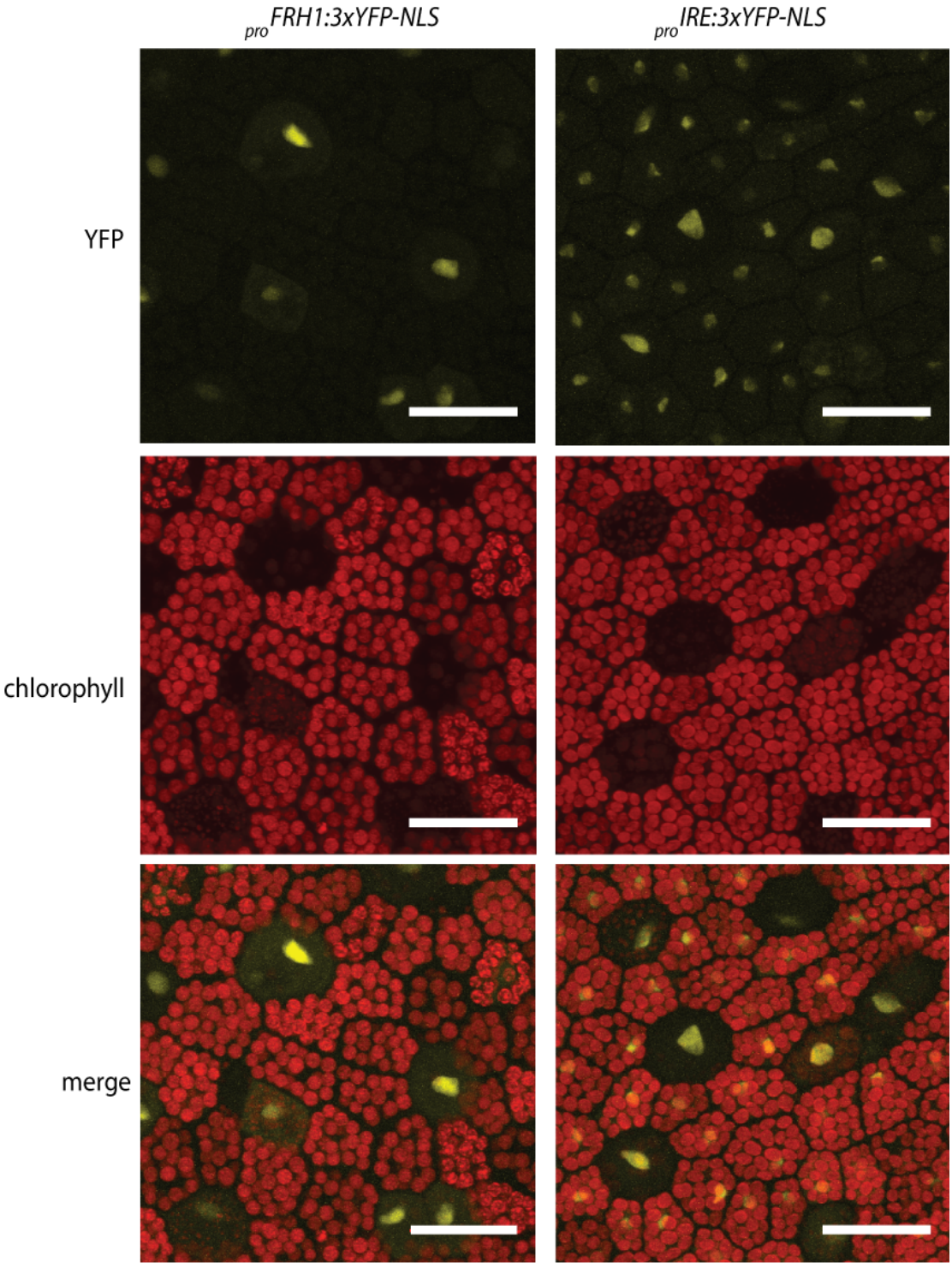

Figure 5.13 Comparison of *MpFRH1* with *MpIRE* promoter expression pattern in the mid region of 1 day old gemmae. Scale bar 50 µm. Rhizoid precursor cells can be distinguished from non-rhizoid precursor cells based on their strongly reduced red chlorophyll autofluorescence.

MpFRH1 promoter may be expressed during gemma development

MpFRH1 is expressed in rhizoid precursor cells, rhizoids and epidermal papillae, while functioning as a negative regulator of the development of these cell types. Thus, as *MpFRH1* also negatively regulates gemma development it is likely that *MpFRH1* is expressed at the bottom of the gemma cup in the cells that give rise to gemmae. However, observing the $_{pro}$*FRH1:3xYFP-NLS* expression pattern at the bottom of gemma cups was not possible as the gemma cups in wild type *M. polymorpha* are full of gemmae, and emptying the gemma cups damages the epidermal cells at the bottom of the cup.

MpFRH1 expression pattern coincides with the expected MpRSL1 expression pattern and the pattern of MpRSL1 activity

As described in chapter 4, *MpRSL1* is required for the development of rhizoid precursor cells, rhizoids, gemmae and epidermal papillae. Thus, *MpRSL1* is likely to be expressed in these cell types. Preliminary analysis of *MpRSL1* promoter expression pattern using plants expressing the *GUS*-reporter gene behind the *MpRSL1* promoter supports this hypothesis (Helene Proust, unpublished data). Thus, *MpFRH1* expression pattern coincides with the pattern of *MpRSL1* expression and activity, giving further support to the hypothesis that *MpFRH1* and *MpRSL1* interact to regulate epidermal cell outgrowth. Furthermore, these findings suggest that *MpFRH1* is likely to either function non-cell autonomously, or be involved in regulation of timing and appropriate level of *MpRSL1* expression during tissue differentiation.

5.4. Discussion

Here, I described the identification and characterisation of *MpFRH1*; a novel liverwort specific miRNA that functions as a negative regulator of rhizoid precursor cell, gemma and epidermal papilla differentiation by negatively regulating the *M. polymorpha* class I *RSL* gene *MpRSL1*. The MpFRH1 miRNA target site on class I *RSL* gene transcripts was perfectly conserved in a range of liverwort species representing the two major liverwort lineages Jugermanniopsida and Marchantiopsida. This suggests that the FRH1 miRNA binding site on liverwort class I *RSL* genes evolved before the divergence of the two lineages in the Late Devonian period approximately 373 Mya (Heinrichs *et al*., 2007). Therefore, the MpFRH1 miRNA may also be ancient and conserved within the liverwort lineage.

21 bp long plant miRNAs have been shown to repress the expression of their target genes by two distinct mechanisms: i) on a transcriptional level by promoting target transcript cleavage, or ii) on a translational level by inhibiting the translation of the target transcript (Voinnet, 2009). In addition, longer 24 bp miRNAs can repress the transcription of their targets by inducing DNA methylation at the target gene loci (Wu *et al*., 2010). Here, I have shown that the 21 bp MpFRH1 miRNA negatively regulates the level of *MpRSL1* transcripts consistent with the hypothesis MpFRH1 miRNA guides *MpRSL1* transcript cleavage. The action of plant miRNAs is in many cases thought to result from a combination of target gene transcript cleavage and translational repression (Aukerman and Sakai, 2003; Chen *et al*., 2004; Bari *et al.*, 2006; Brodersen *et al*., 2008; Beauclair *et al*., 2010; li *et al.,* 2013). Low levels of *MpRSL1* mRNA persist in the *MpFRH1*^{GOF} lines, while the phenotype of the

MpFRH1^{GOF} lines is very similar to the *Mprsl1* loss-of-function lines. These findings suggest the effect of MpFRH1 miRNA on MpRSL1 protein levels may be even more pronounced than the reduction observed in the *MpRSL1* transcript level. In contrast, *MpRSL1* was found to positively regulate *MpFRH1* expression. Together, *MpRSL1* and *MpFRH1* form a negative feedback loop, in which *MpRSL1* activates *MpFRH1* pri-miRNA gene expression, while the MpFRH1 miRNA suppresses *MpRSL1* expression. Such negative feedback loops that fine tune the temporal and spatial expression patterns of developmental regulators are common in multicellular organisms. For example, the miRNA biosynthesis pathway itself is under negative feedback regulation; both *AGO1* and *DCL1* are negatively regulated by miRNAs (Xie *et al.,* 2003; Vaucheret *et al*., 2004; 2006, Axtell *et al*., 2007).

Analysis of the *MpFRH1* promoter activity indicates the *MpFRH1* promoter is highly expressed in cells that give rise to rhizoids. However, *MpFRH1* functions as negative regulator of rhizoid precursor cell differentiation. This suggests, *MpFRH1* may function in the same cells in which it is expressed, and temporally regulate *MpRSL1* expression. *MpFRH1* could provide a mechanism to fine-tune the levels of *MpRSL1* during epidermal cell outgrowth (Fig. 5.13A). Alternatively, the function of MpFRH1 miRNA may be non-cell autonomous. MpFRH1 miRNA may be a mobile signal that moves from rhizoid precursor cells to the neighboring non-rhizoid precursor cells, where it inhibits *MpRSL1* expression and rhizoid precursor cell differentiation (Fig. 5.14B).

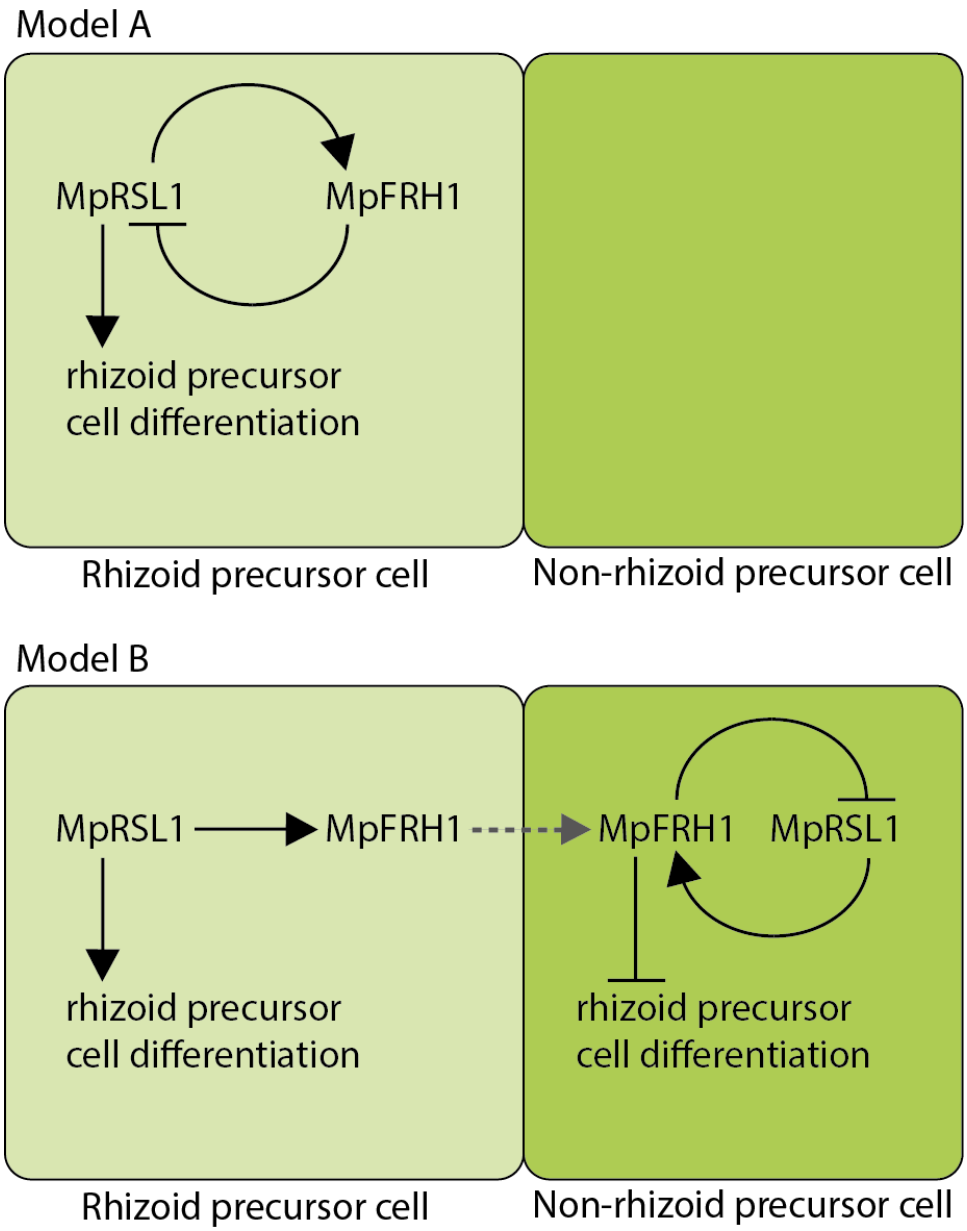

Figure 5.14 Hypothetical models of MpFRH1 miRNA function in *M. polymorpha* rhizoid precursor cell differentiation. In model A, MpFRH1 miRNA and *MpRSL1* are both expressed and active in rhizoid precursor cells. MpRSL1 activates *MpFRH1* expression, while MpFRH1 miRNA provides a negative feedback mechanism that suppresses *MpRSL1* expression resulting in fine-tuning of MpRSL1 levels, or regulation of the timing of *MpRSL1* expression. In model B, *MpRSL1* is expressed in rhizoid precursor cells where it activates the expression of *MpFRH1* pri-miRNA gene. *MpFRH1* pri-miRNA or miRNA moves out of the rhizoid precursor cell to the adjacent non-rhizoid precursor cell, where it suppresses *MpRSL1* expression and inhibits rhizoid precursor cell fate.

miRNAs play a crucial role during establishment of tissue identities in Arabidopsis. Consequently, Arabidopsis mutants defective in genes associated with miRNA biogenesis or function, such as *DCL1* and *AGO1*, are in most cases embryo lethal or have severe developmental abnormalities (Bohmert *et al*., 1998; Jacobsen *et al.,* 1999; Lu and Fedoroff, 2000; Park *et al*., 2002; Seefried *et al*., 2014). Plant miRNAs have been described to be involved in many developmental processes that could be expected to involve miRNA movement. However, so far only two Arabidopsis miRNAs, miR165/166 and miR394, have been experimentally shown to function as non-cell autonomous mobile signals that spatially restrict the expression of their target genes. During the establishment of the radial tissue layer patterning in the Arabidopsis root, the expression of miR165/166 becomes activated in the endodermal cell layer (Carlsbecker *et al.,* 2010). miR165/166 moves from the endodermal layer towards the centre of the root, restricting the expression of its target the class III homeodomain leucine-zipper transcription factor *PHABULOSA* (*PHB*) to the central vascular cylinder (Carlsbecker *et al.*, 2010). This restriction of the *PHB* expression by miR165/166 is required for correct patterning of xylem differentiation. Similarly, non-cell autonomous action of miR394 is required for meristem maintenance in the Arabidopsis shoot apical meristem. miR394 is expressed in the outermost protodermal cell layer of the meristem, from which it moves to the underlying meristematic cell layers, in which it represses its target *LEAF CURLING RESPONSIVENESS* (*LCR*) (Knauer *et al.,* 2013). This repression of *LCR* by miR394 in the inner layers of the meristem allows the activity of the homeodomain protein WUSCHEL, which is required for meristem maintenance. Thus, the ability of miRNAs to function as mobile signals during development has

been demonstrated in plants. However, while there are many examples of mobile proteins that only function non-cell autonomously without affecting their targets in the cells in which they are expressed, in both examples described for miRNAs the distribution of the miRNA target transcript is complementary to the distribution of the miRNA, i.e. the target is also repressed in the cells in which the miRNA is expressed. Thus, as the *MpFRH1* expression pattern co-incidences with the expected pattern of *MpRSL1* expression, it might be considered more likely that *MpFRH1* regulates the temporal dynamics rather than the cell type specific pattern of *MpRSL1* expression.

The role of miRNAs in regulating temporal patterning of their target gene expression has been described for many plant miRNAs. For example, during juvenile development, miR156 suppresses the expression of *SQUAMOSA PROMOTER BINDING PROTEIN-LIKE* (*SPL*) transcription factors that promote the juvenile-to-adult transition (Wu and Poethig, 2006; Wu *et al.*, 2009). The expression of miR156 is sufficient to maintain the juvenile phase, indicating that miR156 regulates the timing of *SPL* expression and juvenile-to-adult transition (Wu *et al*., 2009). Similarly, phosphate starvation induces miR399 that represses its target *PHOSPHATE 2* (*PHO2*) (Bari *et al*., 2006). *PHO2* is a negative regulator of phosphate starvation responses, and thus miR399 regulates the correct timing of phosphate starvation response activation. Therefore, miRNAs are involved in regulating the timing of developmental events and physiological responses in plants.

In some cases the expression domain of the miRNA and its target are not spatially nor temporally separated. The Arabidopsis miR164 co-localises with its

targets *CUP-SHAPED COTYLEDON1 (CUC1)* and *CUC2* transcription factor transcripts in the margins of young leaf and floral primordia (Nikovics *et al*., 2006; Sieber *et al*., 2007). miR164 resistant *CUC1* and *CUC2* were observed to maintain the same expression domain as the wild type proteins, however they were expressed at a higher level (Sieber *et al*., 2007). These findings suggest that miR164 functions to fine-tune the levels of *CUC1* and *CUC2* expression within their expression domain, while the overall pattern of *CUC1* and *CUC2* expression is predominantly established by other factors (Sieber *et al*., 2007). Similarly, an overlapping localisation of miRNA and its target transcripts was observed for *P. hybrida* and *A. majus* miR169 and its targets, NUCLEAR FACTOR-YA (NF-YA) transcription factors during flower development (Cartolano *et al*., 2007). These findings suggest that miRNA and its target are not always expressed in mutually exclusive domains, rather in some cases the miRNA is likely to fine tune the dynamics of the expression of its target gene.

Based on the analysis of the *MpFRH1* promoter activity presented here, it is not possible to evaluate whether the negative regulation of *MpRSL1* by MpFRH1 miRNA is more likely to be temporal or spatial, or whether the two genes are co-expressed. Rhizoid precursor cells on the upper side of the gemmae are already established at the stage after which the gemmae is large enough to survive outside of the gemmae cup, and thus it is not feasible to analyse the temporal dynamics of the *MpFRH1* promoter activity during rhizoid precursor cell differentiation on gemmae. To estimate whether *MpFRH1* miRNA functions in the rhizoid precursor cells, or whether it moves to the neighboring cells and functions non-cell autonomously, localisation of the MpFRH1 miRNA and its target the *MpRSL1*

transcript could be analysed using in RNA situ hybridisation. Furthermore, introducing point mutations into the MpFRH1 miRNA target site on the *MpRSL1* mRNA can be used to generate *MpFRH1* resistant version of *MpRSL1*. Expressing this *MpFRH1* resistant version of *MpRSL1* behind the native *MpRSL1* promoter in the *Mprsl1* mutant background is likely to give an indication of the role of the *MpRSL1* regulation by MpFRH1 miRNA during rhizoid development.

Many land plant miRNA families have ancient origins. 12 miRNA families are shared between the moss *P. patens* and flowering plants, and thus are likely to be conserved across land plants (Jones-Rhoades and Bartel, 2004; Axtell *et al*., 2007; Fattash *et al.,* 2007; Willman and Poethig, 2007; Addo-Quaye *et al*., 2009). Furthermore, based on the presence of the miRNA target sites on the target mRNAs, the targets of these conserved miRNAs are also likely to be highly conserved (Floyd and Bowman, 2004; Axtell and Bartel, 2005; Jones-Rhoades, 2011). In contrast, the unicellular green algae *Chlamydomonas reinhardtii* that is a sister to all land plants and their streptophyte algal ancestors, does not have members of any of the land plant miRNA families (Molnar *et al*., 2007; Zhao *et al*., 2007). Taken together, these findings suggest the 12 conserved land plant miRNA families originated in the streptophyte algae, or in early land plants before the divergence of the moss and vascular plant lineages more than 420 Mya. Furthermore, as nearly all targets of these conserved miRNAs are developmental regulators (Fahlgren *et al*., 2007), the emergence and evolution of these ancient land plant miRNA regulated pathways is likely to have played a role in the evolution of morphological and developmental complexity in land plants.

Despite the fact that many of the miRNA regulatory mechanisms are conserved in land plants, the majority of plant miRNAs are lineage specific or species specific (Axtell *et al.,* 2007; Sunkar *et al*., 2008; Lelandais-Briere *et al*., 2009; Ma *et al.,* 2010; Fahlgren *et al.,* 2010). For example, in total 223 miRNAs belonging to 106 miRNA families have been identified in the moss *P. patens*, and 12 of these families are conserved between *P. patens* and angiosperms (reviewed in Arazi, 2012; Taylor *et al*., 2014). While the number of species specific and lineage specific miRNAs has been suggested to be hugely over-estimated due to low stringency criteria for miRNA annotation and poor taxon sampling (Taylor *et al*., 2014), the emergence of new miRNA families is clearly not unusual. Functional characterisation of lineage or species specific miRNAs has so far only been performed for few flowering plant miRNAs (reviewed in Qin *et al*., 2014). In general, while the conserved miRNAs appear to be involved in developmental processes, the predicted targets of the non-conserved miRNAs in flowering plants suggest more varied functions (Fahlgren *et al*, 2007).

The set of ancient conserved land plant miRNAs identified share perfect or near perfect sequence identity across land plants. However, it is possible that additional miRNA pathways are conserved, but have not been identified as conserved due to divergence of the miRNA sequence and its target binding sequence in different lineages. Axtell *et al*. (2007) identified that the *P. patens* lineage specific miR904 targets the transcripts of three *P. patens AGO1*-like genes. Similarly, the Arabidopsis *AGO1* is targeted by miR168 (Vaucheret *et al.*, 2004, 2006). Both *P. patens* miR904 and Arabidopsis miR168 have their binding site

before just the PAZ-domain on the *AGO1* transcripts. These findings would suggest that this negative regulation of AGO by miRNA evolved in the common ancestor of moss and flowering plants. However, neither the nucleotide sequence of miR904 and miR168 nor the target site sequence on the *AGO1* transcripts are conserved between *P. patens* and Arabidopsis (Axtell *et al*., 2007). Thus, the negative regulation of *AGO1* by miRNAs may be a result of convergent evolution, or alternatively this mechanism may be ancient and the sequences of the miRNA and its target site may have diverged in the moss and flowering plant lineages. Therefore, even though the Arabidopsis class I *RSL* genes do not have conserved FRH1 miRNA binding site, it is possible that they are regulated by miRNA.

Characterisation of bryophyte miRNAs has so far largely been restricted to identification of the miRNA sequences using deep sequencing, predicting putative targets based on target prediction algorithms and in some cases verification of the cleavage of the target transcript by cloning the cleavage products (Floyd and Bowman, 2004; Arazi *et al.,* 2005; Axtell *et al.,* 2007; Addo-Quaye *et al*., 2009). Furthermore, while few bryophyte miRNAs have been assigned predicted functions based on their similarity with flowering plant miRNAs and the conservation of their binding sites on the target mRNAs, the function of the bryophyte specific miRNAs has remained elusive (Floyd and Bowman, 2004; Axtell *et al.,* 2007). Therefore, MpFRH1 is the first functionally characterised lineage specific bryophyte miRNA. Moreover, MpFRH1 is the first liverwort miRNA that can be assigned a function based on the miRNA over-expression phenotype.

Chapter 6

General discussion

Evolution of morphological and developmental complexity was a key to the success of plants in the terrestrial environment. I set out to elucidate the genetic basis behind one of the key morphological adaptations that evolved in the land plant lineage; the development of a specialised rooting structure. To this end, I identified genes required for the development of rhizoids; filamentous rooting cells that are morphologically similar to root hairs of vascular plants and make up the entire rooting structure in the basal land plants bryophytes. The twenty-five genes identified as being required for rhizoid development in the liverwort *M. polymorpha* provide insight both into the mechanism by which rhizoid development is initiated from epidermal cells, and into the genes that function downstream of the initiation mechanism.

The class I *RSL* subfamily basic helix-loop-helix transcription factor MpRSL1 was found to be both required and sufficient for the differentiation of epidermal cells into rhizoid precursor cells in *M. polymorpha* (Chapter 4). These findings suggest that *MpRSL1* is sufficient to switch on the full set of genes required for rhizoid development from thallus epidermal cells, and therefore to activate the entire rhizoid differentiation module. Class I *RSL* genes have also been shown to control rhizoid development in moss *P. patens* and root hair development in flowering plants (Menand *et al*., 2007; Chulmin Kim, unpublished data). Therefore, it is likely that the class I *RSL* gene mechanism was present in the common ancestor of all land plants. Consistent with this hypothesis, the genetic network that controls rhizoid elongation was found to contain many components similar to those required for root hair elongation in flowering plants (Chapter 3). It would be interesting to

see whether class I *RSL* genes also control root hair development in lycophytes, in which axial roots are thought to have evolved independently of the lineage leading to flowering plants (Raven and Edwards, 2001).

During the evolution of organisms' body plans, mutations in the *cis*-regulatory regions of genes that control development can alter spatial and temporal expression patterns of these genes, and can therefore result in re-utilisation of a cell or organ differentiation module in a novel developmental context (Stern and Orgogozo, 2008). *Cis*-regulatory evolution of class I *RSL* genes could have resulted in the entire gametophyte rhizoid module becoming activated in the sporophyte generation in the early land plants. An example of repeated recruitment of an existing genetic mechanism can be observed in leaf evolution. In Arabidopsis, a mechanism mediated by miRNA165/166 and its target the class III homeodomain-leucine zipper transcription factor REVOLUTA controls the patterning of vasculature in leaves (Emery *et al*., 2003). This mechanism is similar to the mechanism that regulates the radial patterning of vascular tissue in the stem (Emery et al., 2003). Therefore, an existing patterning mechanism is likely to have been recruited to function in a novel context in the leaves when the first leaves evolved.

While the role of class I *RSL* genes as regulators of the filamentous rooting cell module is conserved between bryophytes and flowering plants, the genes that function upstream of class I *RSL* genes are not likely to be conserved; no genes involved in patterning of root hair cell fate in Arabidopsis were identified as being required for patterning of rhizoid cell fate in *M. polymorpha* (Chapter 3). Instead, I found *MpRSL1* to be under negative feedback regulation by a novel liverwort

specific miRNA MpFRH1 (Chapter 5). Therefore, during the evolution of the vascular plant sporophyte body plan the class *RSL* gene regulated rooting cell module may have become integrated into a distinct, possibly pre-existing patterning mechanisms. For example, in Arabidopsis a similar patterning mechanism controls the patterning of root hairs in the root epidermis, stomata on the stem epidermis, and trichomes on the leaf epidermis (Berger *et al.,* 1998; Lee and Schiefelbein, 1999; DiChristina *et al*., 1996; Schellmann *et al*., 2002). Therefore, the same patterning mechanism has been utilised several times, and each time a different cell differentiation module has been integrated into this patterning mechanism. Virtually nothing is known about the mechanisms that regulate rhizoid or root hair patterning in species other than Arabidopsis. It remains to be identified where this patterning mechanism originated, and whether the same mechanism has been modified to control root hair patterning in different vascular plant lineages, or whether many distinct patterning mechanisms exist.

In addition to rhizoid development, the class I *RSL* gene *MpRSL1* is required for development of gemmae and mucilage papillae in *M. polymorpha* (Chapter 4). *MpRSL1* functions early in the development of these structures, most likely by promoting outgrowth of an epidermal cell. After the initial outgrowth, distinct downstream signalling pathways must become activated, leading to additional cell divisions in gemmae and mucilage papillae, and cell elongation by tip growth in rhizoids. Similar examples, in which re-wiring pre-existing regulatory networks has led to the development of novel structures can be seen in both the plant and animal kingdoms. The genetic mechanism that controls the maintenance of the stem cell

population within the root apical meristem in Arabidopsis has striking parallels with the mechanism that controls the maintenance of the shoot apical meristem, suggesting that the root meristem maintenance mechanism evolved by modification of existing shoot meristem maintenance mechanism (Stahl *et al*., 2009). Similarly, the development of the morphologically diverse thoracic horns in the genus *Onthophagus* dung beetles is controlled by a genetic network that evolved from a pre-existing genetic network for limb development (Moczek *et al*., 2006a; 2006b). Furthermore, in treehoppers (*Membracidae*), a genetic mechanism for the development of a helmet-like thoracic structure evolved from a pre-existing mechanism that regulates wing development (Prud'homme *et al.,* 2011). Therefore, pre-existing genetic mechanisms can be recruited and re-wired to give rise to novel structures.

Studies on evolution of developmental mechanisms in animals have firmly established that the basic patterning of the animal body plan is regulated by ancient deeply conserved genetic mechanisms mediated by the homeobox-genes (reviewed in Carroll, 2008). Furthermore, as long as 20 years ago genetic evidence suggested that similar genes control the differentiation of structures such as limbs (Panganiban *et al.,* 1997), the eyes (Halder *et al.,* 1995) and the heart (Chan-Thomas *et al.,* 1993) in vertebrates and arthropods that shared a common ancestor more than 500 million years ago (reviewed in Shubin *et al*., 2009). Therefore, the core genetic mechanisms that regulate the development of these morphologically distinct structures must have been established very early in the animal evolution, and have been subsequently built on to generate wide range of organ

morphologies. In contrast, the first pieces of evidence on the mechanisms that regulate plant development in lineages other than flowering plants have only began to emerge within the last decade, and many aspects of these processes remain to be discovered. This project provided some of the first evidence of the genetic basis of rhizoid development in the liverwort lineage and increased the understanding of the evolution of the genetic network for filamentous rooting cell development in land plants. This evidence indicates that rhizoid development in liverworts is carried out by a class I *RSL* gene regulated module of genes that have largely conserved roles in root hair development. Therefore, the class I *RSL* gene regulated cell differentiation module is likely to be widely conserved and have been present in the first land plants. The liverwort class I *RSL* genes either have evolved novel roles in regulation of processes that involve epidermal cell outgrowth, or perhaps more likely this may represent the ancestral function of class I *RSL* genes. Furthermore, in the liverwort lineage class I *RSL* genes are under negative feedback regulation by miRNA that is likely to be ancient and conserved in liverworts. This represents alternative regulation of a pre-existing genetic mechanism that may have evolved after the divergence of the liverwort lineage, highlighting the importance of studying non-angiosperm model species in order to identify the full spectrum of regulatory mechanisms that may act on developmental genes and therefore contribute to the evolution of morphological complexity in land plants.

Appendices

Materials and methods Appendix

TAIL-PCR primers

RB1 CCTGCAGGCATGCAAGCTTGG
RB2 GCTGGCGTAATAGCGAAGAGG
RB3 CCTGAATGGCGAATGCTAGAG
LB1 CAGATAAGGGAATTAGGGTTCCTATAGG
LB2 TATAGGGTTTCGCTCATGTGTTGAGC
LB3 AGTACATTAAAAACGTCCGCAATGTG

AD1 NGTCGASWGANAWGAA
AD2 TGWGNAGSANCASAGA
AD3 AGWGNAGWANCAWAGG
AD4 GTNCGASWCANAWGTT
AD5 NTCGASTWTSGWGTT
AD6 WGTGNAGWANCANAGA

qRT-PCR primers

MpRSL1
AGATGAGTCTGGGGCAACC
GGATGAGCGCTTTAGAGTGG

MpAPT
CGAAAGCCCAAGAAGCTACC
GTACCCCCGGTTGCAATAAG

MpCUL
AGGATGTGGACAAGGATAGACG
GTTGATGTGGCAACACCTTG

MpFRH1
ACAGCTCGGGGGCTGCAGCACAAAT
TCAGGATGGCCAGGGGACACTGAAG

***MpFRH1* ORF1**
CAGGTTGCAGCAGGGAATTC
TCTCACACAAACACAGATGCC

***MpFRH1* ORF2**
ACGATTCAGCCGCAGTCA
CTCAGAAGACACCACCTCGT

***MpFRH1* ORF3**
GCGGGCAAAGATGGAGATTC
TCTGCATCCTTCAGTGTCCC

Cloning primers

***MpFRH1* transcript sequence**
TCGGCACTCTCTTCTGTACA
GGCAAAGCAAATTTATTGACGGG

***MpFRH1* 3.5kb promoter**
GAATTCATTTAAATGAAATCTGAGTTTCC
GGTACCAGGGAGAAAGAGCGCCTGCG

***MpIRE* coding sequence**
ATGGAGGCGGGCTTGCAGA
TCAACTTGGGCCCTTCGGAGA

***MpIRE* 3.5kb promoter**
CCTGTCAAACACTGATAGTTAAACAAGATCAGGCTCATCAGACG
TGAACGATCGGGGAAATTCGTTTAAACAAAATTGACCGTGCACGGAAC

Stem-loop PCR primers

miRFRH1 RT
GTCGTATCCAGTGCAGGGTCCGAGGTATTCGCACTGGATACGACACATTG

miRFRH1 F1
CGGCGTGTGTGAGAAGAGGC

universal R primer
GTGCAGGGTCCGAGGT

TAIL-PCR cycling conditions

1st reaction
93 °C 1 min.
95 °C 1 min.
94 °C 30 sec.
62 °C 1 min.
72 °C 2 min. 30 sec.
Go to step 4 for 4 more cycles
94 °C 30 sec.
25°C 3 min.

Ramp for 72° at 0.2 °C/sec
72 C° 2 min. 30 sec.
94 °C 10 sec.
68 °C 1 min.
72 °C 2 min. 30 sec.
94 °C 10 sec.
68 °C 1 min.
72 °C 2 min. 30 sec.
94 °C 10 sec.
44 °C 1 min.
72 °C 2 min. 30 sec.
Go to step 12 for 14 more cycles
72 °C 5 min.
12 °C forever

2nd reaction
94 °C 10 sec.
64 °C 1 min.
72 °C 2 min. 30 sec.
94 °C 10 sec.
64 °C 1 min.
72 °C 2 min. 30 sec.
94 °C 10 sec.
44 °C 1 min.
72 °C 2 min. 30 sec.
Go to step 2, for 11 more cycles
72 °C 5 min.
12 °C forever

3rd reaction
94 °C 10 sec.
44 °C 1 min.
72 °C 2 min. 30 sec.
Go to step 2, for 19 more cycles
72 °C 5 min.
12 °C forever

qRT-PCR cycling conditions

95 °C 2 min.
95 °C 15 sec.
60/65 °C 30 sec.
72 °C 1 min.
Go to step 2, for 39 more cycles

Chapter 3 Appendix

Table A3.1 Predicted Arabidopsis homologs of the *M. polymorpha* rhizoid development genes.

gene name	predicted function	Arabidopsis homologs
MpALBA	alba-like DNA/RNA-binding protein	At1G76010 At3G07030 At1G20220
MpAP5M	AP-5 complex subunit mu	At2G20790
MpCSLD1 *MpCSLD2*	cellulose synthase-like class D cellulose synthase-like class D	At2G33100 *(CSLD1)* At5G16910 *(CSLD2)* At3G03050 *(CSLD3)* At4G38190 *(CSLD4)* At1G02730 *(CSLD5)* At1G32180 *(CSLD6)*
MpFBA1	fructose-bisphosphate aldolase	At2G21330 *(FBA1)* At4G38970 *(FBA2)* At2G01140 *(FBA3)*
MpGATA1	class A GATA zinc finger transcription factor	At3G24050 *(GATA1)* At2G45050 *(GATA2)* At4G34680 *(GATA3)* At3G60530 *(GATA4)* At5G66320 *(GATA5)* At3G51080 *(GATA6)* At4G36240 *(GATA7)* At3G54810 *(GATA8)* At4G32890 *(GATA9)* At1G08000 *(GATA10)* At1G08010 *(GATA11)* At5G25830 (*GATA12*) At2G28340 *(GATA13)* At3G45170 *(GATA14)*
MpGMP	GDP-mannose pyrophosphorylase	At2G39770 (*GMP1*) At3G55590
MpIRE	AGC-kinase	At5G62310 (*IRE*) At1G48490 At3G17850 At1G45160
MpPI4Kα	1-phosphatidylinositol 4-kinase alpha	At1G49340 At1G51040

Table A3.1 Continued

gene name	predicted function	Arabidopsis homologs
MpPTI	serine/threonine kinase	At2G30740
		At1G06700 *(PTI1-1)*
		At2G30740 *(PTI1-2)*
		At3G59350 *(PTI1-3)*
		At2G43230
		At2G41970
		At2G47060 *(PTI1-4)*
		At3G62220
		At3G17410
		At1G48210
		At1G48220
MpRHM1	rhamnose biosynthesis	At1G78570 (*RHM1*)
		At1G53500 *(RHM2)*
		At3G14790 *(RHM3)*
		At1G63000 (*UER1*)
MpRSL1	bHLH transcription factor	At1G66470 (*RHD6*)
		At5G37800 *(RSL1)*
MpREN	Pleckstrin homology (PH) domain /RhoGAP domain-containing protein	At5G19390
		At5G12150
MpSCD	Rab guanine nucleotide exchange factor	At1G49040 (*SCD1*)
MpSPI	WD-40 repeat protein	At1G03060 (*SPI*)
		At4G02660
MpSRI1	Rab guanine nucleotide exchange factor similar to *S. Cerevisiae RIC1*	At5G28350
		At3G61480
MpSRI2	calcium binding EF-hand family protein similar to *S. Cerevisiae PAN1*	At1G21630
		At1G20760
MpSRI3	unknown protein	At2G41830
		At1G05960
		At5G21080
		At5G26850
MpTHE	CrRLK1 family receptor-like kinase	At5G54380 (*THE1*)
		At3G51550 *(FER*)
		At5G61350
		At3G46290 *(HERK)*
		At5G59700
		At2G21480
		At1G30570 *(HERK2)*
		At4G39110
		At5G28680 *(ANX2)*
		At3G04690 *(ANX1)*
		At5G24010
		At2G39360
		At5G39000
		At5G38990
		At2G23200
		At5G39020
		At5G39030

Table A3.1 Continued

gene name	predicted function	Arabidopsis homologs
MpTMT	tonoplast monosaccharide transporter	At1G20840 *(TMT1)* At4G35300 *(TMT2)* At3G51490 (*TMT3*)
MpWDL	predicted microtubule binding protein /TPX2 domain containing protein	At2G35880 At3G23090 *(WDL3)* At5G28646 *(WVD2)* At1G54460 At3G04630 *(WDL1)* At4G32330 At2G25480 At3G01710
MpXIA	Class XI myosin	At4G33200 *(XI-I)* At2G33240 *(XI-D)* At1G04600 *(XI-A)* At5G43900 *(XI-2)* At1G04160 *(XI-B)* At4G28710 *(XI-H)* At2G20290 *(XI-G)* At5G20490 *(XI-K)* At1G17580 *(XI-1)* At3G58160 *(XI-J)* At1G54560 *(XI-E)* At1G08730 *(XI-C)* At2G31900 *(XI-F)*
MpXF	squalene monooxygenase	At1G58440 At4G37760 At2G22830
MpXUT	xyloglucan-specific galacturonosyltransferase	At5G41250 At2G29040 At2G32740 *(GT13)* At1G63450 *(XUT1)* At2G32750 At4G13990 At2G20370 *(MUR3)* At1G68470 At2G31990 At4G22580 At5G62220 *(GT18)*

Table A3.2 Publications in which mutations in the Arabidopsis homologs of the *M. polymorpha* rhizoid development genes are described to result in a root hair defective phenotype.

gene name	reference
MpRSL1	Masucci and Schiefelbein, 1994; Menand *et al*., 2007
MpCSLD2	Favery et al., 2001; Wang et al., 2001; Bernal *et al*., 2008
MpCSLD1	Favery et al., 2001; Wang et al., 2001; Bernal *et al*., 2008
MpXUT	Pena *et al.*, 2012
MpRHM1	Diet *et al*., 2006; Ringli *et al*., 2008
MpTHE	Duan *et al.*, 2010
MpSCD	Falbel *et al*., 2003
MpSPI	Saedler *et al*., 2009
MpXIA	Peresmylov *et al*., 2009, 2010
MpIRE	Oyama *et al*., 2002
MpXF	Pose *et al*., 2009

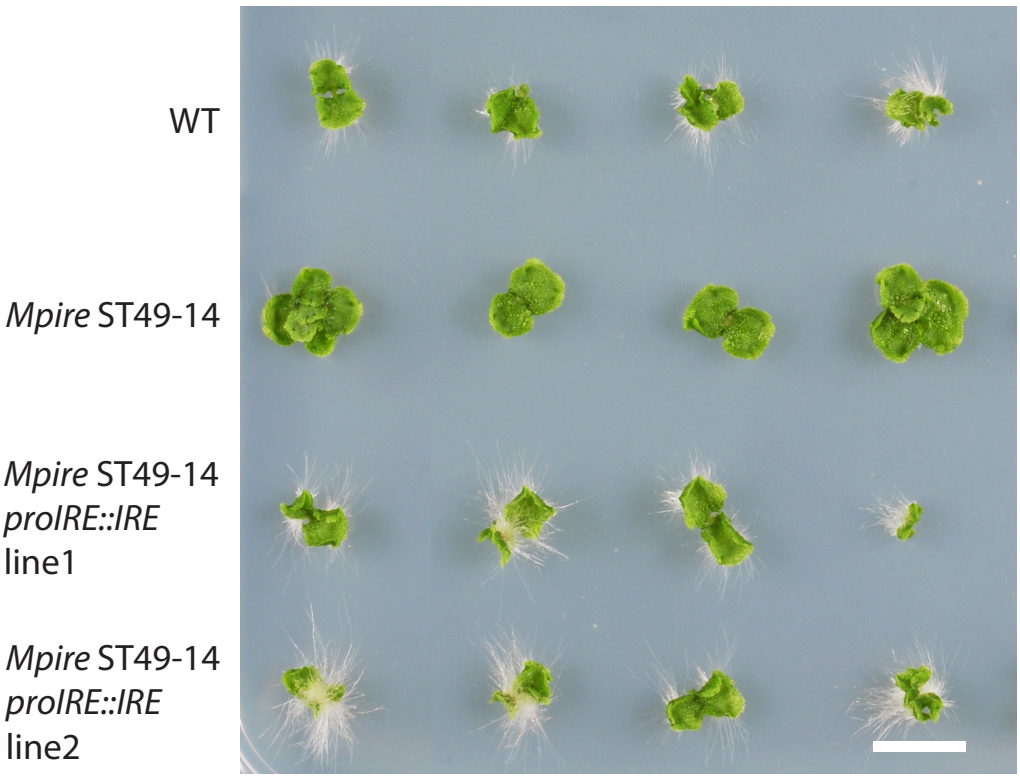

Figure A3.1 *Mpire* mutant ST49-14 rhizoid elongation defect is fully complemented by the full-length *MpIRE* coding sequence driven by the native *MpIRE* promoter. Fourteen day-old gemmae of wild type *M. polymorpha*, *Mpire* mutant ST49-14 and ST49-14 complemented with the wild type *MpIRE* coding sequence driven by the native *MpIRE* promoter. Scale bar 1 cm.

Chapter 5 Appendix

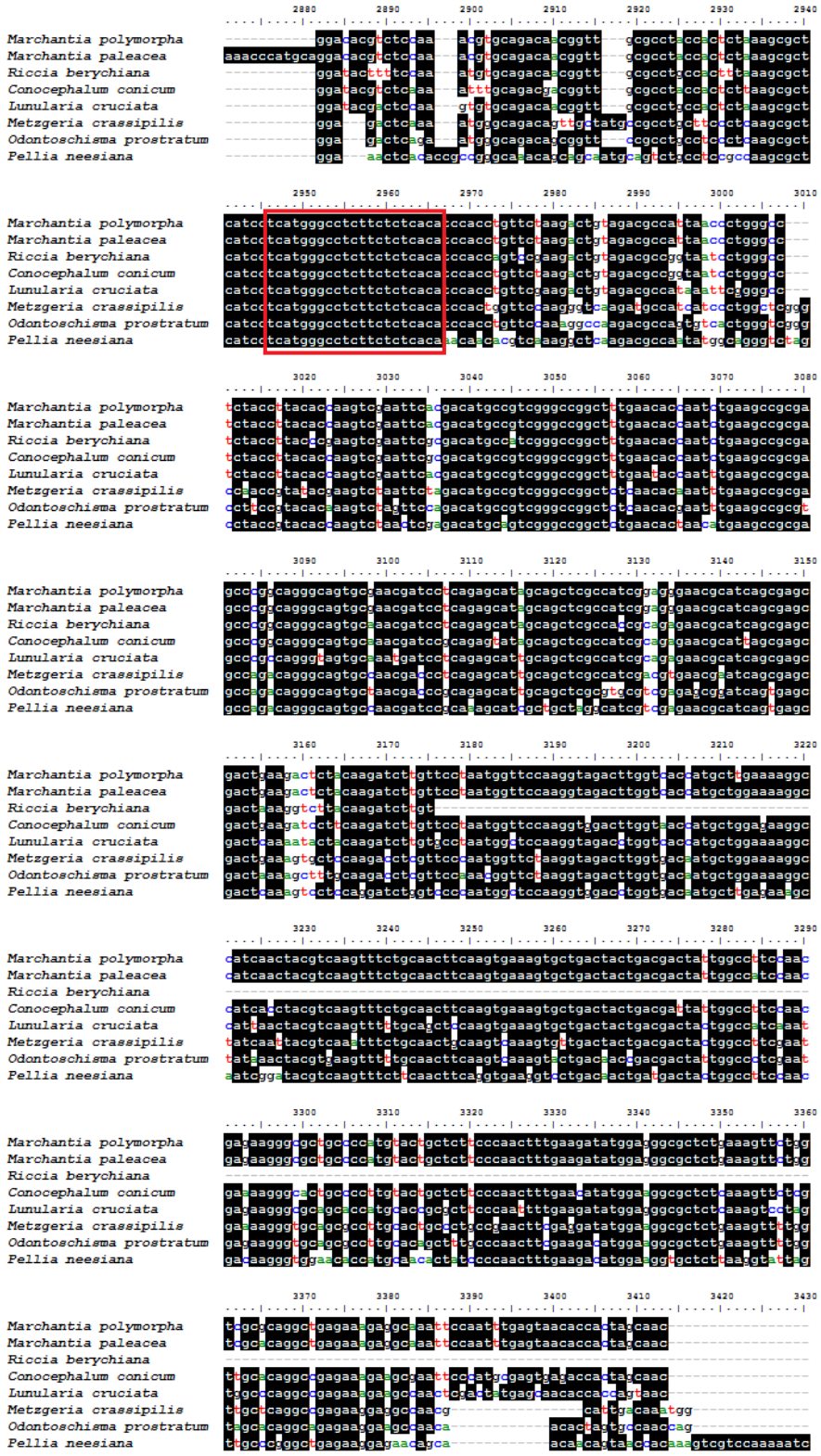

Figure A5.1 multiple sequence alignment of class I *RSL* gene transcripts from the eight liverwort species for which sequence data was available. The red box indicates the FRH1 miRNA binding site.

>*MpFRH1* transcript

tcggcactctcttctgtacaaataagtacttccatcagcagacgacatcagtcttgaacttgctcactcatctccccctccc
ccctccccctcccgcagccctcaacagcgccatagagtcccagacttcccactggccggccccatctgaacctcttctct
tctctcatcggcttctccctagacctgccccgtagttcagtctagctagctcggctcggcgtggcgggcggtggggtagtt
ggttagtccagttccggtataattccagcgctagcagttgctggagttcgtggtgatggtggtggtgtagtagtagtc
atagtgtaccgcattaagatcctctccagtcgcttgagctgcgccacgattctgctcgtgcagcagcttggcttgtggacg
atttgcgtcgttcagatcgaaattcaaccaaaagctgcagcacgaattttggattggatgagcaaccgcagataataga
tagcacagccaaacagcaccgcgtggtggcggccgtcactgacacagacagatagcgagctagatagatagacagat
agacagaaatcttgacattctccaggttgcagcagggaattcggccactttcggttcttgtgcttgcacattggtctcttc
acgcacaaacatcgaacccttgtggcatctgtgtttgtgtgagaagaggccaatctccaagcggaaaaaccccttaaat
tcgaggacgattcagccgcagtcagcagcagtggtcagtcagagtaagtgggtctatgttgtgcgtgaaacagaacac
aattttctcgtgctaacgaggtggtgtcttctgagatcagctccagcgtcatcctcatccatggatcctcaccttcctcaca
ggggatcatcaccatcactcggatagactgccacgcagttttctttggctgcaagcgggcaaagatcgagattctgcac
gggttggcgcactgtagccttaggatggcgtgctccagttacaaacatactcaggatggccaggggacactgaaggat
gcagattcgtagagactccgttcactgatgcaccgaacttgggagctcggatcacaccctcgtgcactcaccacaccgg
caggaggattgattgagaatctagatttgtgctgcagcccccgagctgtatggaattcattacccgtcaataaatttgctt
tgcc

References

Addo-Quaye, C., Snyder, J.A., Park, Y.B., Li, Y.F., Sunkar, R., and Axtell, M.J. (2009). Sliced microRNA targets and precise loop-first processing of MIR319 hairpins revealed by analysis of the *Physcomitrella patens* degradome. RNA **15**: 2112–2121.

Alonso, J.M. et al. (2003). Genome-wide insertional mutagenesis of *Arabidopsis thaliana.* Science **301**: 653–657.

Aravind, L., Iyer, L.M., and Anantharaman, V. (2003). The two faces of Alba: the evolutionary connection between proteins participating in chromatin structure and RNA metabolism. Genome Biol. **4**: R64.

Arazi, T. (2011). MicroRNAs in the moss *Physcomitrella patens*. Plant Mol Biol **80**: 55–65.

Arazi, T., Talmor-Neiman, M., Stav, R., Riese, M., Huijser, P., and Baulcombe, D.C. (2005). Cloning and characterization of micro-RNAs from moss. Plant J **43**: 837–848.

Augustine, R.C., Pattavina, K.A., Tuzel, E., Vidali, L., and Bezanilla, M. (2011). Actin Interacting Protein1 and Actin Depolymerizing Factor Drive Rapid Actin Dynamics in *Physcomitrella patens*. Plant Cell **23**: 3696–3710.

Aukerman, M.J. and Sakai, H. (2003). Regulation of Flowering Time and Floral Organ Identity by a MicroRNA and Its APETALA2-Like Target Genes. Plant Cell **15**: 2730–2741.

Axtell, M.J. (2005). Antiquity of MicroRNAs and Their Targets in Land Plants. Plant Cell **17**: 1658–1673.

Axtell, M.J., Snyder, J.A., and Bartel, D.P. (2007). Common Functions for Diverse Small RNAs of Land Plants. Plant Cell **19**: 1750–1769.

Bari, R., Pant, B.D., Stitt, M., Scheible, W.-D. (2006). PHO2, MicroRNA399, and PHR1 Define a Phosphate-Signaling Pathway in Plants. Plant Physiology **141**: 988–999.

Barnes, C.R. and Land, W. (1908). Bryological papers. II. The origin of the cupule of *Marchantia*. Botanical Gazette **46**: 401-409.

Baumberger, N. and Baulcombe, D.C. (2005). Arabidopsis ARGONAUTE1 is an RNA Slicer that selectively recruits microRNAs and short interfering RNAs. Proc Natl Acad Sci USA. **102**: 11928–11933.

Beauclair, L., Yu, A., and Bouché, N. (2010). microRNA-directed cleavage and translational repression of the copper chaperone for superoxide dismutase mRNA in Arabidopsis. Plant J **62**: 454–462.

Becker, B. and Marin, B. (2009). Streptophyte algae and the origin of embryophytes. Annals of Botany **103**: 999–1004.

Beerling, D.J., Osborne, C.P., and Chaloner, W.G. (2001). Evolution of leaf-form in land plants linked to atmospheric CO2 decline in the Late Palaeozoic era. Nature **410**: 352–354.

Benková, E., Michniewicz, M., Sauer, M., and Teichmann, T. (2003). Local, efflux-dependent auxin gradients as a common module for plant organ formation. Cell **115**: 591-602.

Bennett, T.A. et al. (2014). Plasma Membrane-Targeted PIN Proteins Drive Shoot Development in a Moss. Current Biology **24**: 2776–2785.

Berger, F.F., Linstead, P.P., Dolan, L.L., and Haseloff, J.J. (1998). Stomata Patterning on the Hypocotyl of *Arabidopsis thaliana* is Controlled by Genes Involved in the Control of Root Epidermis Patterning. Dev Biol **194**: 9–9.

Bernal, A.J., Yoo, C.M., Mutwil, M., Jensen, J.K., Hou, G., Blaukopf, C., Sorensen, I., Blancaflor, E.B., Scheller, H.V., and Willats, W.G.T. (2008). Functional Analysis of the Cellulose Synthase-Like Genes CSLD1, CSLD2, and CSLD4 in Tip-Growing Arabidopsis Cells. Plant Physiology **148**: 1238–1253.

Berner, R.A. a model for atmospheric CO2 over phanerozoic time (1991). American Journal of Science **291**, 339-376.

Berner, R.A. (1994). GEOCARB II; a revised model of atmospheric CO 2 over Phanerozoic time. American Journal of Science **294**: 56–91.

Berner, R.A. (1998). The carbon cycle and carbon dioxide over Phanerozoic time: the role of land plants. Philos Trans R Soc Lond, B, Biol. Sci. **353**: 75–82.

Bernhardt, C. (2005). The bHLH genes GL3 and EGL3 participate in an intercellular regulatory circuit that controls cell patterning in the Arabidopsis root epidermis. Development **132**: 291–298.

Bibikova, T.N., Blancaflor, E.B., and Gilroy, S. (1999). Microtubules regulate tip growth and orientation in root hairs of Arabidopsis thaliana. Plant J **17**: 657–665.

Bohmert, K., Camus, I., Bellini, C., Bouchez, D., Caboche, M., and Benning, C. (1998). AGO1 defines a novel locus of Arabidopsis controlling leaf development. EMBO J **17**: 170–180.

Boisson-Dernier, A., Roy, S., Kritsas, K., Grobei, M.A., Jaciubek, M., Schroeder, J.I., and Grossniklaus, U. (2009). Disruption of the pollen-expressed FERONIA homologs ANXUR1 and ANXUR2 triggers pollen tube discharge. Development **136**: 3279–3288.

Boisson-Dernier, A., Lituiev, D.S., Nestorova, A., Franck, C.M., Thirugnanarajah, S., and Grossniklaus, U. (2013). ANXUR Receptor-Like Kinases Coordinate Cell Wall Integrity with Growth at the Pollen Tube Tip Via NADPH Oxidases. PLoS Biol **11**: e1001719.

Bower, F. O. The origin of a land flora (1908). MacMillan & Co., London.

Brandizzi, F. and Wasteneys, G.O. (2013). Cytoskeleton-dependent endomembrane organization in plant cells: an emerging role for microtubules. Plant J **75**: 339–349.

Brodersen, P., Sakvarelidze-Achard, L., Bruun-Rasmussen, M., Dunoyer, P., Yamamoto, Y.Y., Sieburth, L., and Voinnet, O. (2008). Widespread translational inhibition by plant miRNAs and siRNAs. Science **320**: 1185–1190.

Bruex, A., Kainkaryam, R.M., Wieckowski, Y., Kang, Y.H., Bernhardt, C., Xia, Y., Zheng, X., Wang, J.Y., Lee, M.M., Benfey, P., Woolf, P.J., and Schiefelbein, J. (2012). A Gene Regulatory Network for Root Epidermis Cell Differentiation in Arabidopsis. PLoS Genet **8**: e1002446.

Budziszewski, G.J. et al. (2001). Arabidopsis genes essential for seedling viability: isolation of insertional mutants and molecular cloning. Genetics **159**: 1765–1778.

Campbell, E.O. (1954). Structure and Development of *Marchasta Areolata*, Camp. Transactions of the Royal Society of New Zealand **82**: 249–262.

Carlsbecker, A. et al. (2010). Cell signalling by microRNA165/6 directs gene dose-dependent root cell fate. Nature **465**: 316–321.

Carroll, S.B. (2008). Evo-Devo and an Expanding Evolutionary Synthesis: A Genetic Theory of Morphological Evolution. Cell **134**: 25–36.

Cartolano, M., Castillo, R., Efremova, N., Kuckenberg, M., Zethof, J., Gerats, T., Schwarz-Sommer, Z., and Vandenbussche, M. (2007). A conserved microRNA module exerts homeotic control over *Petunia hybrida* and *Antirrhinum majus* floral organ identity. Nat Genet **39**: 901–905.

Chan-Thomas, P.S., Thompson, R.P., Robert, B., Yacoub, M.H., and Barton, P.J. (1993). Expression of homeobox genes Msx-1 (Hox-7) and Msx-2 (Hox-8) during cardiac development in the chick. Dev Dyn **197**: 203–216.

Chen, X. (2004). A microRNA as a translational repressor of APETALA2 in Arabidopsis flower development. Science **303**: 2022–2025.

Cheung, A.Y. and Wu, H.-M. (2011). THESEUS 1, FERONIA and relatives: a family of cell wall-sensing receptor kinases? Current Opinion in Plant Biology **14**: 632–641.

Chiyoda, S., Ishizaki, K., Kataoka, H., Yamato, K.T., and Kohchi, T. (2008). Direct transformation of the liverwort *Marchantia polymorpha L*. by particle bombardment using immature thalli developing from spores. Plant Cell **27**: 1467–1473.

Clowes, F. (2000). Pattern in root meristem development in angiosperms. New Phytologist **146**: 83-94.

Cosgrove, D.J. (2005). Growth of the plant cell wall. Nature Reviews Molecular Cell Biology **6**: 850–861.

Cox, C.J., Li, B., Foster, P.G., Embley, T.M., and Civan, P. (2014). Conflicting Phylogenies for Early Land Plants are Caused by Composition Biases among Synonymous Substitutions. Systematic Biology **63**: 272–279.

Datta, S., Kim, C.M., Pernas, M., Pires, N.D., Proust, H., Tam, T., Vijayakumar, P., and Dolan, L. (2011). Root hairs: development, growth and evolution at the plant-soil interface. Plant Soil **346**: 1–14.

De Smet, I. et al. (2011). Unraveling the Evolution of Auxin Signaling. Plant Physiology **155**: 209–221.

Dharmasiri, N., Dharmasiri, S., and Estelle, M. (2005). The F-box protein TIR1 is an auxin receptor. Nature **435**: 441–445.

Di Cristina, M., Sessa, G., Dolan, L., Linstead, P., Baima, S., Ruberti, I., and Morelli, G. (1996). The Arabidopsis Athb-10 (GLABRA2) is an HD-Zip protein required for regulation of root hair development. Plant J **10**: 393–402.

Diet, A. et al. (2006). The Arabidopsis Root Hair Cell Wall Formation Mutant lrx1 Is Suppressed by Mutations in the RHM1 Gene Encoding a UDP-L-Rhamnose Synthase. Plant Cell **18**: 1630–1641.

Ding, W., Yu, Z., Tong, Y., Huang, W., Chen, H., and Wu, P. (2009). A transcription factor with a bHLH domain regulates root hair development in rice. Cell Research **19:** 1309–1311.

Dittmer, H.J. (1949). Root hair variations in plant species. Am. J. Bot. **36**: 152–155.

Dolan, L. and Costa, S. (2001). Evolution and genetics of root hair stripes in the root epidermis. Journal of Experimental Botany **52**: 413–417.

Dombrovska, O. and Qiu, Y.-L. (2004). Distribution of introns in the mitochondrial gene nad1 in land plants: phylogenetic and molecular evolutionary implications. Molecular Phylogenetics and Evolution **32**: 246–263.

Duan, Q., Kita, D., Li, C., Cheung, A.Y., and Wu, H.-M. (2010). FERONIA receptor-like kinase regulates RHO GTPase signaling of root hair development. Proc Natl Acad Sci USA **107**: 17821–17826.

Duckett, J.G., Ligrone, R., and Renzaglia, K.S. (2014). Pegged and smooth rhizoids in complex thalloid liverworts (Marchantiopsida): structure, function and evolution. Botanical Journal of The Linnean Society **174**: 68–92.

Duckett, J.G., Renzaglia, K.S., and Pell, K. (1991). A light and electron microscope study of rhizoid–ascomycete associations and flagelliform axes in British hepatics with observations on the effects of the fungi on host morphology. New Phytologist **118**: 233–257.

Edwards, D. and Feehan, J. (1980). Records of Cooksonia-type sporangia from late Wenlock strata in Ireland. Nature **287**: 41–42.

Edwards, D., Davies, K.L., and Axe, L. (1992). A vascular conducting strand in the early land plant Cooksonia. Nature **357**: 83-85.

Edwards, D., Duckett, J.G., and Richardson, J.B. (1995). Hepatic characters in the earliest land plants. Nature 374: 635-636.

Edwards, D., Kerp, H., and Hass, H. (1998). Stomata in early land plants: an anatomical and ecophysiological approach. Journal of Experimental Botany **49**: 255–278.

Eklund, D.M. et al. (2015). Auxin Produced by the Indole-3-Pyruvic Acid Pathway Regulates Development and Gemmae Dormancy in the Liverwort *Marchantia polymorpha.* Plant Cell Online.

Eklund, D.M., Thelander, M., Landberg, K., Staldal, V., Nilsson, A., Johansson, M., Valsecchi, I., Pederson, E.R.A., Kowalczyk, M., Ljung, K., Ronne, H., and Sundberg, E. (2010). Homologues of the Arabidopsis thaliana SHI/STY/LRP1 genes control auxin biosynthesis and affect growth and development in the moss *Physcomitrella patens*. Development **137**: 1275–1284.

Emery, J.F., Floyd, S.K., Alvarez, J., Eshed, Y., Hawker, N.P., Izhaki, A., Baum, S.F., and Bowman, J.L. (2003). Radial Patterning of Arabidopsis Shoots by Class III HD-ZIP and KANADI Genes. Current Biology **13**: 1768–1774.

Emms, D.M. and Kelly, S. (2015). OrthoFinder: solving fundamental biases in whole genome comparisons dramatically improves orthogroup inference accuracy. Genome Biol **16**: 1–14.

Fahlgren, N., Jogdeo, S., Kasschau, K.D., Sullivan, C.M., Chapman, E.J., Laubinger, S., Smith, L.M., Dasenko, M., Givan, S.A., Weigel, D., and Carrington, J.C. (2010). MicroRNA Gene Evolution in *Arabidopsis lyrata* and *Arabidopsis thaliana*. Plant Cell **22**: 1074–1089.

Falbel, T.G., Koch, L.M., Nadeau, J.A., Segui-Simarro, J.M., Sack, F.D., and Bednarek, S.Y. (2003). SCD1 is required for cytokinesis and polarized cell expansion in *Arabidopsis thaliana*. Development **130**: 4011–4024.

Fattash, I., Voß, B., Reski, R., Hess, W.R., and Frank, W. (2007). Evidence for the rapid expansion of microRNA-mediated regulation in early land plant evolution. BMC Plant Biology **7**: 13.

Favery, B., Ryan, E., Foreman, J., Linstead, P., Boudonck, K., Steer, M., Shaw, P., and Dolan, L. (2001). KOJAK encodes a cellulose synthase-like protein required for root hair cell morphogenesis in Arabidopsis. Genes & Development **15**: 79–89.

Finet, C., Timme, R.E., Delwiche, C.F., and Marlétaz, F. (2010). Multigene Phylogeny of the Green Lineage Reveals the Originand Diversification of Land Plants. Current Biology **20**: 2217–2222.

Finka, A., Saidi, Y., Goloubinoff, P., Neuhaus, J.-M., Zrÿd, J.-P., and Schaefer, D.G. (2008). The knock-out of ARP3a gene affects F-actin cytoskeleton organization altering cellular tip growth, morphology and development in moss *Physcomitrella patens*. Cell Motil Cytoskeleton **65**: 769–784.

Flores-Sandoval, E., Eklund, D.M., and Bowman, J.L. (2015). A Simple Auxin Transcriptional Response System Regulates Multiple Morphogenetic Processes in the Liverwort *Marchantia polymorpha*. PLoS Genet **11**: e1005207.

Floyd, S.K. Zalewski, C.S., Bowman, J.L. (2006). Evolution of Class III Homeodomain-Leucine Zipper Genes in Streptophytes. Genetics **173**: 373–388.

Floyd, S.K. and Bowman, J.L. (2004). Gene regulation: ancient microRNA target sequences in plants. Nature **428**: 485–486.

Foreman, J., Demidchik, V., Bothwell, J.H., Mylona, P., Miedema, H., Torres, M.A., Linstead, P., Costa, S., Brownlee, C., and Jones, J.D. (2003). Reactive oxygen species produced by NADPH oxidase regulate plant cell growth. Nature **422**: 442–446.

Forrest, L.L., Davis, E.C., Long, D.G., and Crandall-Stotler, B.J. (2006). Unraveling the evolutionary history of the liverworts (Marchantiophyta): multiple taxa, genomes and analyses. The Bryologist **109**: 303-334.

Friis, E.M., Pedersen, K.R., and Crane, P.R. (2006). Cretaceous angiosperm flowers: Innovation and evolution in plant reproduction. Palaeogeography, Palaeoclimatology, Palaeoecology **232**: 251–293.

Fujita, T., Sakaguchi, H., Hiwatashi, Y., Wagstaff, S.J., Ito, M., Deguchi, H., Sato, T., and Hasebe, M. (2008). Convergent evolution of shoots in land plants: lack of auxin polar transport in moss shoots. Evol Dev **10**: 176–186.

Galway, M.E., Heckman, J.W., and Schiefelbein, J.W. (1997). Growth and ultrastructure of Arabidopsis root hairs: the rhd3 mutation alters vacuole enlargement and tip growth. Planta **201**: 209–218.

Gensel, P.G. (2008). The Earliest Land Plants. Annu Rev Ecol Evol Syst **39**: 459–477.

Graham, L.E.L., Cook, M.E.M., and Busse, J.S.J. (2000). The origin of plants: body plan changes contributing to a major evolutionary radiation. Proc Natl Acad Sci USA **97**: 4535–4540.

Gruber, A.R., Lorenz, R., Bernhart, S.H., Neubock, R., and Hofacker, I.L. (2008). The Vienna RNA Websuite. Nucleic Acids Research **36**: W70–W74.

Guindon, S., Dufayard, J.F., Lefort, V., Anisimova, M., Hordijk, W., and Gascuel, O. (2010). New Algorithms and Methods to Estimate Maximum-Likelihood Phylogenies: Assessing the Performance of PhyML 3.0. Systematic Biology **59**: 307–321.

Guo, R., Xue, H., and Huang, L. (2003). Ssh10b, a conserved thermophilic archaeal protein, binds RNA in vivo. Molecular Microbiology **50**: 1605–1615.

Halder, G., Callaerts, P., and Gehring, W.J. (1995). Induction of ectopic eyes by targeted expression of the eyeless gene in Drosophila. Science **267**: 1788–1792.

Hay, A. and Tsiantis, M. (2010). KNOX genes: versatile regulators of plant development and diversity. Development **137**: 3153–3165.

Heinrichs, J., Hentschel, J., Wilson, R., and Feldberg, K. (2007). Evolution of leafy liverworts (Jungermanniidae, Marchantiophyta): estimating divergence times from chloroplast DNA sequences using penalized likelihood with integrated fossil evidence. Taxon **56**: 31-44.

Hellens, R., Mullineaux, P., and Klee, H. (2000). Technical Focus: a guide to Agrobacterium binary Ti vectors. Trends in Plant Science **5**: 446–451.

Hernick, L.V., Landing, E., and Bartowski, K.E. (2008). Earth's oldest liverworts—*Metzgeriothallus sharonae sp.* nov. from the Middle Devonian (Givetian) of eastern New York, USA. Review of Palaeobotany and Palynology **148**: 154–162.

Humphreys, C.P., Franks, P.J., Rees, M., Bidartondo, M.I., Leake, J.R., and Beerling, D.J. (2010). Mutualistic mycorrhiza-like symbiosis in the most ancient group of land plants. Nature Communications **1**: 103.

Inoue, N., Yamada, S.-Y., Nagata, Y., and Shimmen, T. (2002). Rhizoid differentiation in Spirogyra: position sensing by terminal cells. Plant and Cell Physiology **43**: 479–483.

Ishizaki, K., Chiyoda, S., Yamato, K.T., and Kohchi, T. (2008). Agrobacterium-Mediated Transformation of the Haploid Liverwort *Marchantia polymorpha L*., an Emerging Model for Plant Biology. Plant and Cell Physiology **49**: 1084–1091.

Ishizaki, K., Johzuka-Hisatomi, Y., Ishida, S., Iida, S., and Kohchi, T. (2013). Homologous recombination-mediated gene targeting in the liverwort *Marchantia polymorpha*. Nature Scientific Reports **3**.

Ishizaki, K., Nonomura, M., Kato, H., Yamato, K.T., and Kohchi, T. (2012). Visualization of auxin-mediated transcriptional activation using a common auxin-responsive reporter system in the liverwort *Marchantia polymorpha*. J Plant Res **125**: 643–651.

Jacobsen, S.E., Running, M.P., and Meyerowitz, E.M. (1999). Disruption of an RNA helicase/RNAse III gene in Arabidopsis causes unregulated cell division in floral meristems. Development **126**: 5231-5243.

Jang, G., Yi, K., Pires, N.D., Menand, B., and Dolan, L. (2011). RSL genes are sufficient for rhizoid system development in early diverging land plants. Development **138**: 2273–2281.

Johnson, C.M., Stout, P.R., Broyer, T.C., and Carlton, A.B. (1957). Comparative chlorine requirements of different plant species. Plant and Soil **4**: 337-353.

Jones-Rhoades, M.W. (2011). Conservation and divergence in plant microRNAs. Plant Mol Biol **80**: 3–16.

Jones-Rhoades, M.W. and Bartel, D.P. (2004). Computational identification of plant microRNAs and their targets, including a stress-induced miRNA. Molecular Cell **14**: 787–799.

Karas, B., Murray, J., Gorzelak, M., Smith, A., Sato, S., Tabata, S., Szczyglowski, K. (2005). Invasion of *Lotus japonicus* root hairless 1 by *Mesorhizobium loti* Involves the Nodulation Factor-Dependent Induction of Root Hairs. Plant Physiology **137**: 1331–1344.

Karas, B., Amyot, L., Johansen, C., Sato, S., Tabata, S., Kawaguchi, M., and Szczyglowski, K. (2009). Conservation of Lotus and Arabidopsis Basic Helix-Loop-Helix Proteins Reveals New Players in Root Hair Development. Plant Physiology **151**: 1175–1185.

Karol, K.G., McCourt, R.M., Cimino, M.T., Delwiche, C.F. (2001). The Closest Living Relatives of Land Plants. Science **294**: 2351–2353.

Kato, H., Ishizaki, K., Kouno, M., Shirakawa, M., Bowman, J.L., Nishihama, R., and Kohchi, T. (2015). Auxin-Mediated Transcriptional System with a Minimal Set of Components Is Critical for Morphogenesis through the Life Cycle in *Marchantia polymorpha*. PLoS Genet **11**: e1005084.

Katoh, K. and Standley, D.M. (2013). MAFFT Multiple Sequence Alignment Software Version 7: Improvements in Performance and Usability. Molecular Biology and Evolution **30**: 772–780.

Kaul, K.N., Mitra, G.C., and Tripathi, B.K. (1962). Responses of *Marchantia* in aseptic culture to well-known auxins and antiauxins. Annals of Botany **26**: 447-466.

Kenrick, P. and Crane, P.R. (1997). The origin and early evolution of plants on land. Nature **389**: 33–39.

Kepinski, S. and Leyser, O. (2005). The Arabidopsis F-box protein TIR1 is an auxin receptor. Nat Cell Biol **435**: 446–451.

Kerp, H., Trewin, N.H., and Hass, H. (2004). New gametophytes from the Early Devonian Rhynie chert. Transactions of the Royal Society of Edinburgh: Earth Sciences **94**: 411–428.

Kessler, S.A., Lindner, H., Jones, D.S., and Grossniklaus, U. (2015). Functional analysis of related CrRLK1L receptor-like kinases in pollen tube reception. EMBO Rep **16**: 107–115.

Kim, C.M., Park, S.H., Je, B.I., Park, S.H., Park, S.J., Piao, H.L., Eun, M.Y., Dolan, L., and Han, C.D. (2007). OsCSLD1, a Cellulose Synthase-Like D1 Gene, Is Required for Root Hair Morphogenesis in Rice. Plant Physiology **143**: 1220–1230.

Kim, Y.J., Zheng, B., Yu, Y., Won, S.Y., Mo, B., and Chen, X. (2011). The role of Mediator in small and long noncoding RNA production in *Arabidopsis thaliana.* The EMBO Journal **30**: 814–822.

Knauer, S., Holt, A.L., Rubio-Somoza, I., Tucker, E.J., Hinze, A., Pisch, M., Javelle, M., Timmermans, M.C., Tucker, M.R., and Laux, T. (2013). A Protodermal miR394 Signal Defines a Region of Stem Cell Competence in the Arabidopsis Shoot Meristem. Developmental Cell **24**: 125–132.

Komatsu, A., Terai, M., Ishizaki, K., Suetsugu, N., Tsuboi, H., Nishihama, R., Yamato, K.T., Wada, M., and Kohchi, T. (2014). Phototropin Encoded by a Single-Copy Gene Mediates Chloroplast Photorelocation Movements in the Liverwort *Marchantia polymorpha L.* Plant Physiology **166**: 411-427.

Koshino-Kimura, Y., Wada, T., Tachibana, T., Tsugeki, R., Ishiguro, S., Okada, K. (2005). Regulation of CAPRICE Transcription by MYB Proteins for Root Epidermis Differentiation in Arabidopsis. Plant and Cell Physiology **46**: 817–826.

Krysan, P.J., Young, J.C., Jester, P.J., Monson, S., Copenhaver, G., Preuss, D., and Sussman, M.R. (2002). Characterization of T-DNA insertion sites in *Arabidopsis thaliana* and the implications for saturation mutagenesis. OMICS **6**: 163–174.

Kubota, A., Kita, S., Ishizaki, K., and Nishihama, R. (2014). Co-option of a photoperiodic growth-phase transition system during land plant evolution. Nature Communications **5**: 3668.

Kurata, T. et al. (2005). Cell-to-cell movement of the CAPRICE protein in Arabidopsis root epidermal cell differentiation. Development **132**: 5387–5398.

Kurihara, Y. and Watanabe, Y. (2004). Arabidopsis micro-RNA biogenesis through Dicer-like 1 protein functions. Proc. Natl. Acad. Sci. U.S.A. **101**: 12753–12758.

Kurihara, Y., Takashi, Y., and Watanabe, Y. (2006). The interaction between DCL1 and HYL1 is important for efficient and precise processing of pri-miRNA in plant microRNA biogenesis. RNA **12**: 206–212.

Kusano, H., Testerink, C., Vermeer, J.E.M., Tsuge, T., Shimada, H., Oka, A., Munnik, T., and Aoyama, T. (2008). The Arabidopsis Phosphatidylinositol Phosphate 5-Kinase PIP5K3 Is a Key Regulator of Root Hair Tip Growth. Plant Cell **20**: 367–380.

Kwasniewski, M., Nowakowska, U., Szumera, J., Chwialkowska, K., and Szarejko, I. (2012). iRootHair: A Comprehensive Root Hair Genomics Database. Plant Physiology **161**: 28–35.

LaRue, C.D. and Narayanaswami, S. (1957). Auxin inhibition in the liverwort Lunularia. New Phytologist **56**: 61–70.

Lee, M.M. and Schiefelbein, J. (2002). Cell pattern in the Arabidopsis root epidermis determined by lateral inhibition with feedback. Plant Cell **14**: 611-618.

Lee, M.M. and Schiefelbein, J. (1999). WEREWOLF, a MYB-related protein in Arabidopsis, is a position-dependent regulator of epidermal cell patterning. Cell **99**: 473–483.

Lelandais-Briere, C., Naya, L., Sallet, E., Calenge, F., Frugier, F., Hartmann, C., Gouzy, J., and Crespi, M. (2009). Genome-Wide *Medicago truncatula* Small RNA Analysis Revealed Novel MicroRNAs and Isoforms Differentially Regulated in Roots and Nodules. Plant Cell **21**: 2780–2796.

Li, S. et al. (2013). MicroRNAs Inhibit the Translation of Target mRNAs on the Endoplasmic Reticulum in Arabidopsis. Cell **153**: 562–574.

Li, Y., Rosso, M.G., Ulker, B., and Weisshaar, B. (2006). Analysis of T-DNA insertion site distribution patterns in *Arabidopsis thaliana* reveals special features of genes without insertions. Genomics **87**: 645–652.

Linkies, A., Graeber, K., Knight, C., and Leubner-Metzger, G. (2010). The evolution of seeds. New Phytologist **186**: 817–831.

Long, J.A., Moan, E.I., Medford, J.I., and Barton, M.K. (1996). A member of the KNOTTED class of homeodomain proteins encoded by the STM gene of Arabidopsis. Nature **379**: 66–69.

Lu, C. and Fedoroff, N. (2000). A mutation in the Arabidopsis HYL1 gene encoding a dsRNA binding protein affects responses to abscisic acid, auxin, and cytokinin. Plant Cell **12**: 2351–2366.

Lukowitz, W., Nickle, T.C., Meinke, D.W., Last, R.L., Conklin, P.L., and Somerville, C.R. (2001). Arabidopsis cyt1 mutants are deficient in a mannose-1-phosphate guanylyltransferase and point to a requirement of N-linked glycosylation for cellulose biosynthesis. Proc Natl Acad Sci USA **98**: 2262–2267.

MA, Z., Coruh, C., and Axtell, M.J. (2010). *Arabidopsis lyrata* Small RNAs: Transient MIRNA and Small Interfering RNA Loci within the Arabidopsis Genus. Plant Cell **22**: 1090–1103.

Mallory, A.C. and Vaucheret, H. (2006). Functions of microRNAs and related small RNAs in plants. Nat Genet **38** Suppl: S31–6.

Maravolo, N.C. and Voth, P.D. (1966). Morphogenic effects of three growth substances on *Marchantia* gemmalings. Botanical Gazette **127**: 79–86.

Marella, H.H., Sakata, Y., and Quatrano, R.S. (2006). Characterization and functional analysis of ABSCISIC ACID INSENSITIVE3-like genes from *Physcomitrella patens*. Plant J **46**: 1032–1044.

Marsh, V.L., Peak-Chew, S.Y., and Bell, S.D. (2005). Sir2 and the Acetyltransferase, Pat, Regulate the Archaeal Chromatin Protein, Alba. Journal of Biological Chemistry **280**: 21122–21128.

Masucci, J.D. and Schiefelbein, J.W. (1994). The rhd6 Mutation of Arabidopsis thaliana Alters Root-Hair Initiation through an Auxin- and Ethylene-Associated Process. Plant Physiology **106**: 1335–1346.

McConaha, M. (1941). Ventral structures effecting capillarity in the Marchantiales. Am. J. Bot. **128**: 301–306.

McCourt, R.M., Delwiche, C.F., and Karol, K.G. (2004). Charophyte algae and land plant origins. Trends in Ecology & Evolution **19**: 661–666.

McElver, J. et al. (2001). Insertional mutagenesis of genes required for seed development in *Arabidopsis thaliana*. Genetics **159**: 1751–1763.

Menand, B., Yi, K., Jouannic, S., Hoffmann, L., Ryan, E., Linstead, P., Schaefer, D.G., and Dolan, L. (2007). An Ancient Mechanism Controls the Development of Cells with a Rooting Function in Land Plants. Science **316**: 1477–1480.

Miyazaki, S., Murata, T., Sakurai-Ozato, N., Kubo, M., Demura, T., Fukuda, H., and Hasebe, M. (2009). ANXUR1 and 2, Sister Genes to FERONIA/SIRENE, Are Male Factors for Coordinated Fertilization. Current Biology **19**: 1327–1331.

Moczek, A.P., Cruickshank, T.E., and Shelby, A. (2006a). When ontogeny reveals what phylogeny hides: gain and loss of horns during development and evolution of horned beetles. Evolution **60**: 2329–2341.

Moczek, A.P., Rose, D., Sewell, W., and Kesselring, B.R. (2006b). Conservation, innovation, and the evolution of horned beetle diversity. Dev Genes Evol **216**: 655–665.

Molnár, A., Schwach, F., Studholme, D.J., Thuenemann, E.C., and Baulcombe, D.C. (2007). miRNAs control gene expression in the single-cell alga *Chlamydomonas reinhardtii.* Nature **447**: 1126–1129.

Monshausen, G.B., Bibikova, T.N., Messerli, M.A., Shi, C., and Gilroy, S. (2007). Oscillations in extracellular pH and reactive oxygen species modulate tip growth of Arabidopsis root hairs. Proc Natl Acad Sci USA **104**: 20996–21001.

Mosquna, A., Katz, A., Decker, E.L., Rensing, S.A., Reski, R., and Ohad, N. (2009). Regulation of stem cell maintenance by the Polycomb protein FIE has been conserved during land plant evolution. Development **136**: 2433–2444.

Niklas, K.J. and Kutschera, U. (2009). The evolutionary development of plant body plans. Functional Plant Biol **36**: 682.

Nikovics, K., Blein, T., Peaucelle, A., Ishida, T., Morin, H., Aida, M., and Laufs, P. (2006). The Balance between the MIR164A and CUC2 Genes Controls Leaf Margin Serration in Arabidopsis. Plant Cell **18**: 2929–2945.

Nordahl Petersen, T., Brunak, S., Heijne, von, G., and Nielsen, H. (2011). SignalP 4.0: discriminating signal peptides from transmembrane regions. Nat. Methods **8**: 785–786.

O'Hanlon, M.E. (1926). Germination of Spores and Early Stages in Development of Gametophyte of *Marchantia polymorpha*. Botanical Gazette **82**: 215–222.

Oka, T., Nemoto, T., and Jigami, Y. (2007). Functional analysis of Arabidopsis thaliana RHM2/MUM4, a multidomain protein involved in UDP-D-glucose to UDP-L-rhamnose conversion. J Biol Chem **282**: 5389–5403.

Okada, S. et al. (2000). Construction of male and female PAC genomic libraries suitable for identification of Y-chromosome-specific clones from the liverwort, *Marchantia polymorpha*. Plant J **24**: 421–428.

Okano, Y., Aono, N., and Hiwatashi, Y. (2009). A polycomb repressive complex 2 gene regulates apogamy and gives evolutionary insights into early land plant evolution. Proc Natl Acad Sci USA **106**: 16321–16326.

Ono, K., Ohyama, K., and Gamborg, O.L. (1978). Regeneration of the liverwort *Marchantia polymorpha L*. From protoplasts isolated from cell suspension culture. Plant Science Letters **14**: 225–229.

Oyama, T.T., Shimura, Y.Y., and Okada, K.K. (2002). The IRE gene encodes a protein kinase homologue and modulates root hair growth in Arabidopsis. Plant J **30**: 289–299.

Pan, X. (2005). Site Preferences of Insertional Mutagenesis Agents in Arabidopsis. Plant Physiology **137**: 168–175.

Panganiban, G. et al. (1997). The origin and evolution of animal appendages. Proc Natl Acad Sci USA. **94**: 5162–5166.

Park, S., Szumlanski, A.L., Gu, F., Guo, F., and Nielsen, E. (2011). A role for CSLD3 during cell-wall synthesis in apical plasma membranes of tip-growing root-hair cells. Nat Cell Biol **13**: 973–980.

Park, W., Li, J., Song, R., Messing, J., and Chen, X. (2002). CARPEL FACTORY, a Dicer homolog, and HEN1, a novel protein, act in microRNA metabolism in *Arabidopsis thaliana*. Current Biology **12**: 1484-1495.

Pattison, R.J. and Amtmann, A. (2009). N-glycan production in the endoplasmic reticulum of plants. Trends in Plant Science **14**: 92–99.

Pena, M.J., Kong, Y., York, W.S., and O'Neill, M.A. (2012). A Galacturonic Acid-Containing Xyloglucan Is Involved in Arabidopsis Root Hair Tip Growth. Plant Cell **24**: 4511–4524.

Peremyslov, V.V., Prokhnevsky, A.I., and Dolja, V.V. (2010). Class XI Myosins Are Required for Development, Cell Expansion, and F-Actin Organization in Arabidopsis. Plant Cell **22**: 1883–1897.

Peremyslov, V.V., Prokhnevsky, A.I., Avisar, D., and Dolja, V.V. (2008). Two Class XI Myosins Function in Organelle Trafficking and Root Hair Development in Arabidopsis. Plant Physiology **146**: 1109–1116.

Perrin, R.M., Wang, Y., Yuen, C.Y.L., Will, J., and Masson, P.H. (2007). WVD2 is a novel microtubule-associated protein in *Arabidopsis thaliana*. Plant J **49**: 961–971.

Pires, N. and Dolan, L. (2010). Origin and Diversification of Basic-Helix-Loop-Helix Proteins in Plants. Molecular Biology and Evolution **27**: 862–874.

Pires, N.D., Yi, K., Breuninger, H., Catarino, B., Menand, B., and Dolan, L. (2013). Recruitment and remodeling of an ancient gene regulatory network during land plant evolution. Proc Natl Acad Sci USA **110**: 9571–9576.

Pitts, R.J., Cernac, A., and Estelle, M. (1998). Auxin and ethylene promote root hair elongation in Arabidopsis. Plant J **16**: 553–560.

Pocock, K. and Duckett, J.G. (1985). On the occurrence of branched and swollen rhizoids in British hepatics: their relationships with the substratum and associations with fungi. New Phytologist **91**: 281-304.

Prigge, M.J., Lavy, M., Ashton, N.W., and Estelle, M. (2010). *Physcomitrella patens* Auxin-Resistant Mutants Affect Conserved Elements of an Auxin-Signaling Pathway. Current Biology **20**: 1907–1912.

Prud'homme, B., Minervino, C., Hocine, M., Cande, J.D., Aouane, A., Dufour, H.D., Kassner, V.A., and Gompel, N. (2011). Body plan innovation in treehoppers through the evolution of an extra wing-like appendage. Nature **473**: 83–86.

Qi, Y., Denli, A.M., and Hannon, G.J. (2005). Biochemical Specialization within Arabidopsis RNA Silencing Pathways. Molecular Cell **19**: 421–428.

Qin, Z., Li, C., Mao, L., and Wu, L. (2014). Novel insights from non-conserved microRNAs in plants. Front Plant Sci **5**: 586.

Qiu, Y.-L. et al. (2006). The deepest divergences in land plants inferred from phylogenomic evidence. Proc Natl Acad Sci USA **103**: 15511–15516.

Raven, J.A. and Edwards, D. (2001). Roots: evolutionary origins and biogeochemical significance. Journal of Experimental Botany **52**: 381–401.

Rensing, S.A. et al. (2008). The *Physcomitrella* Genome Reveals Evolutionary Insights into the Conquest of Land by Plants. Science **319**: 64–69.

Rensing, S.A., Ick, J., Fawcett, J.A., Lang, D., Zimmer, A., Van de Peer, Y., and Reski, R. (2007). An ancient genome duplication contributed to the abundance of metabolic genes in the moss *Physcomitrella patens*. BMC Evolutionary Biology **7**: 130.

Ringli, C., Bigler, L., Kuhn, B.M., Leiber, R.M., Diet, A., Santelia, D., Frey, B., Pollmann, S., and Klein, M. (2008). The Modified Flavonol Glycosylation Profile in the Arabidopsis rol1 Mutants Results in Alterations in Plant Growth and Cell Shape Formation. Plant Cell **20**: 1470–1481.

Rogers, K. and Chen, X. (2013). Biogenesis, Turnover, and Mode of Action of Plant MicroRNAs. Plant Cell **25**: 2383–2399.

Rounds, C.M. and Bezanilla, M. (2013). Growth Mechanisms in Tip-Growing Plant Cells. Annu. Rev. Plant Biol. **64**: 243–265.

Ruijter, J.M., Ramakers, C., Hoogaars, W.M.H., Karlen, Y., Bakker, O., van den Hoff, M.J.B., and Moorman, A.F.M. (2009). Amplification efficiency: linking baseline and bias in the analysis of quantitative PCR data. Nucleic Acids Research **37**: e45–e45.

Russell, J. and Bulman, S. (2004). The liverwort *Marchantia foliacea* forms a specialized symbiosis with arbuscular mycorrhizal fungi in the genus Glomus. New Phytologist **165**: 567–579.

Saavedra, L., Balbi, V., Lerche, J., Mikami, K., Heilmann, I., and Sommarin, M. (2011). PIPKs are essential for rhizoid elongation and caulonemal cell development in the moss *Physcomitrella patens*. Plant J **67**: 635–647.

Saedler, R., Jakoby, M., Marin, B., Galiana-Jaime, E., and Hülskamp, M. (2009). The cell morphogenesis gene SPIRRIGin Arabidopsis encodes a WD/BEACH domain protein. Plant J **59**: 612–621.

Saint-Marcoux, D., Proust, H., Dolan, L., and Langdale, J.A. (2015). Identification of Reference Genes for Real-Time Quantitative PCR Experiments in the Liverwort *Marchantia polymorpha*. PLoS ONE **10**: e0118678.

Sakakibara, K., Nishiyama, T., Sumikawa, N., Kofuji, R., Murata, T., Hasebe, M. (2003). Involvement of auxin and a homeodomain-leucine zipper I gene in rhizoid development of the moss *Physcomitrella patens*. Development **130**: 4835–4846.

Sakakibara, K., Ando, S., Yip, H.K., Tamada, Y., Hiwatashi, Y., Murata, T., Deguchi, H., Hasebe, M., and Bowman, J.L. (2013). KNOX2 Genes Regulate the Haploid-to-Diploid Morphological Transition in Land Plants. Science **339**: 1067–1070.

Sakakibara, K., Nishiyama, T., Deguchi, H., and Hasebe, M. (2008). Class 1 KNOX genes are not involved in shoot development in the moss *Physcomitrella patens* but do function in sporophyte development. Evol Dev **10**: 555–566.

Sarkar, P., Bosneaga, E., and Auer, M. (2009). Plant cell walls throughout evolution: towards a molecular understanding of their design principles. Journal of Experimental Botany **60**: 3615–3635.

Sayou, C. et al. (2014). A Promiscuous Intermediate Underlies the Evolution of LEAFY DNA Binding Specificity. Science **343**: 645–648.

Schellmann, S., Schnittger, A., Kirik, V., Wada, T., Okada, K., Beermann, A., Thumfahrt, J., Jürgens, G., and Hulskamp, M. (2002). TRIPTYCHON and CAPRICE mediate lateral inhibition during trichome and root hair patterning in Arabidopsis. EMBO J **21**: 5036–5046.

Schindelin, J. et al. (2012). Fiji: an open-source platform for biological-image analysis. Nat Methods **9**: 676–682.

Seefried, W.F., Willmann, M.R., Clausen, R.L., and Jenik, P.D. (2014). Global Regulation of Embryonic Patterning in Arabidopsis by MicroRNAs. Plant Physiology **165**: 670–687.

Shubin, N., Tabin, C., and Carroll, S. (2009). Deep homology and the origins of evolutionary novelty. Nature **457**: 818–823.

Sieber, P., Wellmer, F., Gheyselinck, J., Riechmann, J.L., and Meyerowitz, E.M. (2007). Redundancy and specialization among plant microRNAs: role of the MIR164 family in developmental robustness. Development **134**: 1051–1060.

Singer, S.D. and Ashton, N.W. (2007). Revelation of ancestral roles of KNOX genes by a functional analysis of *Physcomitrella* homologues. Plant Cell Reports **26**: 2039–2054.

Solovyev, V.V. and Shahmuradov, I.A. (2003). PromH: promoters identification using orthologous genomic sequences. Nucleic Acids Research **31**: 3540–3545.

Song, S.K., Ryu, K.H., Kang, Y.H., Song, J.H., Cho, Y.H., Yoo, S.D., Schiefelbein, J., and Lee, M.M. (2011). Cell Fate in the Arabidopsis Root Epidermis Is Determined by Competition between WEREWOLF and CAPRICE. Plant Physiology **157**: 1196–1208.

Stahl, Y., Wink, R.H., Ingram, G.C., and Simon, R. (2009). A Signaling Module Controlling the Stem Cell Nichein Arabidopsis Root Meristems. Current Biology **19**: 909–914.

Steemans, P., Herisse, A.L., Melvin, J., Miller, M.A., Paris, F., Verniers, J., and Wellman, C.H. (2009). Origin and Radiation of the Earliest Vascular Land Plants. Science **324**: 353–353.

Stein, W.E., Berry, C.M., Hernick, L.V., and Mannolini, F. (2012). Surprisingly complex community discovered in the mid-Devonian fossil forest at Gilboa. Nature **482**: 78–81.

Stern, D.L. and Orgogozo, V. (2009). Is genetic evolution predictable? Science **323**: 741–746.

Stern, D.L. and Orgogozo, V. (2008). The loci of evolution: how predictable is genetic evolution? Evolution **62**: 2155–2177.

Sunkar, R., Zhou, X., Zheng, Y., Zhang, W., and Zhu, J.-K. (2008). Identification of novel and candidate miRNAs in rice by high throughput sequencing. BMC Plant Biology **8**: 25.

Szabados, L. et al. (2002). Distribution of 1000 sequenced T-DNA tags in the Arabidopsis genome. Plant J **32**: 233–242.

Tam, T.H.Y., Catarino, B., and Dolan, L. (2015). Conserved regulatory mechanism controls the development of cells with rooting functions in land plants. Proc Natl Acad Sci USA **112**: 3959–3968.

Tamura, K., Stecher, G., Peterson, D., Filipski, A., and Kumar, S. (2013). MEGA6: Molecular Evolutionary Genetics Analysis Version 6.0. Molecular Biology and Evolution **30**: 2725–2729.

Tanahashi, T. (2005). Diversification of gene function: homologs of the floral regulator FLO/LFY control the first zygotic cell division in the moss *Physcomitrella patens*. Development **132**: 1727–1736.

Tarén, N. (1958). Factors Regulating the Initial Development of Gemmae in *Marchantia Polymorpha*. The Bryologist **61**: 191–204.

Taylor, R.S., Tarver, J.E., Hiscock, S.J., and Donoghue, P.C.J. (2014). Evolutionary history of plant microRNAs. Trends in Plant Science **19**: 175–182.

Taylor, T. N., Taylor, E.L., Krings, M. (2009). Paleobotany: The biology and evolution of fossil plants. 2nd Ed. Academic Press.

Taylor, T.N., Kerp, H., and Hass, H. (2005). Life history biology of early land plants: deciphering the gametophyte phase. Proc Natl Acad Sci USA **102**: 5892–5897.

Taylor, W.A. (1995). Spores in earliest land plants. Nature **373**: 391-392.

Timme, R.E. and Delwiche, C.F. (2010). Uncovering the evolutionary origin of plant molecular processes: comparison of Coleochaete (Coleochaetales) and *Spirogyra* (Zygnematales) transcriptomes. BMC Plant Biology **10**: 96.

Timme, R.E., Bachvaroff, T.R., and Delwiche, C.F. (2012). Broad phylogenomic sampling and the sister lineage of land plants. PLoS ONE **7**: e29696.

Tougane, K., Komatsu, K., Bhyan, S.B., Sakata, Y., Ishizaki, K., Yamato, K.T., Kohchi, T., and Takezawa, D. (2010). Evolutionarily Conserved Regulatory Mechanisms of Abscisic Acid Signaling in Land Plants: Characterization of ABSCISIC ACID INSENSITIVE1-Like Type 2C Protein Phosphatase in the Liverwort *Marchantia polymorpha*. Plant Physiology **152**: 1529–1543.

Turmel, M., Pombert, J.F., Charlebois, P., Otis, C., and Lemieux, C. (2007). The Green Algal Ancestry of Land Plants as Revealed by the Chloroplast Genome. Int. J Plant Sci **168**: 679–689.

Vanneste, S. and Friml, J. (2009). Auxin: A Trigger for Change in Plant Development. Cell **136**: 1005–1016.

Varkonyi-Gasic, E., Wu, R., Wood, M., Walton, E.F., and Hellens, R.P. (2007). Protocol: a highly sensitive RT-PCR method for detection and quantification of microRNAs. Plant Methods **3**: 12.

Vashishta B. R., Sinha, A. K., Kumar, A (2011). Botany for degree students, Part III Bryophyta. S. Chand & Company Ltd., Ram Nagar, New Delhi, India.

Vaucheret, H., Vazquez, F., Crete, P., Bartel, D.P. (2004). The action of ARGONAUTE1 in the miRNA pathway and its regulation by the miRNA pathway are crucial for plant development. Genes & Development **18**: 1187–1197.

Vaucheret, H., Mallory, A.C., and Bartel, D.P. (2006). AGO1 Homeostasis Entails Coexpression of MIR168 and AGO1 and Preferential Stabilization of miR168 by AGO1. Molecular Cell **22**: 129–136.

Viaene, T. et al. (2014). Directional Auxin Transport Mechanisms in Early Diverging Land Plants. Current Biology **24**: 2786–2791.

Vidali, L., Burkart, G.M., Augustine, R.C., Kerdavid, E., Tuzel, E., and Bezanilla, M. (2010). Myosin XI Is Essential for Tip Growth in *Physcomitrella patens.* Plant Cell **22**: 1868–1882.

Villalobos, L.I.A. et al. (2012). a combinatorial TIR1/AFB–Aux/IAA co-receptor system for differential sensing of auxin. Nature Chemical Biology **8**: 477–485.

Voinnet, O. (2009). Origin, Biogenesis, and Activity of Plant MicroRNAs. Cell **136**: 669–687.

Voth, P.D. and Hamner, K.C. (1940). Responses of *Marchantia polymorpha* to nutrient supply and photoperiod. Botanical Gazette **102**: 169–205.

Wang, X., Cnops, G., Vanderhaeghen, R., De Block, S., Van Montagu, M., and Van Lijsebettens, M. (2001). AtCSLD3, a cellulose synthase-like gene important for root hair growth in arabidopsis. Plant Physiology **126**: 575–586.

Watt, G., Leoff, C., Harper, A.D., Bar-Peled, M. (2004). A Bifunctional 3,5-Epimerase/4-Keto Reductase for Nucleotide-Rhamnose Synthesis in Arabidopsis. Plant Physiology **134**: 1337–1346.

Wellman, C.H. and Gray, J. (2000). The microfossil record of early land plants. Philos Trans R Soc Lond, B, Biol. Sci. **355**: 717–731

Wellman, C.H., Osterloff, P.L., and Mohiuddin, U. (2003). Fragments of the earliest land plants. Nature **425**: 282–285.

Wickett, N.J. et al. (2014). Phylotranscriptomic analysis of the origin and early diversification of land plants. Proc Natl Acad Sci USA **111**: E4859–68.

Willmann, M.R. and Poethig, R.S. (2007). Conservation and evolution of miRNA regulatory programs in plant development. Current Opinion in Plant Biology **10**: 503–511.

Wodniok, S., Brinkmann, H., Glöckner, G., Heidel, A.J., Philippe, H., Melkonian, M., and Becker, B. (2011). Origin of land plants: do conjugating green algae hold the key? BMC Evolutionary Biology **11**: 104.

Wu, G. and Poethig, R.S. (2006). Temporal regulation of shoot development in *Arabidopsis thaliana* by miR156 and its target SPL3. Development **133**: 3539–3547.

Wu, G., Park, M.Y., Conway, S.R., Wang, J.-W., Weigel, D., and Poethig, R.S. (2009). The Sequential Action of miR156 and miR172 Regulates Developmental Timing in Arabidopsis. Cell **138**: 750–759.

Wu, L., Zhou, H., Zhang, Q., Zhang, J., Ni, F., Liu, C., and Qi, Y. (2010). DNA Methylation Mediated by a MicroRNA Pathway. Molecular Cell **38**: 465–475.

Xie, Z., Kasschau, K.D., and Carrington, J.C. (2003). Negative Feedback Regulation of Dicer-Like1 in Arabidopsis by microRNA-Guided mRNA Degradation. Current Biology **13**: 784–789.

Xu, B. et al. (2014). Contribution of NAC Transcription Factors to Plant Adaptation to Land. Science **343**: 1505–1508.

Yi, K., Menand, B., Bell, E., and Dolan, L. (2010). A basic helix-loop-helix transcription factor controls cell growth and size in root hairs. Nat Genet **42**: 264–267.

Yin, Y., Huang, J., and Xu, Y. (2009). The cellulose synthase superfamily in fully sequenced plants and algae. BMC Plant Biology **9**: 99.

Zhao, T., Li, G., Mi, S., Li, S., Hannon, G.J., Wang, X.J., and Qi, Y. (2007). A complex system of small RNAs in the unicellular green alga *Chlamydomonas reinhardtii*. Genes & Development **21**: 1190–1203.